Neural correlates of memory impairment and rescue in a mouse model of Down syndrome

Maria Alemany González

TESI DOCTORAL UPF / 2019

THESIS SUPERVISOR

Dra. M. Victoria Puig Velasco

Neurosciences Research Programme,
Hospital del Mar Research Institute (IMIM)

DEPARTMENT CEXS UPF-PHD PROGRAMME IN BIOMEDICINE

Als meus pares.

Acknowledgements

Em sento molt afortunada d'haver estat tan ben rodejada aquests últims anys de persones que han fet que aquesta sigui una etapa molt feliç. A nivell de feina, a nivell d'amistat i a nivell de suport, gràcies a tots.

Primer de tot volia agrair a la Vicky tot el que m'ha permès viure durant aquests anys. Gràcies per confiar en mi des del principi i donar-me la oportunitat de ser la primera estudiant del teu laboratori. Gràcies per la paciència, pels ànims i per ensenyar-me a ser optimista i a creure en mi. Gràcies per transmetre'm aquesta passió per estudiar els "ritmes del cervell" i per ser un gran model de resiliència. He après molt amb tu. Hem passat moltes hores reunides, ens hem exaltat i hem celebrat resultats que ens han encantat, i tot i haver passat moments més complicats sempre ho hem superat. He vist néixer i créixer el Puig Lab i tinc moltes ganes de seguir veient com puja. He pogut veure la teva gran implicació, l'esforç i dedicació, les ganes que hi ha darrera i t'ho ben mereixes. Gràcies per tot, Vicky!

Y ahora vienes tu, Thomas, quien ha tenido la gran paciencia de enseñarme a hacer aquellas cirugías que tan imposibles veía, quien me introdujo al mundo de la electrofisiología y me formó desde el principio. Gracias también por hacerme un poco más "trouble-shooter" y por confiar en mi cuando ni yo lo hacía. Gracias Thomas, compartir contigo estos años ha sido una suerte. Aunque al principio ha sido duro, ha valido la pena! Ya sabes que pienso que

eres una pieza clave en el Puig Lab y que espero que muchos estudiantes puedan seguir formándose contigo! Gracias!

Jordi, ja no estàs al lab però com si hi fossis, compartir amb tu la primera etapa va ser una sort i no has deixat mai de ser un gran suport i amic, gràcies! No oblidaré mai les bones estones que hem viscut els quatre, des de Tortosa fins a San Diego! Que segueixin! Pau, a ti también tengo mucho que agradecerte, a nivel técnico i a nivel personal has sido también una pieza clave durante estos años, muchas gracias! Y ya sabes que te considero una de las grandes adquisiciones del Puig Lab, a nivel personal y profesional. Cristina, la segona estudiant de doctorat del Puig Lab! Gràcies per estar sempre disposada a donar un cop de mà i pel suport constant, he après molt de la teva manera optimista d'encarar les dificultats i estic segura que faràs una tesi preciosa i t'ho passaràs molt bé! Marta, m'ha encantat tenir-te pel laboratori. Gràcies pel suport, per la feina ben feta i per endolçar-nos molts dies amb els teus dots pastissers, estic segura que en la teva nova etapa seguiràs tenint molt d'èxit, molta sort! Amanda, we have shared many times after work and you have always motivated me! Thank you! Pablo, el surfero currante, sabemos que te espera una tesis complicada pero estoy segura que lo vas a hacer genial, no me preocupas porque eres muy capaz! Gracias también por el soporte que me has dado y ánimo! Meli, I hope you keep always having this positive energy because the people around you can feel it and enjoy it, thank you!

I què dir de la resta de companys de l'IMIM.. he tingut la sort de passar per tres despatxos diferents i així compartir estones amb molts de vosaltres. Euli, que ja has volat a fer el postdoc però no per això et deixo de tenir molt present. Gràcies per ser un pilar aquests anys, per calmar-me en les meves angoixes i ser una gran amiga dins i fora de la feina. Em sento molt afortunada d'haver-te conegut i vull que tot i la distància seguim fent pinya! Sort en tinc també de l'Àlex, gràcies pel suport, per les bones estones plegats i ànims amb el que queda! Anna, també companya d'aquest camí, ha estat un plaer compartir-lo amb tu, molta sort en la recta final! Carla! Juntes també ens hem desfogat i ens hem donat suport, gràcies i ànims que ja casi ho tens! Natalia, Laura, Jose, Jordi, Cristina, Rafa, Patricia, Óscar, Eva i companyes del segon i tercer despatx.. Aida, Patricia, Thais, Gemma, Olga, Maria, Neus... gràcies pels bons moments compartits i pel suport, he après molt de tots vosaltres. També vull destacar la sort que he tingut de compartir amistat amb dues persones molt especials, la Laia i la Neus. Laia, ja des de ben aviat que vam connectar i ha estat clau tenir-te aquest temps, ets una valenta i t'admiro molt! Gràcies! Neus, al final d'aquesta etapa he pogut seure al teu costat i m'has ajudat molt, m'has donat calma i suport i estic encantada d'haver-te conegut, gràcies! També vull agrair al lab de la Mara el suport que m'han donat. Gracias Mara por confiar en mi, transimitirme el interés de estudiar la discapacidad intelectual e introducirme en el necesario mundo de la divulgación científica. Linus i Julia, els meus companys de viatge, ha estat tot un plaer compartir tants moments amb vosaltres. Maria, gracias! Siempre dispuesta a echarme un

cable, ha sido un placer! Edu, sempre has tingut unes paraules d'ànims que m'han fet guanyar seguretat, gràcies!

A la Julia, al Marc i a la Berta, amb camins diferents des de sortir de Biologia Humana però sempre pendents i cuidant-nos, gràcies amics! Gemma, què dir-te, tot ho hem viscut molt juntes i no podria haver compartit aquests dies amb ningú millor que tu, gràcies! A les nenes, m'heu donat molta energia i trobades de les nostres m'han posat molt les piles! Gràcies! En especial gràcies Martona, per ser-hi sempre! Maria i Lucia, sempre pendents i transmetent ànims, gràcies! Blanca, Maria i amics de la coral, també heu estat una part clau del meu dia a dia, els dimarts cantant i rodejada de vosaltres han estat un privilegi. Marta, pels nostres moments de barri i els que ens queden. Violeta, la meva germana triada, gràcies per ser-hi!

I finalment, i el més important, gràcies família. Sobretot a vosaltres, pares. Gràcies per tot i per tant. No podria tenir més sort. M'ho heu donat tot, m'heu cuidat infinit i sempre heu cregut molt en mi i donat suport a totes les meves decisions. Heu estat un gran model a seguir i he après a gaudir del camí per molt que hagi estat complicat en més d'una ocasió. M'heu donat serenor, tranquil·litat i felicitat. Papa, gràcies per contagiar-me aquest "gaudir cada dia de les petites coses". Mama, gracias por hacer de mi la persona que soy ahora, por toda la dedicación, porque gracias a ello que soy muy feliz. Per acabar, em faré meva la frase del Jesús Vidal als Goya, ''Me gustaría tener un hijo como yo por tener unos padres como vosotros''. Gràcies!

Maria Alemany González was supported by a predoctoral fellowship “Formación Personal Investigador” (FPI) awarded by the Spanish Ministry of Economy and Competitiveness (MINECO: BES-2014-070429) during the period 2015-2019. The work presented in this thesis received financial support from MINECO´s projects SAF2013-49129-C2-2-R during the period 2015-2016 and SAF2016-80726-R during the period 2016-2019. This work also received financial support from the Foundation Jerome Lejeune (project #1419) during the period 2015-2018.

Abstract

Understanding the neural correlates of intellectual disability is still a central and unresolved problem in neuroscience. In this thesis we have unraveled several candidate neural substrates of memory impairment and rescue using a well-established mouse model of Down syndrome (DS) and three validated pro-cognitive strategies. DS is the most common form of intellectual disability and results from one of the most complex genetic perturbations that is compatible with survival, trisomy 21. DS is accompanied by abnormal neuro-architecture, deficient synaptic plasticity, and excitation-inhibition imbalance in critical brain regions for learning and memory such as the prefrontal cortex (PFC) and the hippocampus (HPC). Here, we recorded neural activity simultaneously from the PFC and HPC of trisomic Ts65Dn male and female mice and their non-trisomic littermates during quiet wakefulness, natural sleep and memory acquisition and retrieval via the novel object recognition task. Trisomic mice showed recognition memory deficits that were accompanied by hypersynchronised neural activity in the PFC and HPC and exaggerated PFC-HPC functional connectivity, particularly at theta ranges. We speculate that this pathological theta hypersynchronisation in TS mice is caused by an overinhibition as it was rescued by blocking the GABAergic system with α5IA, a $GABA_A$ receptor inverse agonist. We also assessed whether memory deficits could be caused by poor memory consolidation during sleep and found that Ts65Dn mice showed ripple alterations that predicted poor memory performance and were rescued by two

non-pharmacological pro-cognitive treatments, epigallocatechin-3-galate (EGCG) and environmental enrichment (EE). Detailed analyses of neural activity while animals were performing the memory task revealed that memory acquisition depends on PFC-to-HPC theta connectivity whereas memory retrieval depends on HPC-to-PFC low gamma connectivity. Both memory biomarkers predicted successful memory performance in healthy mice, were disrupted in trisomic mice and rescued by EGCG and EE in male and female trisomic mice, respectively. This strongly suggests that PFC-HPC theta and gamma connectivity contribute to memory acquisition and retrieval. Collectively, we identified unique neurophysiological biomarkers that are candidate cellular mechanisms underlying intellectual disability and sleep disturbances in DS. This thesis also highlights potential neural substrates of cognitive rescue taking advantage of three promising therapeutic strategies in DS.

Resumen

Comprender los sustratos neurales de la discapacidad intelectual sigue siendo un problema central y sin resolver en el campo de las neurociencias. En esta tesis doctoral hemos combinado estudios en un modelo murino de síndrome de Down (SD) con tres estrategias procognitivas validadas e identificado varios sustratos neurales que pueden explicar el déficit y la mejora cognitiva en discapacidad intelectual. El SD es la forma más común de discapacidad intelectual y surge como consecuencia de una de las perturbaciones genéticas más complejas compatibles con la supervivencia, la trisomía 21. Las personas con SD presentan anomalías en la estructura del cerebro, una plasticidad sináptica deficiente y un desequilibrio excitación-inhibición en áreas cerebrales críticas para el aprendizaje y la memoria, como la corteza prefrontal (CPF) y el hipocampo (HPC). En esta tesis hemos registrado actividad neural simultáneamente en la CPF y el HPC de ratones trisómicos Ts65Dn (TS) y sus hermanos no trisómicos, tanto machos como hembras, durante vigilia y sueño y durante la adquisición y recuperación de memoria en una tarea de reconocimiento de objetos. Los ratones trisómicos mostraron déficits en la memoria de reconocimiento de objetos que correlacionaron con una hipersincronización de actividad neural en la CPF y el HPC y un exceso de conectividad prefronto-hipocampal (PFC-HPC), predominantemente a frecuencias theta. Especulamos que esta hipersincronicidad patológica en theta está causada por una excesiva inhibición ya que se corrige bloqueando el sistema GABAérgico con α5IA, un

agonista inverso de los receptores $GABA_A$. Además, hemos explorado si los déficits de memoria podrían estar causados por una consolidación de memoria deficiente durante el sueño. Los ratones trisómicos presentaron alteraciones en los eventos "ripples" hipocampales que predijeron los déficits de memoria y se corrigieron con dos tratamientos no farmacológicos procognitivos, la epigallocatechin-3-galato (EGCG) y el enriquecimiento ambiental (EA). Un análisis detallado de la actividad neural durante la realización de la tarea reveló que la adquisición de memoria depende de conectividad CPF-a-HPC a frecuencias theta mientras que la recuperación de memoria depende de conectividad HPC-a-CPF a frecuencias gamma. Ambos biomarcadores fueron buenos predictores de los índices de memoria en ratones sanos, estaban alterados en ratones TS y se normalizaron con EGCG en machos trisómicos y con EA en hembras trisómicas. Esto sugiere que la conectividad entre la CPF y el HPC a frecuencias theta y gamma es clave para la adquisición y recuperación de memoria. En conclusión, hemos identificado biomarcadores neurofisiológicos únicos en el circuito CPF-HPC de ratones TS durante diferentes estados cerebrales que podrían subyacer las alteraciones en la adquisición y recuperación de memoria y en el sueño en el SD. Esta tesis también resalta nuevas dianas potencialmente útiles para el tratamiento de la discapacidad intelectual mediante la descripción de los sustratos neurales de tres estrategias terapéuticas prometedoras para el SD.

Table of Contents

Acknowledgements iii
Abstract ix
Table of Contents xv
List of figures xix
List of tables xxiii
1. INTRODUCTION 3
1.1. Brain oscillations 3
1.1.1. Brain oscillations in prefrontal cortex and hippocampus during behaviour and cognition 4
1.1.2. Prefronto - hippocampal communication encodes cognition 7
1.2. The prefronto – hippocampal circuit in cognitive disorders 9
1.2.1. Cognitive impairment in Down syndrome 11
1.2.2. Mouse models of Down syndrome 13
1.2.3. The Ts65Dn mouse model of Down syndrome 14
1.2.4. Cellular alterations of the prefrontal cortex and hippocampus in individuals with Down syndrome 17
1.2.5. Cellular alterations in the prefrontal cortex and hippocampus in animal models of Down syndrome 18
1.3. Pro-cognitive interventions in Down syndrome 20
1.3.1. Non-pharmacological intervention: Chronic oral epigallocatechin-3-gallate 21
1.3.2. Pharmacological intervention: acute $GABA_A$ receptor α5 subunit inverse agonist 23
1.3.3. Cognitive stimulation: Early environmental enrichment 24
2. HYPOTHESES AND OBJECTIVES 29
3. MATERIALS AND METHODS 35
3.1. Experimental mice 35

3.2. In vivo electrophysiology in freely moving mice 35
3.2.1. Surgery 35
3.2.2. Neurophysiological recordings 37
3.3. Memory assessment with the novel object recognition task ... 38
3.4. Pro-cognitive therapeutic strategies in Down syndrome 40
3.4.1. Epigallocatechin-3-gallate 40
3.4.2. $GABA_A$ α5 inverse agonist 40
3.4.3. Environmental enrichment 41
3.5. Data analyses 41
3.5.1. Power spectral analyses 41
3.5.2. Phase-amplitude coupling 42
3.5.3. Functional connectivity measures 44
3.5.4. Analyses of ripples during NREM sleep 46
3.6. Statistical analyses 46
3.7. Histology 47
4. CHAPTER I. NEURAL CORRELATES OF MEMORY IMPAIRMENT IN Ts65Dn MICE 51
4.1. Prefronto-hippocampal circuit alterations during quiet wakefulness and natural sleep in Ts65Dn mice 51
4.1.1. Quiet wakefulness 51
4.1.2. Natural sleep 60
4.2. Prefronto-hippocampal circuit alterations during memory acquisition and retrieval in Ts65Dn mice 70
4.2.1. Recognition memory impairment in Ts65Dn mice 72
4.2.2. Neural substrates of memory acquisition and retrieval in healthy mice 75
4.2.3 Neural substrates of memory acquisition and retrieval impairments in Ts65Dn mice 80
4.3. Prefronto-hippocampal neurophysiological biomarkers predict memory performance 85

5. CHAPTER II. NEURAL CORRELATES OF COGNITIVE AMELIORATION IN Ts65Dn MICE 93
5.1. Chronic oral treatment with epigallocatechin-3-gallate in young adult Ts65Dn male mice 93
5.2. Acute IP treatment with α5IA in old adult Ts65Dn male mice 99
5.3. Environmental enrichment in Ts65Dn female mice 106
6. DISCUSSION 123
7. CONCLUSIONS 135
8. BIBLIOGRAPHY 139

List of figures

Figure 3.2.1. Diagram of electrode implantation in the PFC and HPC of the mouse brain 36

Figure 3.5.1. Analytical strategy to measure phase-amplitude cross-frequency coupling 43

Figure 3.5.2. Taxonomy of two methods used for quantifying non-directed and directed functional connectivity 44

Figure 3.5.3. Toy scenario to illustrate phase synchronisation 45

Figure 3.7.1. Representative images of brain sections stained with Cresyl violet 47

Figure 4.1.1: General locomotor activity in Ts65Dn and WT mice during quiet wakefulness 52

Figure 4.1.10: NREM-REM-awake classification in WT mice using supervised Gaussian Naïve Bayes classifier 62

Figure 4.1.11: Oscillatory power in PFC and HPC of Ts65Dn and WT mice during NREM sleep 64

Figure 4.1.12: Hippocampal ripples in WT and Ts65Dn mice during NREM sleep 65

Figure 4.1.13: Phase synchronization of prefronto-hippocampal circuits in Ts65Dn and WT mice during NREM sleep 66

Figure 4.1.14: Oscillatory power in PFC and HPC of Ts65Dn and WT mice during REM sleep 68

Figure 4.1.15: Prefrontal and hippocampal phase-amplitude comodulograms in WT and Ts65Dn mice during REM sleep 69

Figure 4.1.16: Phase synchronization of prefronto-hippocampal circuits in WT and Ts65Dn mice during REM sleep 70

Figure 4.1.2: Mean firing rate of individual neurons in PFC and HPC of Ts65Dn and WT mice during quiet wakefulness 53

Figure 4.1.3: Mean oscillatory power in the PFC and HPC of Ts65Dn and WT male mice during quiet wakefulness 54

Figure 4.1.4: Mean oscillatory power in the PFC and HPC of Ts65Dn and WT female mice during quiet wakefulness 55

Figure 4.1.5: Prefrontal and hippocampal phase-amplitude comodulograms in Ts65Dn and WT male mice during quiet wakefulness 56

Figure 4.1.6: Prefrontal and hippocampal phase-amplitude modulation indices in Ts65Dn and WT mice during quiet wakefulness 57

Figure 4.1.7: Phase synchronization of prefronto-hippocampal circuits in Ts65Dn and WT mice during quiet wakefulness 58

Figure 4.1.8: Correlation between mean firing rate of individual neurons in PFC and locomotion in Ts65Dn and WT mice during quiet wakefulness 59

Figure 4.1.9: Example of a neural recording in a non-trisomic mouse during natural sleep 61

Figure 4.2.1: Different phases of the novel object recognition test 71

Figure 4.2.10: Network activity in the PFC-HPC circuit during object familiarization in WT and Ts65Dn mice 81

Figure 4.2.11: Network activity in the PFC-HPC circuit during the 24-hour memory test in WT and Ts65Dn mice 83

Figure 4.2.12: Network activity in the PFC-HPC circuit during the 24-hour memory test in WT and Ts65Dn specific to female mice 84

Figure 4.2.13 - Putative alterations of the PFC-HPC circuit during memory acquisition and retrieval in Ts65Dn mice 85

Figure 4.2.2: PFC and HPC activity recorded during the novel object recognition test in a WT mouse 72

Figure 4.2.3: Behavioural readouts of the NOR task in WT and Ts65Dn mice 74

Figure 4.2.4: Behavioural readouts of novel and familiar explorations in WT and Ts65Dn mice 75

Figure 4.2.5: Schematic representation of memory acquisition in the familiarization phase of the NOR task 77

Figure 4.2.6: PFC-HPC network activity during memory acquisition in WT mice 77

Figure 4.2.7: Schematic representation of memory retrieval in the 24-hour memory test of the NOR task 78

Figure 4.2.8: PFC-HPC network activity during memory retrieval in WT mice 79

Figure 4.2.9: PFC-HPC theta and gamma connectivity during memory acquisition (familiarization phase) and retrieval (24-hour memory test) in the NOR task 80

Figure 4.3.1: Correlations between PFC-HPC neurophysiological biomar-kers and memory performance in WT and Ts65Dn male mice 88

Figure 4.3.2: Correlations between PFC-HPC neurophysiological biomar-kers and memory performance in TS and WT female mice 90

Figure 5.1.1: Protocol for the behavioural and neurophysiological assessment of chronic oral EGCG treatment of as a memory enhancer 94

Figure 5.1.2: Behavioural effects of chronic oral treatment with EGCG in male mice 95

Figure 5.1.3: Effects of chronic EGCG on neural activity of the PFC-HPC circuit during quiet wakefulness and sleep 96

Figure 5.1.4: Effects of chronic EGCG on neural activity of the PFC-HPC circuit during memory acquisition and retrieval 98

Figure 5.2.1: Protocol for the behavioural and neurophysiological assessment of an acute injection of α5IA as a memory enhancer 100

Figure 5.2.2: Behavioural effects of acute α5IA in Ts65Dn mice 101

Figure 5.2.3: Acute α5IA effects on neural activity of the PFC-HPC network in Ts65Dn mice 104

Figure 5.3.1: Protocol for the behavioural and neurophysiological assessment of post-weaning environmental enrichment 107

Figure 5.3.2: Behavioural effects of environmental enrichment during post-weaning periods in WT and Ts65Dn female mice 108

Figure 5.3.3: Effects of EE on neural activity of the PFC-HPC circuit in WT and Ts65Dn female mice during quiet wakefulness 110

Figure 5.3.4: Effects of EE on neural activity of the PFC-HPC circuit in WT and Ts65Dn female mice during NREM sleep..... 112

Figure 5.3.5: Effects of EE on neural activity of the PFC-HPC circuit in WT and Ts65Dn female mice during REM sleep..... 113

Figure 5.3.6: Effects of EE on neural activity of PFC-HPC network in WT and Ts65Dn mice during memory acquisition and retrieval in the NOR task..... 115

Figure 5.3.7: Effects of EE on correlations between PFC-HPC neurophysiological biomarkers and memory performance in WT and Ts65Dn mice..... 116

List of tables

Table 1 - Behavioural, sleep, cognitive, neuromorphological and electrophysiological alterations in DS subjects and DS mouse models..... 15

Table 2 - Therapeutic approaches investigated in DS subjects and Ts65Dn mice..... 21

Table 3 - PFC-HPC network alterations in Ts65Dn mice compared to WT mice.. 85

Table 4 - Summary of the pro-cognitive and neural activity effects of the three treatments on the PFC-HPC circuit in TS mice: comparison between EGCG, α5IA and EE. 119

1. INTRODUCTION

1. INTRODUCTION

1.1. Brain oscillations

Brain oscillations, also called brain rhythms or waves, are rhythmic fluctuations of electrical activity generated by the synchronization of neuron populations organised in neural networks. Neurons in these networks experience changes of the membrane voltage that we can record as electrical signals in intracellular or extracellular unitary recordings or in extracellular local field potentials (LFP) that capture population fluctuations. Neural oscillations coordinate activity to optimize local information processing and signal communication between brain regions (Ward, 2003; Buzsáki and Watson, 2012). The mammalian brain exhibits several oscillatory rhythms that occur at different frequencies ranging from 0.05 to 500 Hz that are typically associated with different brain functions or states. The main brain oscillations occur at delta (1.5 – 4 Hz), theta (4-10 Hz), beta (10-30 Hz) and gamma (30-80 Hz) frequency ranges. These rhythms can coexist temporally in the same or different brain structures and interact with each other to encode specific physiological functions. Faster oscillations are confined to small neural populations as a result of the limited speed of neural communication (due to slow axon conduction and synaptic delays) while slow oscillations recruit a larger number of neurons (Uhlhaas et al., 2009). The relationship between anatomical architecture and oscillatory patterns force brain operations to happen simultaneously at different spatial and temporal scales. This naturally prompts that the phase of slower rhythms modulates the power of faster rhythms

(Buzsaki and Draguhn, 2004). This modulation or cross-frequency phase-amplitude coupling represents a well characterized mechanism of hierarchical organization of brain rhythms, generally described between theta and gamma oscillations.

1.1.1. Brain oscillations in prefrontal cortex and hippocampus during behaviour and cognition

Multiple studies suggest that cognition might be the consequence of frequency-specific interactions of distributed regions coordinated by rhythmic brain oscillations. Specifically, two key brain regions known to be involved in cognitive processing are the prefrontal cortex (PFC) and the hippocampus (HPC) (Helfrich and Knight, 2016).

The **PFC** consists of an interconnected set of neocortical areas broadly connected with all sensory and motor systems and subcortical structures, including the HPC. This sophisticated architecture allows the processing of different types of information needed for complex behaviours. Moreover, the PFC exerts top-down control of its targeted areas during brain processing. The PFC orchestrates task-relevant large networks and is required when cognitive control and executive function are needed (Miller, 2000). Therefore, disruptions of the PFC can compromise the encoding, consolidation, and retrieval of declarative memories (Helfrich and Knight, 2016; Headley and Paré, 2017).

The **HPC** was associated with memory 50 years ago with the case study of patient H.M., a man who became amnesic after the removal of the medial temporal lobe as a surgical intervention to treat epileptic seizures. H.M. was severely impaired in declarative memory but his perceptual, working memory and motor skill learning remained intact (Scoviille and Milner, 1957; Corkin et al., 1997). Moreover, H.M. was not able to recall memories that occurred closely before the onset of amnesia while he could recollect remote memories, suggesting that HPC-mediated memory processing occurs both during learning and consolidation of memories (Eichenbaum, 2004). The HPC is key for encoding novel experiences. In rodents, for example, damage to the HPC impairs acquisition of contextual fear memories (Kim and Fanselow, 1992). The HPC may also participate in memory consolidation, whereby memories are gradually transferred from the HPC to the cortex for long-term storage (Alvarez and Squire, 1994).

The PFC and HPC play relevant roles in both declarative learning and memory and they do so likely via neural oscillations. Delta (1.5 – 4 Hz), theta (4-10 Hz) and gamma (30-80 Hz) oscillations are the three main rhythms that contribute to cognitive processing. The PFC shows prominent **theta oscillations** during the performance of spatial tasks and PFC neurons fire in phase with hippocampal theta oscillations during spatial memory formation (Negrón-Oyarzo et al., 2018). The HPC also exhibits large amplitude theta oscillations during movement, exploration, sniffing and REM sleep. In fact, the place field-specific firing of CA1 pyramidal cells shows a theta-

phase dependence during active explorations (Csicsvari et al., 2007). **Gamma oscillations** happen throughout the cortex and in the HPC during waking and sleep and coordinate local spiking. Gamma activity in the HPC correlates with successful encoding and retrieval. Specifically, the strength of spike- gamma coherence during encoding predicts recognition in a visual preferential looking task in macaques (Siapas et al., 2005) and also correlates with memory retrieval in rodents (Trimper et al., 2017). Moreover, HPC gamma oscillations play a role in object-location memory encoding in rats (Zheng et al., 2016; Trimper et al., 2017). On the other hand, it has been demonstrated that PFC gamma oscillations are required for attentional processing (Paneri and Gregoriou, 2017).

Interestingly, gamma oscillations are modulated by the phase of ongoing slower oscillations such as delta and theta mostly in the HPC, but also in the PFC. In particular, the depolarizing phase of the theta oscillation increases local gamma oscillations (Bragin et al., 1995). Gamma oscillations nested within delta and theta cycles are believed to integrate spatially distributed local network activity forming coherent representations within large functional networks. More especifically, HPC **theta-gamma coupling** may be key for long-term memory (Tort et al., 2009), where increases during learning and predicts correct memory choices in rats. In humans, long-term memory encoding has been also associated with increased cross-frequency coupling between PFC theta and gamma oscillations (Friese et al., 2013).

Brain oscillations during **sleep** strongly contribute to consolidate and re-form important memories for long-term storage. Sleep can be divided into two physiologically distinct states with different roles in memory, slow-wave sleep (SWS or NREM) and rapid eye movement sleep (REM). NREM sleep is characterized by large slow waves (0.5 – 4 Hz) in the PFC and irregular activity in the HPC, such as **sharp wave ripples (SWRs)** (100 – 300 Hz), an intrinsic self-organized process which plays a key role in memory consolidation by reactivating HPC and cortical patterns that occurred during past experiences (Ramadan et al., 2009). In fact, SWRs also occur in quiet epochs during task performance to coordinate the replay of prior trajectories and so disrupting SWRs impairs the acquisition of memory-guided spatial navigation tasks (Ego-Stengel and Wilson, 2009). On the other hand, REM sleep resembles to waking states showing smaller-amplitude gamma waves through the PFC and prominent theta oscillations with theta-nested gamma waves in the HPC. Interestingly, increased REM sleep predicts better performance in procedural tasks in humans while deprivation of REM sleep in rats impairs memory for complex tasks, suggesting that REM sleep also plays an important role in cognition (Smith, 2001; Watson and Buzsáki, 2015).

1.1.2. Prefronto - hippocampal communication encodes cognition

Many electrophysiological, functional imaging, lesion and optogenetic studies have revealed interactions between the PFC and the HPC during a variety of behavioural tasks that are dynamically

modulated by cognitive demands. The PFC and HPC are connected **anatomically** by several direct and indirect pathways. In both rodents and primates the medial PFC receives monosynaptic projections from the ventral HPC. In addition, there is a monosynaptic projection from the PFC to the dorsal HPC in mice. In parallel with monosynaptic connections there are also several indirect routes that favour bidirectional interactions between the two structures through the nucleus reuniens (NR) of the thalamus and the lateral entorhinal cortex (Condé et al., 1995; Vertes, 2006).

In addition, the PFC and HPC are **functionally** connected. Several studies have highlighted the importance of PFC-HPC communication in brain operations that support cognitive processing including learning and memory. PFC-HPC **theta** synchrony emerges specifically during working memory demands in rats (Jones and Wilson, 2005) and increases gradually during spatial learning (Sigurdsson et al., 2010; Rosen et al., 2015; Sigurdsson and Duvarci, 2015). PFC-HPC theta interactions also play an important role in long-term memory, specifically in its consolidation and its transfer to the neocortex, as reported in (Brincat and Miller, 2015) where they found that PFC-HPC theta connectivity decreases with associative learning in monkeys. Finally, PFC-HPC theta connectivity is also involved in motivational and emotional behaviours, specifically, PFC-vHPC theta synchrony increases in anxiogenic environments (Adhikari et al., 2010), consistent with the vHPC role in emotional behaviour. On the other hand, PFC-HPC **gamma** connectivity is particularly

linked to spatial working memory (SWM), an essential feature of goal-directed actions that consists in catching relevant spatial cues and maintained them updated for a proper execution of adaptive behaviours. Specifically, PFC-HPG gamma synchrony is critical for encoding, but not for maintenance or retrieval, of spatial cues in mice and successful encoding of these cues is predicted by higher connectivity (Spellman et al., 2015). In agreement, PFC-HPC gamma connectivity in humans also correlates with memory performance in a spatial working memory task (Bähner et al., 2015). Altogether, both PFC-HPC connectivity at theta and gamma frequencies support different types of behaviours and memory in rodents, primates and humans.

1.2. The prefronto – hippocampal circuit in cognitive disorders

Many psychiatric, neurological and neurodevelopmental disorders are associated with cognitive impairment. Therefore, ”cognitive disorders” are prevalent, with a steady increase in rates in the past half-century and create conspicuous social problems in developed countries. Despite the growth in the last decade in our knowledge of brain mechanisms of cognition, there have been no major breakthroughs in the treatment of cognitive diseases. Network activities in the PFC and HPC and their interactions are disrupted in psychiatric and neurological disorders and may contribute to their pathophysiology. Most of these alterations have been described in **schizophrenia** and correlated with memory deficits. Sigurdsson et al demonstrated that the Df(16)A+- mouse model of schizophrenia

shows reduced PFF-HPC theta coherence during a spatial working memory task that predicts poor learning rate and impaired memory performance (Sigurdsson et al., 2010). Consistently, del Pino et al demonstrated that the Erbb4 mouse model of squizophrenia also shows diminished PFC-HPC theta connectivity in resting-state conditions that correlate with poor working memory performance (del Pino et al., 2013). In humans, fMRI studies in squizophrenia patients also revealed aberrant functional networks related to abnormal memory performance in working memory and episodic memory. Specifically, it has been suggested an "hypofrontality" hypothesis for working memory deficits and a frontotemporal dysconnectivity underlying episodic memory abnormalities (Carter et al., 1998; Crossley et al., 2009).

In addition, alterations in the PFC-HPC circuit have been reported in other brain disorders that concur with memory impairments such as Autism spectrum disorder (ASD) or Alzheimer's disease (AD). **Alzheimer's disease** is a progressive neurodegenerative disorder basically affecting deterioration of memory, judgment and reasoning accompanied by accumulation of extracellular insoluble beta amyloid plaques and selective synaptic and neural loss that impair PFC and HPC function. Verret L et al demonstrated that the hAPP mouse model of AD shows network hypersynchrony, primarily during reduced gamma oscillatory activity, that correlates with memory deficits in a context-dependent habituation task (Verret et al., 2012). Moreover, functional studies in humans reported that AD patients show increased activity in the right dorsal

lateral PFC and enhanced functional connectivity within the prefrontal regions during the performance of memory tasks, suggesting that AD patients may use excess neural projection in PFC to compensate impaired memory function (Horwitz et al., 1995; Grady et al., 2003; Rosano et al., 2005). Electrophysiology and fMRI studies in rodents and humans strongly suggest that the PFC-HPC circuit plays a key role in fundamental cognitive processes and that its disruption might be a common element of pathogenesis in neuronal disorders that course with memory impairments.

1.2.1. Cognitive impairment in Down syndrome

Down syndrome (DS; trisomy 21) is the most common genetic cause of intellectual disability with a prevalence of 1 over 800 live births and consists on a chromosomic alteration with total or partial triple copy -aneuploidy- of human chromosome 21 (Hsa21). DS individuals suffer cognitive deficits, but also early onset Alzheimer's disease, increased frequencies of congenital heart disease, gastrointestinal anomalies, and leukemia. Despite its prevalence, little research has been conducted to understand the biology of this syndrome and even less research has been devoted to develop cognitive therapies. This might be due to the complexity of the syndrome that involves overexpression of hundreds of genes which confers a wide variety of physical affections and neuropsychological profiles (Dierssen, 2012).

The neurocognitive profile in DS is basically characterized by deficits in the structure-function of an episodic memory network constituted by the frontal and medial temporal lobes, specifically affecting the PFC and the HPC. The main cognitive disabilities found in DS individuals affect spatial learning, language acquisition and comprehension, but memory is the most compromised cognitive domain, affecting **long-term, short-term and working memory** abilities (Pennington et al., n.d.; Chapman and Hesketh, 2000; Nadel, 2003; Abbeduto et al., 2007). With only a few exceptions, these memory abilities are impaired across DS lifespan (Godfrey and Lee, 2018). While behavioural research studies have provided a great knowledge about memory impairments in DS, functional research is needed to examine behaviour-brain relations in DS and employing analogues memory tasks for murine models of DS is key for understanding the neural underpinnings of the complex memory difficulties in DS.

Interestingly, it has been postulated that sleep disruptions could influence memory impairment in DS and that addressing them might be a strategy to improve cognitive outcomes in this population (Hoffmire et al., 2014). DS individuals suffer from upper respiratory airways alterations that contribute to obstructive sleep apnea syndrome (OSAS) and sleep fragmentation. It has been hypothesized that loss of sleep quality contributes to some of the everyday intellectual difficulties in DS people as it has been shown that non-DS population with OSAS show compromised executive function, working memory and attention and reduced metabolic

markers and atrophy in the PFC and HPC (Fernandez and Edgin, 2013). Moreover, longitudinal EEG studies indicate that DS infants spend less time in SWS and in REM sleep, show less spindle activity and excessive sleep fragmentation than non-DS infants (Ellingson and Peters, 1980). However, more research is needed to determine exactly how and when sleep contributes to cognitive outcomes in DS.

1.2.2. Mouse models of Down syndrome

For the study of the neurobiology of DS, genetically engineered animals provide a very useful tool to disentangle the mechanisms that underlie DS phenotypes. The mouse models mimic different endophenotypes of DS that range from structural and functional features to behavioral and cognitive aspects (see Table 1). In the genetic domain, mouse models of DS can be divided in two main groups, trisomic models with broad triplications or translocations of Hsa21-associated genes, such as Ts65Dn (see section below), Dp(16)1Yey/+ , Ts2Cje and Ts1Cje, and models with triplication of few extragenomic genes or a single gene. Among the second group, the transgenic TgDyrk1a mouse is of special interest because it carries one extra copy of the gene DYRK1A present in Hsa21 (Altafaj et al., 2001). DYRK1A is a major candidate gene to underlie the cognitive disability in DS. It is expressed during neurodevelopment and has a critical role in neurogenesis and neuronal differentiation (Tejedor and Hämmerle, 2011). The Dyrk1a protein is a dual-specificity tyrosine phosphorylation-regulated kinase that interacts with many substrates and proteins

involved in cellular processes relevant for cognition, such as synaptic function, and is mainly expressed in cortex, cerebellum and hippocampus (Guimera et al., 1999). As summarized in Table 1, most of DS models recapitulate several **behavioural, sleep, cognitive, neuromorphological and electrophysiological alterations** present in DS subjects. Specifically, the Ts65Dn mouse is the model that mimics more DS endophenotypes. DS mouse models show reduced attention and hyperactivity and sleep disturbances such as reduced NREM sleep and delayed sleep rebound. At the cognitive level, DS mice show many alterations ranging from disturbances in context discrimination, spatial learning and memory, working and reference memory, novel object recognition memory and operant conditioning. These mice also recapitulate DS neuro-morphological alterations such as reduced brain volume, decreased neuronal density, impaired neurogenesis, dendritic pathology and reduced synaptic density. In addition, TS mice also show aberrant overinhibition. Only a little is known from electrophysiological studies in DS, however, DS subjects show EEG abnormalities and altered event-related potentials, while most DS models show impaired HPC LTP (Rueda et al., 2012).

1.2.3. The Ts65Dn mouse model of Down syndrome

As we have reviewed in the previous section, the Ts65Dn transgenic mouse is the best characterized animal model of DS. Ts65Dn bears segmental trisomy for a distal region of murine chromosome Mmu16 that contains approximately 55% of Hsa21 conserved genes (Reeves et al., 1995).

		DS	Trisomic mouse models				DYRK1A overexpression
		Subjects	Ts65Dn	Dp(16)1Yey/+	Ts2Cje	Ts1Cje	TgDyrk1a
Behavioural alterations	Motor skills and coordination	Impaired	Delayed acquisition				Altered acquisition
	Activity and attention	Reduced attention	Hyperactivity and reduced attention			Normal activity	Hyperactivity
Sleep alterations		Sleep fragmentation	Reduced NREM and delayed sleep rebound			Delayed sleep rebound	
Cognitive alterations	Context discrimination		Impaired	Impaired			
	Spatial learning and memory	Impaired	Impaired	Impaired		Impaired	Impaired
	Working and reference memory	Impaired	Impaired				Impaired reference memory
	Novel object recognition memory	Impaired	Impaired				Impaired
	Operant conditioning		Impaired				
Neuro-morphological alterations	Brain volume	Reduced	Reduced		Reduced	Reduced	
	Neuronal density	Reduced	Reduced		Reduced	Not affected	
	Neurogenesis	Impaired	Impaired		Impaired	Impaired	
	Dendrites and dendritic spines	Impaired	Impaired		Impaired	Impaired	Impaired
	Synaptic density		Reduced			Impaired	Impaired
	Inhibition		+ Inh. – Exc. synapses + GABA neurons			Impaired	Desinhibition PFC PV+ neurons
Electrophysiology		Abnormal EEG coherence and event-related potentials	Impaired HPC LTP and disordered spiking CA1 pyramidal neurons	Impaired HPC LTP		Impaired HPC LTP	Decreased PFC firing rate and gamma power

Table 1 - Behavioural, sleep, cognitive, neuromorphological and electrophysiological alterations in DS subjects and DS mouse models. Adapted from (Rueda et al., 2012).

However, Ts65Dn present trisomy for approximately 60 Mmu17 genes contained in but non-orthologous to Hsa21 and lacks a number of Hsa21 orthologous genes present in Mmu10 and Mmu11 (Duchon et al., 2011). Despite this construct limitations, Ts65Dn mouse model is a highly valuable tool to investigate DS neuropathology as it has been described extensively at the behavioral and structural levels (Table 1). Specifically, Ts65Dn mice show delayed acquisition of motor skills, hyperactivity and reduced attention, and reduced NREM sleep together with delayed sleep rebound (Coussons-Read and Crnic, 1996; Colas et al., 2008; Powers et al., 2016) . Ts65Dn mice also show cognitive alterations that depend basically on the PFC-HPC circuit such as impaired context discrimination abilities, altered spatial learning and memory in the morris water maze (MWM), deficits in working and reference memory and impaired recognition memory in the novel object recognition task, a test that measures the ability to discriminate object novelty versus familiarity (Escorihuela et al., 1998; Hyde et al., 2001; Hunter et al., 2003; Fernandez and Garner, 2008). Moreover, most of the pro-cognitive treatments assessed in DS mice have been tested in Ts65Dn mice, giving further support to consider the Ts65Dn mouse model as a great tool to investigate neuropathology of DS and to assess pro-cognitive therapies in preclinical studies.

However, most of these studies have been performed in males while female are underrepresented in DS research. Importantly, there is evidence that sex differences in cognitive profiles exist in DS, as it

has been reported that DS female outperformed males on a subset of cognitive tets. However, only a few studies using the Ts65Dn mouse model have considered sex differences. As examples, female Ts65Dn mice show less basal forebrain cholinergic neurons (Kelley et al., 2014) and display higher biochemical and behavioural reaction to stress and anxiety than (Martinez-Cue et al., 2006) WT mice. Gender differences in learning responses have also been reported by Martinez-Cue et al, where they found that enriched environment only improved spatial memory acquisition in TS females while deteriorated acquisition in TS males, suggesting that gender plays a significant modulatory role (Martínez-Cué et al., 2002). Therefore, future studies should consider gender as a confounding factor in the behavioural and physiological assessment of TS mice.

1.2.4. Cellular alterations of the prefrontal cortex and hippocampus in individuals with Down syndrome

The majority of **cellular alterations** identified in the brain of DS individuals occur in the PFC and HPC. Remarkably, DS subjects show reduced density of neocortical neurons and dendritic atrophy. More specifically, dendritic branching complexity and dendritic spine densities are below euploid levels in the PFC and the HPC (Marin-Padilla, 1976; Suetsugu and Mehraein, 1980; Becker et al., 1986). This is of special interest for this thesis because dendritic spines represent the main receptive support of neurons and form the postsynaptic site for glutamatergic contacts, playing a key role in experience-dependent neuroplasticity and therefore in learning and

memory processes (Sorra and Harris, 2000; Newpher and Ehlers, 2009). From a more macroscopic perspective, neuroimaging studies using magnetic resonance imaging (MRI) have revealed smaller HPC and larger parahippocampal gyrus in DS subjects (Teipel et al., 2003; White et al., 2003). At a **functional** level, functional MRI (fMRI) studies have reported that DS individuals show widespread increased synchrony between brain regions with only a small subset of strong, distant connections showing under-connectivity. In addition, higher connectivity rates correlated with lowest performance IQ (Anderson et al., 2013). More recently, Pujol and colleagues have shown that DS individuals display higher regional connectivity in a ventral brain system involving the amygdala/anterior temporal region and the ventral aspect of the frontal cortices. On the other hand, DS individuals showed lower functional connectivity in dorsal executive networks involving dorsal PFC and anterior cingulate cortices. Interestingly, functional connectivity measures correlated with scores on adaptive behavior related to communication skills (Pujol et al., 2015)

1.2.5. Cellular alterations in the prefrontal cortex and hippocampus in animal models of Down syndrome

Cognitive deficits reported in DS mice are associated with **neuro-morphological alterations** in the PFC and the HPC (see Table 1). Specifically, Ts65Dn mice show decreased neural density in HPC CA1 (Ayberk Kurt et al., 2004) and both hippocampal and neocortical pyramidal and granule neurons show aberrant neuro-architecture. More specifically, neurons in Ts65Dn mice have

shorter and less branched dendrites and the number of spines is reduced but they are larger and exhibit larger presynaptic terminals (Dierssen, 2003; Belichenko et al., 2007).

In addition, **synaptic alterations** in TS mice also might contribute to cognitive deficits. Density of excitatory synapses is reduced in DG, CA1 and CA3, while inhibitory synapses decreased specifically in the DG (Ayberk Kurt et al., 2004), leading to a **excitatory-inhibitory imbalance** in TS mice. This imbalance of excitatory-inhibitory synapses results in an enhancement of inhibition in specific brain regions that has functional consequences in GABAergic and glutamatergic transmission (Belichenko et al., 2007). These alterations lead to aberrant synaptic plasticity, specifically to impaired long-term potentiation (LTP) and long-term depression (LTD) in the HPC (Siarey et al., 1999; Kleschevnikov et al., 2004; Costa and Grybko, 2005), raising the possibility that HPC synaptic physiology alterations contribute to failed performance on cognitive tasks in DS.

However, only a few ***in vivo*** **electrophysiology** studies in awake mice have been implemented in mouse models of DS. Ruiz-Mejias and colleagues have reported decreased firing rate and gamma power in prefrontal networks of anesthetized and awake TgDyrk1A mice accompanied by a dysfunction of cortical fast-spiking interneurons (Ruiz-Mejias et al., 2016). In addition, two studies have focused on studying network alterations underlying sleep disturbances and spatial memory impairments in DS models. First,

Colas et al. reported that Ts65Dn mice showed increased wake in the expense of NREM sleep accompanied by increased theta power in REM and NREM sleep and decreased delta power during NREM sleep measured with cortical EEG (Colas et al., 2008). More recently, Raveau and colleagues demonstrated that the trisomic Dp(16)1Yey mouse model of DS, during post-exploratory rest periods, showed disordered spiking patterns of hippocampal CA1 pyramidal neurons and less coordinated activity during sharp wave ripples (SWRs) that correlated with poorer spatial memory (Raveau et al., 2018). However, no studies have focused on investigating the neural activity patterns in the PFC-HPC circuit during sleep, including SWRs, and during memory processing in mouse models of DS

1.3. Pro-cognitive interventions in Down syndrome

So far most of the therapeutic approaches to DS have been based on treatment strategies used in other diseases such as Alzheimer's, unspecific dietary protocols or early interventions that are only effective in the short term. However, research in DS mouse models has led to a number of promising new therapies and some of them have been tested clinically in DS subjects. Some of these therapies focus on targeting neurogenesis (e.g., **environmental enrichment**, fluoxetine and lithium), others target overinhibition (e.g., **α5IA,** picrotoxin and PTZ) while another set of therapies normalize protein overexpression levels to correct detrimental effects of gene overdose such as **epigallocatechin-3-gallate** (see Table 2) (Rueda et al., 2012).

Promising cognitive therapies in DS		DS subjects	Ts65Dn
Target	Therapy		
DYRK1A overexpression	EGCG	- Improves visual recognition memory, inhibitory control and adaptive behaviour - Rescues excessive intracortical facilitation	- Rescues short-term spatial WM and recognition memory - Normalizes LTP
Overinhibition	α5IA		- Rescues spatial learning and recognition memory
Multiple (e.g. Neurogenesis)	Environmental enrichment	- Improves cognition	- Rescues spatial memory - Restores HPC synaptic plasticity - Restores neurogenesis - Reduces overinhibition

Table 2 – Therapeutic approaches investigated in DS subjects and Ts65Dn mice.

1.3.1. Non-pharmacological intervention: Chronic oral epigallocatechin-3-gallate

As mentioned above, normalizing protein overexpression levels to reverse the deleterious effects of gene overdose in DS is one pro-cognitive strategy. The best candidate is the normalization of DYRK1A overexpression which encodes a serine-threonine kinase that is expressed in the developing and adult nervous system and plays pleiotropic roles in neurodevelopment in physiological and pathological conditions. Specifically, DYRK1A overexpression leads to premature neuroprogenitor cells (NPC) differentiation and inhibition of NPC proliferation, reduces neurogenesis and increases astrogliogenesis in DS (Yabut et al., 2010). In agreement, the TgDyrk1A mouse model, which overexpresses DYRK1A only, is able to recapitulate many DS alterations (see Table 1) (Altafaj et al.,

2001). Noteworthy, reducing Dyrk1A kinase activity has proven useful to rescue some DS phenotypes. Chronic treatment with non-pharmacological epigallocatechin-3-gallate (EGCG), a major polyphenolic constituent of green tea, inhibits Dyrk1A kinase activity and ameliorates cognition in both DS subjects and models. Importantly, EGCG-treated DS subjects for 12 months exhibited improved visual recognition memory, inhibitory control and adaptive behaviour (de la Torre et al., 2016). More recently, preclinical studies showed that EGCG-treated Fragile X syndrome patients also exhibited improved visual episodic memory and functional competences (de la Torre et al., 2019). In Ts65Dn mice, oral chronic administration of EGCG in the drinking water rescued spatial learning deficits in the MWM and object recognition memory impairment in the NOR task (Table 2) (De La Torre et al., 2013; Catuara-Solarz et al., 2016). In addition, EGCG also rescued visuospatial learning, reference memory and object recognition memory impairment in TgDyrk1A mice (De la Torre et al., 2014).

In addition, EGCG-treated DS subjects exhibited higher regional functional connectivity in the frontal cortex and rescued excessive intracortical facilitation, suggesting that EGCG might improve cognitive abilities via the normalization of over-excitability in the cerebral cortex (de la Torre et al., 2016). Complementary studies in DS models helped to further elucidate candidate underlying mechanisms of EGCG pro-cognitive effects. EGCG rescued brain morphological alterations in TgDyrk1A mice while prevented premature neuronal maturation and normalized HPC long-term

potentiation (LTP) in Ts65Dn mice, suggesting that EGCG might alleviate cognitive impairments in DS by modulating synaptic plasticity deficits (Xie et al., 2008).

1.3.2. Pharmacological intervention: acute $GABA_A$ receptor α5 subunit inverse agonist

Pharmacological interventions have been also considered to mitigate cognitive impairments through the correction of the excitatory-inhibitory imbalance, that has been attributed to underlie abnormal brain function in individuals with DS. Accordingly, several pharmacological interventions that aimed to reduce GABAergic transmission have provided promising preclinical results in the cognitive domain in DS mouse models. Non-competitive $GABA_AR$ antagonists (e.g. PTX, PTZ and Bilobalide) can restore impaired DS phenotypes in mice but produce convulsant side effects that preclude their use for therapeutic interventions in DS individuals (Contestabile et al., 2017). As an alternative to $GABA_AR$ antagonists, Braudeau and colleagues evaluated the pro-cognitive effects of an inverse agonist selective for the $GABA_A$ receptor subunit α5-subtype (α5IA), largely expressed in the HPC, and showed that α5IA restored spatial learning and recognition memory deficits in Ts65Dn mice and enhanced learning-evoked immediate early gene products in the HPC, perirhinal and posterior cingulate cortices (Braudeau et al., 2011) (Table 2). In addition, α5IA potentiates LTP in healthy mouse hippocampal slices (Dawson et al., 2005). Altogether, these results suggest that α5IA

might improve learning and memory deficits by correcting over-inhibition and LTP deficits in Ts65Dn mice.

1.3.3. Cognitive stimulation: Early environmental enrichment

DS phenotypes can be also be ameliorated by cognitive stimulation. In fact, early intervention programs are the main available therapy at the moment for DS and are focused on infants and young individuals. **Early intervention programs** are aimed at providing cognitive stimulation and special education to impulse children's developmental skills, such as speech, language and nonverbal communication, motor and problem-solving abilities, attention, learning and memory. Several studies have shown that early intervention programs have beneficial effects on children and young adults with DS that develop faster skill acquisition, less abnormal patterns of functioning, better communication and social inclusion and better executive function (Engevik et al., 2016; Guralnick, 2016). Moreover, the combination of cognitive and physical exercise improves health and wellbeing in DS adults (Heller et al., 2004; Morgan et al., 2004).

Environmental enrichment (EE) is the main paradigm used to study the effects of experience and environmental stimulation in experimental settings. It consists in housing mice in a large cage with a combination of social and cognitive stimulation. EE housing requires multiple number of animals with varying sets of toys that are changed regularly to promote novelty (HEBB and DO, 1947).

Some studies have demonstrated that EE not only improves learning and memory but also increases brain weight, neurotransmitter content, synaptic plasticity, dendritic spine growth, as well as promotes adult hippocampal neurogenesis, all associated with cognitive enhancement (van Praag et al., 2000; Baroncelli et al., 2009, 2010; Voss et al., 2013). From a functional perspective, EE enhances gamma oscillations and increases interhemispheric asymmetry in the HPC in rats (Shinohara et al., 2013).

Relevant to this thesis, post-weaning mice under EE conditions show better spatial memory in the MWM in Ts65Dn female mice but not in their male counterparts (Martínez-Cué et al., 2002). Intriguingly, in enriched non-trisomic mice pyramidal cells are markedly more branched and more spinous than non-enriched controls but EE has little effects on the morphology of cortical and hippocampal neurons in Ts65Dn mice (Dierssen, 2003). Finally, EE during adulthood reduces brain inhibition levels and promotes the recovery of spatial memory abilities and hippocampal synaptic plasticity in Ts65Dn mice (Begenisic et al., 2011).

2. HYPOTHESES AND OBJECTIVES

2. HYPOTHESES AND OBJECTIVES

Significance

The main aim of this thesis is to unravel the neural substrates of intellectual disability to find new avenues for cognitive amelioration in brain disorders. We address this question in two different and complementary ways: first, we investigate the neural substrates of memory impairment in a well-established mouse model of Down syndrome and second, we investigate the neural substrates of memory amelioration by three largely distinct therapeutic strategies

Hypotheses

(1) Neural mechanisms in the prefronto-hippocampal circuit are abnormal in Ts65Dn mice during distinct brain states becoming major contributors to their cognitive impairment.

(2) Abnormal ripples during NREM sleep contribute to memory impairment in TS mice.

(3) Recognition memory acquisition and retrieval are encoded by neural activity of the prefronto-hippocampal circuit in healthy mice.

(4) Ts65Dn mice exhibit alterations in the prefronto-hippocampal circuit that prevent proper memory processing.

(5) Promising cognitive therapies proven to be useful to ameliorate intellectual disability in Down syndrome influence key neurophysiological biomarkers of the prefronto-hippocampal circuit.

Objectives

The specific aims of this thesis are:

1. To identify abnormal neural activity patterns in the prefronto-hippocampal circuit of Ts65Dn mice relative to their non-trisomic littermates in three different brain states: quiet wakefulness, NREM and REM sleep.

2. To unravel distinct pathological neural activities in males versus females Ts65Dn mice and understand how these evolve with age.

3. To decipher the contribution of the prefronto-hippocampal circuit in the neural mechanisms of memory acquisition and retrieval in non-trisomic healthy mice.

4. To understand how anomalous neural activity in the prefronto-hippocampal circuit cause deficient memory acquisition and retrieval in Ts65Dn mice.

5. To determine the neural mechanisms of memory amelioration by three distinct pro-cognitive strategies in Ts65Dn mice:

    a. Epigallocatechin-3-galate
    b. $GABA_A$ α5 inverse agonist
    c. Environmental enrichment

3. MATERIALS AND METHODS

3. MATERIALS AND METHODS

3.1. Experimental mice

Ts65Dn mice and their wild-type littermates were obtained by repeated backcross of B6EiC4Sn.BLiA-Ts(1716)65Dn/DnJ females with C57BL/6 × 6JOlaHsd (B6C3F1/OlaHsd) hybrid males. The parental generation was obtained from the Jackson Laboratory (Bar Harbor, ME) and a colony was generated and maintained at the Barcelona Biomedical Research Park (PRBB) Animal Facility. Mice were genotyped using multiplex PCR detecting the fusion product between chromosome 16 and 19 in trisomic mice and ~25% of the offspring presented trisomy. All procedures had authorization from the PRBB Animal Research Ethics Committee and the local government (Generalitat de Catalunya), and were carried out in accordance with the guidelines of the European Union Council (2003/65/CE) and Spanish regulations (BOE 252/34367-91, 2005).

3.2. In vivo electrophysiology in freely moving mice

3.2.1. Surgery

We used stereotrodes (two-wire electrodes) to record neural activity. Stereotrodes were custom made using 25 μm tungsten wire (Advent Research Materials, UK) and twisted with an electrode twister designed by Open Ephys. Electrode insulation was achieved using a heat gun and tips were welt to golden pins. Mice were induced with a mixture of ketamine/xylacine and placed in a stereotaxic apparatus. Anesthesia was maintained with continuous 0.5-4% isofluorane. Small craniotomies were drilled above the

medial PFC and HPC. Five micro-screws were screwed into the skull to stabilize the implant, and the one on top of the cerebellum was used as a general ground. Three tungsten electrodes, one stereotrode and one single electrode (we used one of the electrodes of a stereotrode), were implanted in the prelimbic region of the medial PFC (AP: 1.5, 2.1 mm; ML: ± 0.6, 0.25 mm; DV: -1.7 mm from bregma) and three more were implanted in CA1 region of the HPC (AP: -1.8, 2.5 mm; ML: -1.3, 2.3 mm; DV: -1.15, 1.25 mm). The recorded hemisphere was randomly chosen in each animal. In addition, three reference electrodes were implanted in corpus callosum and lateral ventricles (AP: 1, 0.2, -1; ML: 1, 0.8, 1.7; DV: -1.25, -1.4, -1.5, respectively). At the time of implantation, the electrodes had impedances that ranged from 100 to 400 kOhm. After surgery animals were allowed at least one week to recover during which they were extensively monitored and received both analgesia and anti-inflammatory treatments. Additionally, animals were handled and familiarized with the implant connected to the recording cable. Implanted mice were individualized in home cages from the day of surgery to prevent the implants from being damaged over the recovery week and during the experimental days.

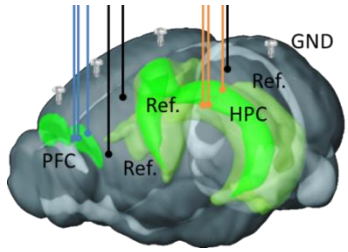

Figure 3.2.1. Diagram of electrode implantation in the PFC and HPC of the mouse brain.

3.2.2. Neurophysiological recordings

We recorded single-unit activity (SUA) and local field potentials (LFPs) in freely-moving mice with the multi-channel Open Ephys system at a sampling rate of 30 kHz with Intan RHD2132 amplifiers equipped with an accelerometer. We used the accelerometer´s signals in the X, Y and Z axis to monitor locomotion. We quantified the variance of the instantaneous acceleration module (Acc; variance (Root square[X2, Y2, Z2])) that was maximum during exploration and decreased as the animals were in quiet alertness and natural sleep. Recorded signals from each electrode were filtered offline to extract SUA and LFPs. SUA was estimated by first subtracting the raw signal from each electrode with the signal from a nearby referencing electrode to remove artifacts related to animals´ movement. Next, referenced signals were filtered between 450-6000 Hz and the spikes from individual neurons were sorted using principal component analysis with Offline Sorter v3 (Plexon Inc.). To obtain LFPs, signals were detrended, notch-filtered to remove 50 Hz artifacts and down-sampled to 1 kHz with custom-written scripts in Python. Signals were then imported into MATLAB (MathWorkds, Natick, MA) where all LFP-related analyses were implemented. The frequency bands considered for the band-specific analyses included delta (1-4 Hz), theta (8-12 Hz), beta (15-25 Hz), low gamma (30-50 Hz), and high gamma (50-80 Hz). High frequency oscillations (HFO, 100-200 Hz) were also considered during sleep (see below).

3.2.2.1. Quiet, NREM and REM sleep

Recordings during quiet wakefulness were performed with animals constrained in a small box (12 cm * 8 cm) that allowed them to move but not to walk. Recordings during natural sleep were implemented following the familiarization phase of the NOR task to better capture neural signals related to memory consolidation. Accelerometer measures and LFP signals from the PFC and the HPC were used to identify epochs of REM and NREM sleep. NREM sleep was behaviourally defined as presenting stillness (low amplitude variations of the accelerometer), eyes closed and large amplitude slow oscillations in the PFC and HPC. Only periods of deep NREM sleep prior to REM episodes were considered for analysis. REM epochs were defined as stillness, eyes closed and prominent hippocampal theta rhythms.

3.3. Memory assessment with the novel object recognition task

We tested long-term recognition memory using a well-established non-operant task that relies on mice innate instinct to explore novel objects in the environment (Leger et al., 2013). The test was implemented in three phases: habituation and familiarization during the first day and long-term memory test 24 hours after familiarization (Fig. 3a). Mice were first habituated to an empty maze for 10 min. Five minutes later, mice were placed again in the maze where they could explore two identical objects located at the end of the two lateral arms for 10 min. Twenty-four hours later, in

the test phase, mice were presented with one familiar and one novel object for 10 min. Memory acquisition was investigated during the familiarization phase by comparing neural signals during the first 5 explorations (early explorations) versus the last 5 explorations (late explorations) of the session irrespective of side. Memory retrieval was investigated during the 24-hour memory test by comparing neural signals during explorations of familiar versus novel objects. We used a custom-designed T-maze (8 cm wide x 30 cm long x 20 high) made of aluminium, that was located on an aluminium platform and grounded for electrophysiological recordings. The novel-familiar object pairs were previously validated as in (Gulinello et al., 2018) and mice were always tested with different pairs of objects in different experiments (e.g., pre- vs. post-EGCG periods). The arm of the maze where the novel object was placed was randomly chosen across experiments. Any investigative behaviour with the objects such as head orientation or sniffing at a distance of <= 2 cm or when touching with the nose was considered object exploration. Exploratory events were detected online using a custom-designed joystick with a right and left button that were pressed continuously during the time of explorations. Button presses were automatically aligned to the electrophysiological file by sending TTL pulses to the acquisition system. In addition, each session was videotaped via a videocamera located on top of the maze. Object recognition memory was defined by the discrimination index (DI), the exploration time for the novel object minus the exploration time for the familiar object divided by the total amount of exploration of both objects.

$$DI = \frac{[\textbf{Novel}\ \text{Object Exploration Time} - \textbf{Familiar}\ \text{Object Exploration Time}]}{\textbf{Total}\ \text{Exploration Time}}$$

Discrimination indices vary between +1 and -1, where a positive score indicates more time spent with the novel object, a negative score indicates more time spent with the familiar and a zero score indicates a null preference (Leger et al., 2013).

3.4. Pro-cognitive therapeutic strategies in Down syndrome

3.4.1. Epigallocatechin-3-gallate

Young-adult male mice were administered EGCG in drinking water for one month. EGCG solution was prepared freshly from a green tea leaf extract [Mega Green Tea Extract, Decaffeinated, Life Extension®, USA; 45% EGCG content (326.25 mg) per capsule] every 3 days (EGCG concentration: 90 mg/mL for a dose of 2–3 mg per day).

3.4.2. $GABA_A$ α5 inverse agonist

Old-adult male mice were administered 3-(5-methylisoxazol-3-yl)-6-[(1-methyl-1,2, 3-triazol-4-yl)methyloxy]-1, 2, 4-triazolo[3, 4-a]phthalazine (a5IA). It was synthesized by Orga-Link SARL (Magny-les-Hameaux, France), according to Sternfeld et al. (2004), and prepared by Marie Claude Potier (Centre de Researche de l'Institut du Cerveau et de Moelle Epinière, CNRS, Paris, France). The hydrochloride salt was prepared by dissolving first the base in

hot ethanol and later adding a solution of 5% hydrochloric acid in ethanol. After cooling, the precipitate formed was collected by filtration, washed with cold ethanol and dried (Braudeau et al., 2011c). α5IA and vehicle (solubilization solution) were injected intraperitoneally (i.p.) at a dose of 5 mg/kg.

3.4.3. Environmental enrichment

Female mice were assigned randomly to either control or enriched conditions after weaning for 7 weeks. The non-enriched environment consisted in standard Plexiglas cages (20x12x12 cm height) were mice were housed in groups of 2-3 while mice in EE conditions were housed in groups of 4-6 in a two levels (55x80x50 cm height) cage with various plastic toys that were changed every 3 days to maintain novelty. Mice had surgery during the first week after completing the rearing in both conditions and after one week of recovery were ready to start the experiments. EE mice were individualized from the day of surgery to prevent the implants from being damaged but enrichment (i.e., new toys) was maintained in their standard home cages over the recovery week and during the experimental days.

3.5. Data analyses

3.5.1. Power spectral analyses

Analyses of LFPs signals during quiet wakefulness and natural sleep were performed averaging neural signals over discrete epochs of different duration (quiet wakefulness: 3 min; NREM sleep: 1 min; REM sleep: 10 s) that were chosen based on the stability of the

brain state. For LFPs analyses during memory performance on the T-maze measures were computed only within the time windows of object exploration triggered by button presses on the joystick. Only explorations longer than 600 ms were considered. Results for each exploration were obtained by averaging 1 second non-overlapping windows. We used the multitaper fast Fourier transform method (time frequency bandwidth; TW = 5 and K = 9 tapers; 1-100 Hz range; non-overlapping sliding window of 5 seconds for power spectrum, 2 seconds for spectrograms, 1 second for object explorations) with the Chronux toolbox (Bokil et al., 2010).

3.5.2. Phase-amplitude coupling

To quantify the intensity of phase-amplitude coupling we used the modulation index (MI) described in (Tort et al., 2009). First, low frequency (delta and theta) phases were divided into 18º bins (i.e., each cycle is divided into 20 bins) and gamma (low, high gamma) and high frequency oscillations (HFO) amplitude were calculated for each phase bin. MI measures the divergence of the phase-amplitude distribution and is higher as further away is from the uniform distribution (i.e., no modulation) (Fig. 3.5.1). In order to choose specific frequency band pairs for the MI quantification we represented overall MI in two-dimensional pseudocolour comodulation maps. A warmer colour indicates coupling between the phase of the low frequency band (x axis) and the amplitude of the high frequency band (y axis) while blue depicts absence of coupling. As previously described (REFS), our MI maps showed highly selective comodulation between bands relevant for cognition.

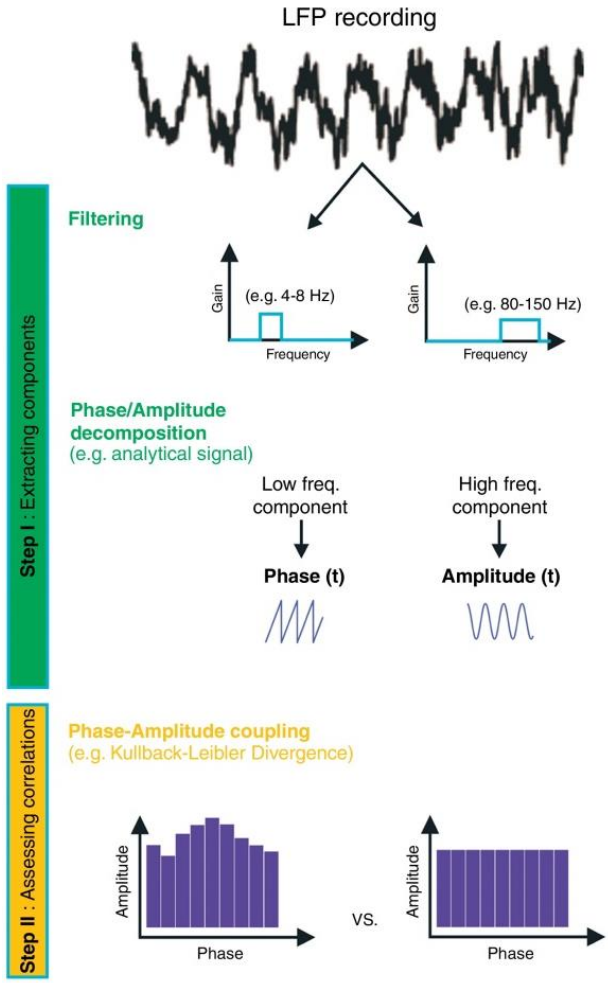

Figure 3.5.1. Analytical strategy to measure phase-amplitude cross-frequency coupling – Step 1. Band-pass filtering and extraction of phase and amplitude signals for the relevant frequency bands. **Step 2.** Assessing correlations between amplitude and phase to quantify how much the histogram of mean amplitude versus phase deviates from the uniform distribution. Figure from (Aru et al., 2015).

3.5.3. Functional connectivity measures

To quantify functional connectivity between the PFC and the HPC we used two different approaches. Non-directed connectivity was assessed using weighed phase lag index (wPLI) while directionality was explored using phase slope index (PSI).

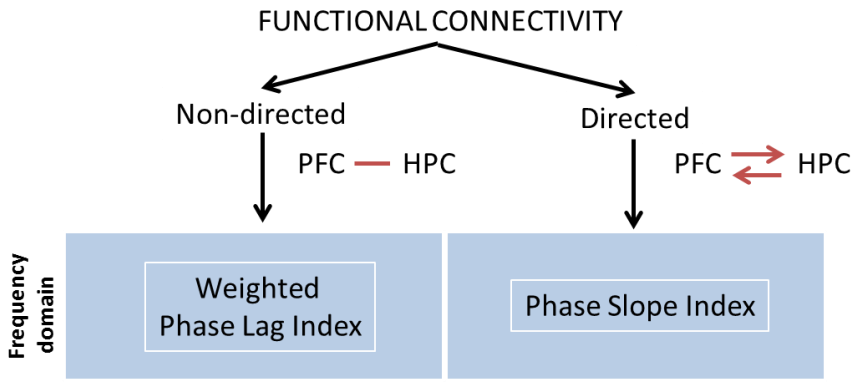

Figure 3.5.2. Taxonomy of two methods used for quantifying non-directed and directed functional connectivity. Adapted from (Bastos and Schoffelen, 2016)

3.5.3.1. Weighed Phase Lag Index (wPLI)

To assess non-directed functional connectivity between LFP signals in the PFC and HPC we used the wPLI as in (Vinck et al., 2011; Hardmeier et al., 2014), a measure of phase synchronization (Fig. 3.5.3). First, instantaneous phases from LFP signals recorded simultaneously in both areas were determined by Hilbert transformation. wPLI measures the asymmetry in the distribution of phase differences for each frequency band between the two time-series resulting in values ranging between 0 and 1, being a higher

value a high asymmetric distribution as a consequence of a consistent phase-lag between signals in the two areas. wPLI reduces the probability of detecting false positive connectivity in the case of volume conducted noise sources with near zero phase lag and shows higher sensitivity in detecting real phase synchronization.

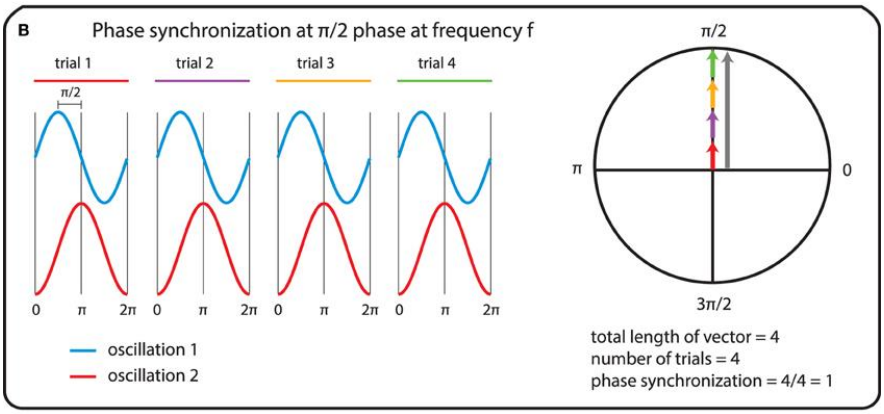

Figure 3.5.3. Toy scenario to illustrate phase synchronisation. The left panel depicts two signals (oscillation 1 and oscillation 2) that are observed for four trials and the right panel show the vector sums of the cross-spectral densities. In this scenario, the phase difference between the two oscillations is consistent across observations (90º each) showing a perfect non-zero phase synchronisation. Figure from (Bastos and Schoffelen, 2016)

3.5.3.2. Phase Slope Index (PSI)

To estimate the unidirectional flow of information between neural signals of the PFC and HPC, we used the Phase Slope Index as in (Nolte et al., 2007). PSI is a robust measure based on the conceptual temporal argument supporting that the driver is earlier than the recipient and contains information about the future of the recipient.

It quantifies the consistency of the direction of the change in the phase difference across frequencies. Given a specific bandwidth parameter, it computes for each frequency bin the change in the phase difference between close frequency bins, weighted with the coherence. Then, when phase difference changes consistently across frequencies, and there is coherence, PSI deviates from zero (Bastos and Schoffelen, 2016). Positive slope reflects an HPC-to-PFC flow of information in a specific frequency range while a negative slope reflects the opposite.

3.5.4. Analyses of ripples during NREM sleep

Raw signals were down-sampled to 1.25 kHz and bandpass filtered between 100-600 Hz. Sharp-wave ripple events were detected by thresholding (>3 SDs) the filtered signals using ripple detection scripts from Valero et al (Valero et al., 2017). Time-frequency analyses of ripples were calculated using multitaper spectral estimation in sliding windows with 97.7% overlap and frequency resolution of 10 Hz.

3.6. Statistical analyses

All data are represented as the mean +- S.E.M. We used independent T tests and nonparametric Mann-Whitney tests to compare measures across genotypes. Paired T tests and nonparametric Wilcoxon tests were used to assess effects within each genotype. To assess interactions between genotype and treatment we used two-way and repeated measures ANOVA with Bonferroni post-hoc correction when appropriate. To identify

significant correlations between neurophysiological measures and DIs, Pearson or Spearman correlations were used for parametric and non-parametric distributions, respectively.

3.7. Histology

On the last day of electrophysiological recordings, small electrolytic lesions of the recording sites were carried out via electrical stimulation of the electrodes (5 mA for 2 s) under anaesthesia. Then, mice were sacrificed and their brains extracted and preserved in 2-methylbutane. Brains were sliced into 30 μm sections with a cryostat. Electrode placements were confirmed histologically by staining the brain slices using the Nissl method. Electrodes with tips outside the targeted areas were discarded from data analyses.

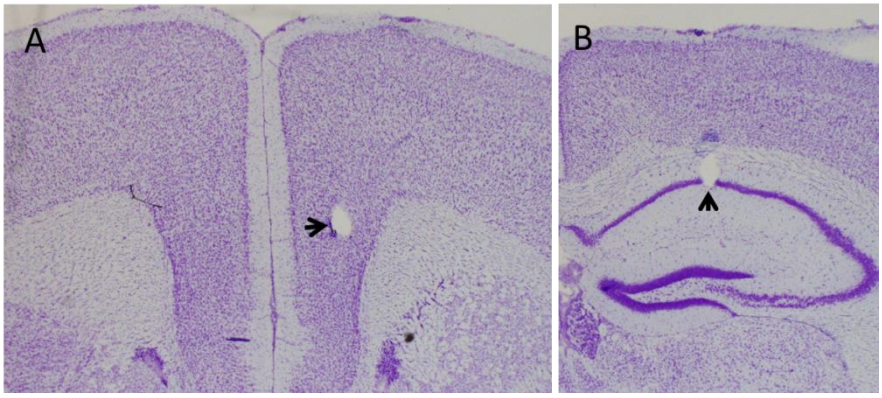

Figure 3.7.1. Representative images of brain sections stained with Cresyl violet. Arrows denote the location of electrode tips in the mPFC **(A)** and the HPC **(B)**.

4. CHAPTER I. NEURAL CORRELATES OF MEMORY IMPAIRMENT IN Ts65Dn MICE

4. CHAPTER I. NEURAL CORRELATES OF MEMORY IMPAIRMENT IN Ts65Dn MICE

In this chapter, we explore alterations in prefronto-hippocampal neural networks of Ts65Dn mice to unravel the neurophysiological correlates of memory impairment in DS. We recorded neural activity simultaneously from the PFC and HPC of Ts65Dn (TS) mice and their wild-type (WT) non-trisomic littermates during distinct brain states: quiet wakefulness, natural sleep (NREM and REM), memory acquisition and memory retrieval.

4.1. Prefronto-hippocampal circuit alterations during quiet wakefulness and natural sleep in Ts65Dn mice

4.1.1. Quiet wakefulness

We first investigated neural activity alterations in the prelimbic medial PFC and the CA1 region of the HPC of TS mice compared to their WT littermates. TS mice typically display higher locomotion rates than WT mice (Faizi et al., 2011). To control for this, recordings were carried out in a small box (animals could move but not walk) (Fig. 4.1.1A) where the two genotypes showed comparable activity as measured by accelerometer rates (independent T test; males, WT n = 10, TS n = 12 mice; P = 0.2; females, WT n = 6, TS n = 7 mice; P = 0.15) (Fig. 4.1.1B,C)

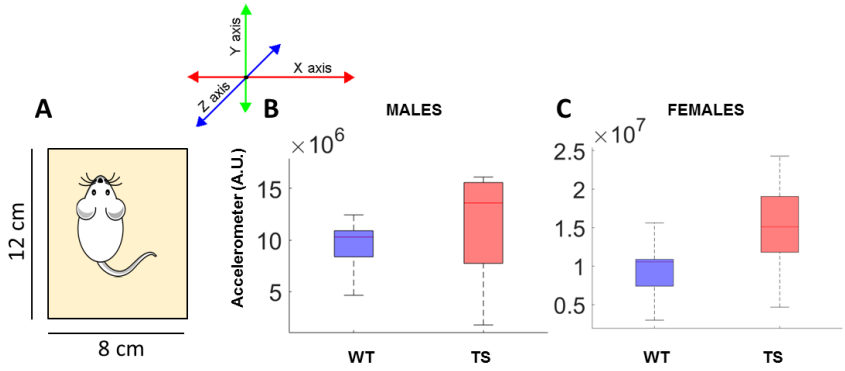

Figure 4.1.1: General locomotor activity in Ts65Dn and WT mice during quiet wakefulness – (A) Recordings during quiet wakefulness were carried out in a box of 12 x 8 cm where animals could move but not walk. **(B)** Mean locomotion (variance of the acceleration module) of alert WT (blue) and TS (red) male and **(C)** female mice. Data are represented as mean ± S.E.M. in all figures. A.U. arbitrary units.

During quiet wakefulness individual prefrontal neurons showed increased spiking rates in TS male mice than WT mice (independent T test, P = 0.03), whereas in HPC they were moderately reduced (P = 0.05) (Fig. 4.1.2A). TS female mice showed increased spiking rates in PFC and HPC (P = 0.02 for both areas) (Fig. 4.1.2B). TS males also showed larger power of theta oscillations (8-12 Hz) in both PFC and HPC (P = 0.04 for both areas), and in the HPC theta rhythms were slightly faster (WT = 7.55 ± 0.15, TS = 8.07 ± 0.16 Hz; P = 0.03) (Fig. 4.1.3). We note that amplified theta in PFC and HPC did not correlate with animals general mobility (n = 22 mice; ACC; [PFC] R = 0.17, P = 0.44; [HPC] R = 0.25, P = 0.24). The power of gamma oscillations was only slightly higher in TS mice in the HPC (WT vs TS gamma power; unpaired T test, P = 0.17 and P = 0.21 for low and high gamma, respectively).

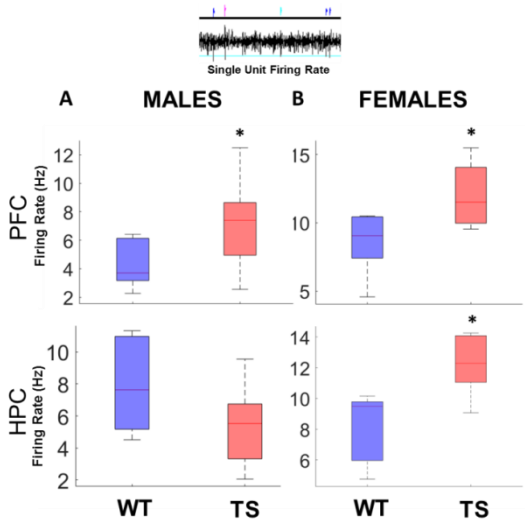

Figure 4.1.2: Mean firing rate of individual neurons in PFC and HPC of Ts65Dn and WT mice during quiet wakefulness – (A) Mean firing rate of single units in PFC (upper panels) and HPC (lower panels) for WT (blue) and TS (red) male and **(B)** female mice. *p ≤ 0.05, **p ≤ 0.01, ***p ≤ 0.001 in all figures.

TS females showed more pronounced alterations in oscillatory power than TS males, including a greater increase of theta power in PFC and HPC (P = 0.02 for both areas) (Fig. 4.1.4). In addition, they also showed augmented power of PFC low gamma (30-50 Hz) (P = 0.01) and HPC beta (18-25 Hz) (independent T test; P = 0.004), low gamma (30-50 Hz) (P = 0.005) and high gamma (50-80 Hz) (P = 0.009) oscillations relative to WT female mice (Fig. 4.1.4).

Previous studies have suggested that lower-to-faster amplitude modulation is involved in information processing such as memory encoding.

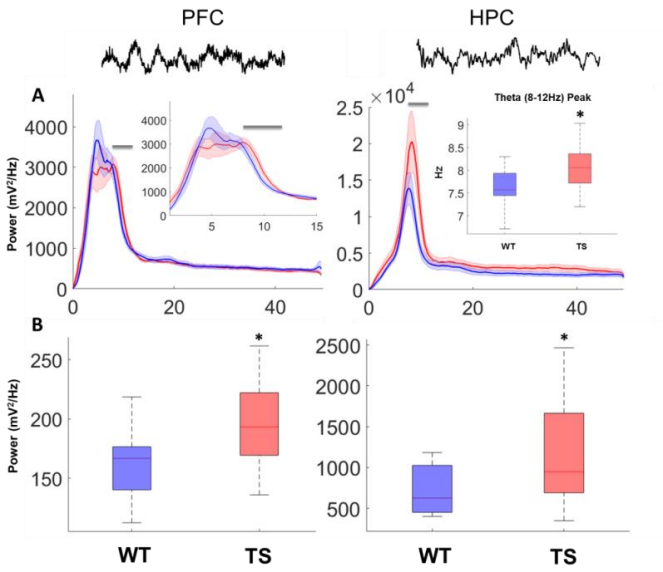

Figure 4.1.3: Mean oscillatory power in the PFC and HPC of Ts65Dn and WT male mice during quiet wakefulness – (A) Power spectra of signals in PFC and HPC in WT and TS mice. Grey bars mark significant differences between genotypes. Insets show amplification of power spectra at lower frequencies (left) and quantification of HPC mean theta peak frequency (right). **(B)** Theta power (8-12 Hz) in PFC and HPC. Above, representative traces from LFPs simultaneously recorded from the PFC and HPC in one mouse during quiet wakefulness.

For example, theta and gamma oscillations co-occur and interact with each other. Gamma amplitude is strongly modulated by the theta phase (Nyhus and Curran, 2010) and, in fact, theta-gamma coupling in the HPC may be key for associative memory (Tort et al., 2009). So, we next examined the phase-amplitude cross-frequency coupling (CFC) between lower frequencies and higher frequencies in the PFC and the HPC. More specifically, we quantified the phase-amplitude modulation index (MI) of delta and theta oscillations with gamma and high frequency oscillations (100-200 Hz).

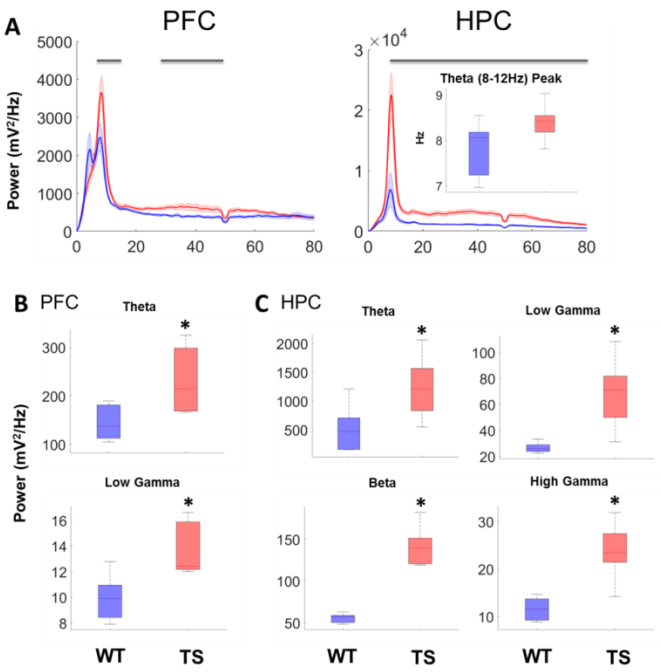

Figure 4.1.4: Mean oscillatory power in the PFC and HPC of Ts65Dn and WT female mice during quiet wakefulness – (A) Power spectra of signals in PFC and HPC of WT (blue) and TS (red) mice. Inset shows HPC mean theta peak frequency. **(B)** PFC LFP power at theta and low gamma and **(C)** HPC LFP power in theta, beta, low gamma and high gamma in WT and TS.

We represented the overall MI in two-dimensional comodulation maps for both regions and genotypes. A warmer colour indicates coupling between the phase of the low frequency band (x axis) and the amplitude of the high frequency band (y axis) while blue depicts absence of coupling (Fig. 4.1.5). TS male mice exhibited increased delta-high gamma modulation in PFC compared to WT mice (independent T test, P = 0.04) (Fig. 4.1.6A) while TS female mice did not (P = 0.52) (Fig. 4.1.6B).

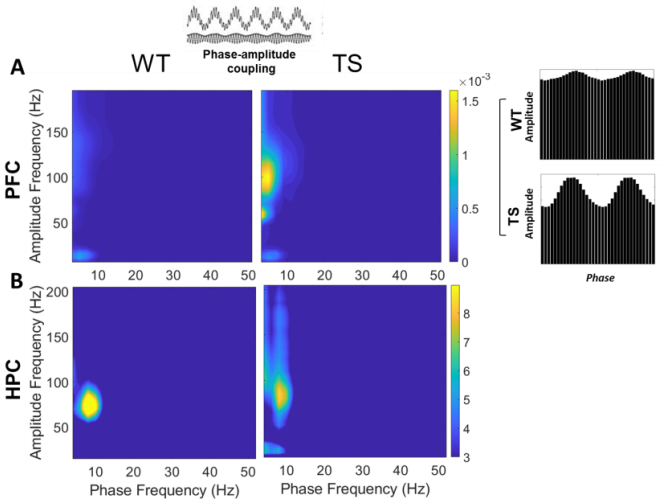

Figure 4.1.5: Prefrontal and hippocampal phase-amplitude comodulograms in Ts65Dn and WT male mice during quiet wakefulness – (A) Mean phase-amplitude comodulogram map of WT and TS mice and two representative genotype examples of gamma amplitude modulation by theta phase in PFC. **(B)** Mean phase-amplitude comodulogram map of WT and TS mice in HPC.

In HPC, theta-low gamma coupling and theta-high frequency (HFO) coupling was consistently stronger in both TS male ($P = 0.03$ for both couplings) and female mice ($P = 0.02$ for both couplings) (Fig. 4.1.6A,B). These results unravel an aberrant local hypersynchronisation in the PFC and HPC of TS mice.

We next investigated the dynamics of long-range connectivity between the PFC and the HPC. We measured PFC-HPC synchrony using weighted phase lag index (wPLI), a measure of phase synchronization between LFP signals that minimizes the effects of volume-conduction, noise and sample size (Vinck et al., 2011).

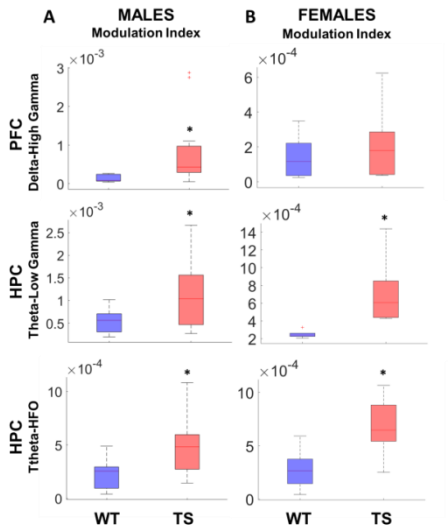

Figure 4.1.6: Prefrontal and hippocampal phase-amplitude modulation indices in Ts65Dn and WT mice during quiet wakefulness – (A) PFC delta-gamma MI, HPC theta-high gamma and -HFO MI in WT and TS male and **(B)** female mice.

Both male (Fig. 4.1.7A) and female (Fig. 4.1.7B) TS mice showed increased PFC-HPC connectivity during quiet wakefulness compared to their WT littermates. Specifically, TS male mice showed robust increases of PFC-HPC phase synchronization at delta (independent T test; P = 0.03), theta (P = 0.01) and beta (P = 0.03) frequencies (Fig. 4.1.7C). On the other hand, TS female mice showed augmented theta (P = 0.07), beta (P = 0.04), low gamma (P = 0.002) and high gamma (P = 0.004) frequencies (Fig. 4.1.7D). So, excessive PFC-HPC long-range synchronization may contribute to trisomic phenotypes.

Finally, we investigated whether neural activity biomarkers could predict locomotor activity in TS mice. TS mice are hyperactive and,

although not significant, general mobility (i.e., accelerometer rate) was slightly higher in our TS mice relative to WT mice during quiet wakefulness (Fig. 4.1.1A).

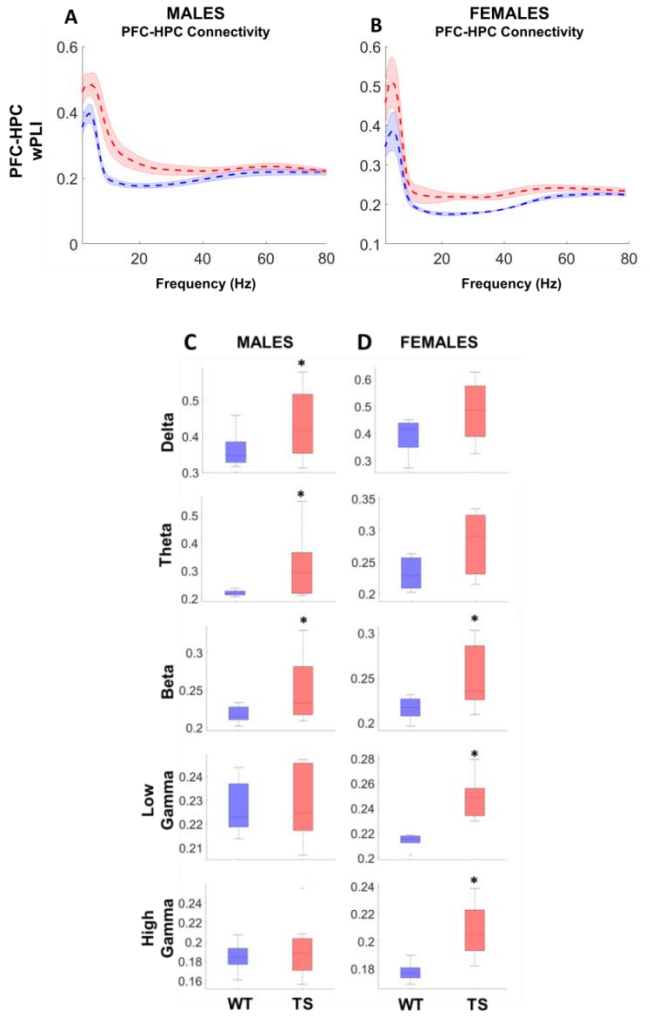

Figure 4.1.7: Phase synchronization of prefronto-hippocampal circuits in Ts65Dn and WT mice during quiet wakefulness – (A) Mean weighted phase lag index (wPLI) between PFC and HPC in WT and TS male and **(B)** female mice. **(C)** PFC-HPC wPLI at delta, theta, beta, low gamma and high gamma in WT and TS male and **(D)** female mice.

Firing rate of individual neurons in PFC was the only abnormal measure that correlated specifically with movement in TS mice. It correlated positively with accelerometer rates in both TS male (Correlation; R = 0.63, P = 0.03) and female (R = 0.89, P = 0.03) mice, but not in WT mice (males: R = -0.55, P = 0.15; females: R = 0.17, P = 0.74) (Fig. 4.1.8). Previous studies have reported that lesions of the PFC produce impulsivity and locomotor hyperactivity, suggesting that PFC is particularly important for behavioural inhibition (Brennan and Arnsten, 2008). Along these lines, we speculate that PFC excessive firing rates may affect the execution of top-down commands and compromise attention and behavioural inhibition in TS mice.

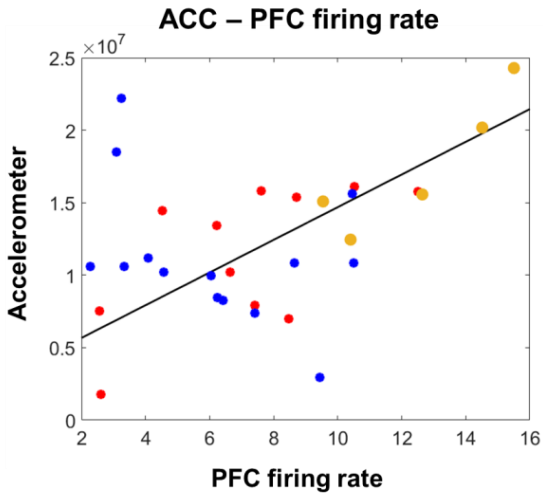

Figure 4.1.8: Correlation between mean firing rate of individual neurons in PFC and locomotion in Ts65Dn and WT mice during quiet wakefulness – Correlation between the variance of the accelerometer module and PFC firing rates. Black line, linear regression of data from TS male (R = 0.63; red dots) and female (R = 0.89; orange dots) mice. Blue dots represent WT mice.

4.1.2. Natural sleep

We also investigated abnormal prefronto-hippocampal neuro-dynamics during sleep. Sleep is involved in memory consolidation and requires the interaction of numerous brain structures including the PFC and the HPC. Natural sleep is divided in two distinct states known as slow-wave sleep (SWS or NREM) and rapid eye movement sleep (REM). These two states appear in cyclical and stereotyped patterns during a given episode of sleep. A light form of NREM sleep first emerges that progresses into deeper NREM states with larger slow waves (0.5-4 Hz). Later, there are retreats back to superficial NREM epochs but each sleep cycle concludes with a REM sleep episode. During NREM sleep the HPC generates high-frequency oscillations, known as sharp-wave ripple (SPW-R) complexes, which have been proposed to promote synaptic plasticity necessary for memory consolidation (Buzsáki, 1986). REM-associated LFPs are similar to those of the wake state, with prominent theta oscillations and theta-nested gamma waves in the HPC accompanied by smaller amplitude gamma waves in the neocortex (Watson and Buzsáki, 2015). We recorded LFPs in WT and TS mice during natural sleep and later classified NREM and REM epochs based on the neurophysiological biomarkers mentioned above (PFC slow waves, HPC theta oscillations) combined with accelerometer rates (near zero during sleep) and video recordings (Fig. 4.1.9).

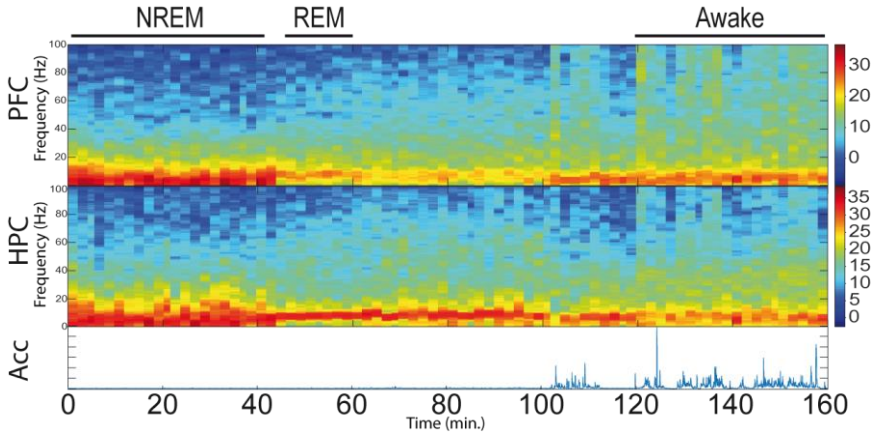

Figure 4.1.9: Example of a neural recording in a non-trisomic mouse during natural sleep - Spectrogram of PFC and HPC LFP during natural sleep in a WT mouse containing awake, NREM and REM epochs. Instantaneous acceleration module (Arbitrary Units) is shown below.

In addition, we built a supervised classifier based on the Gaussian Naïve Bayes Classifier algorithm to discriminate between awake, NREM and REM stages in WT mice. First, we evaluated which pairs of PFC and HPC neural features were more powerful to discriminate between the three brain states. We found that the highest classification accuracies were achieved using PFC delta with high gamma activity (Fig. 4.1.10A) and PFC low-gamma with HPC theta activity (Fig. 4.1.10B), underscoring that PFC delta and gamma activity and HPC theta are great biomarkers for sleep scoring. The model was able to generalize and successfully predict brain states in other WT mice (Fig. 4.1.10C).

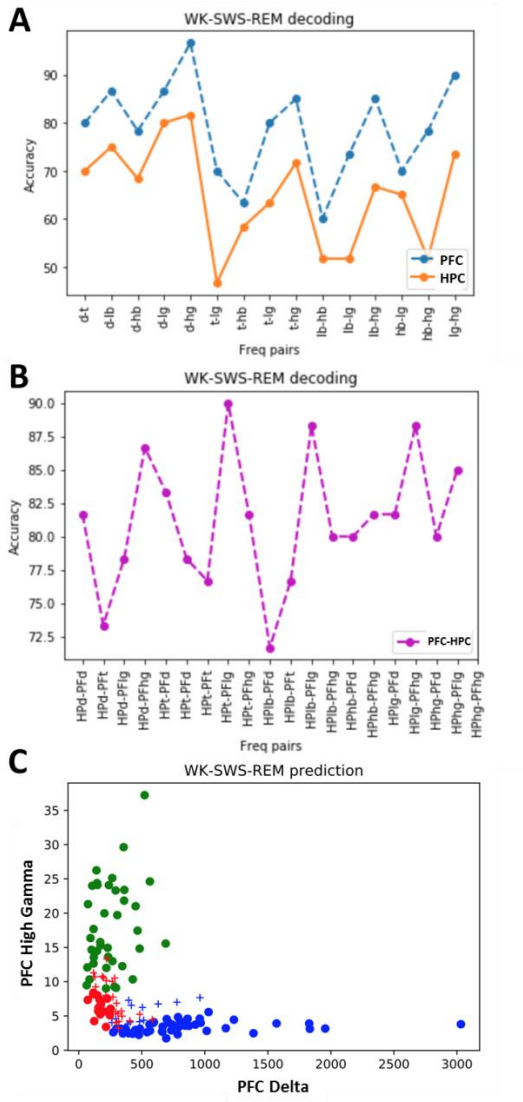

Figure 4.1.10: NREM-REM-awake classification in WT mice using supervised Gaussian Naïve Bayes classifier -(A) Comparison of accuracies between neurophysiological feature pairs within the PFC (blue) and the HPC (orange) and **(B**) between the PFC and the HPC that better discriminate between awake, NREM and REM sleep. **(C**) Trained model using PFC delta and high-gamma power classifies successfully awake-NREM-REM states in one WT mouse.

However, we performed manual sleep scoring in our analyses to avoid misleading classifications due to genotype differences in neural activity.

4.1.2.1. NREM sleep

During NREM sleep, PFC activity exhibits large amplitude slow waves while HPC neural signals are dominated by short high-frequency oscillations (~100 ms, 100–250 Hz) referred to as sharp wave ripples (SWRs). Relevant to this study, PFC and HPC NREM-associated neural rhythms, and particularly SWRs, may be critical for offline information processing including memory consolidation (Buzsáki, 2015). TS male mice showed smaller slow waves (i.e., reduced power below 4 Hz) and increased low gamma activity in PFC compared to their WT littermates (WT n = 9, TS n = 11 mice; independent T test; P = 0.03 and P = 0.01, respectively) (Fig. 4.1.11A,B). On the other hand, TS female mice showed also increased low and high gamma activity in PFC (WT n = 6, TS n = 7 mice; independent T test; P = 0.02 and P = 0.006, respectively) as well as in the HPC (P = 0.01 for both) (Fig. 4.1.11C,D).

We additionally detected ripple events in the HPC and compared several of their features across genotypes (Fig. 4.1.12A). The number of ripples per minute was not significantly different between genotypes (independent T test; P = 0.63). However, in males, TS ripples occurred at lower frequencies (P = 0.03) and were larger in amplitude (P = 0.04).

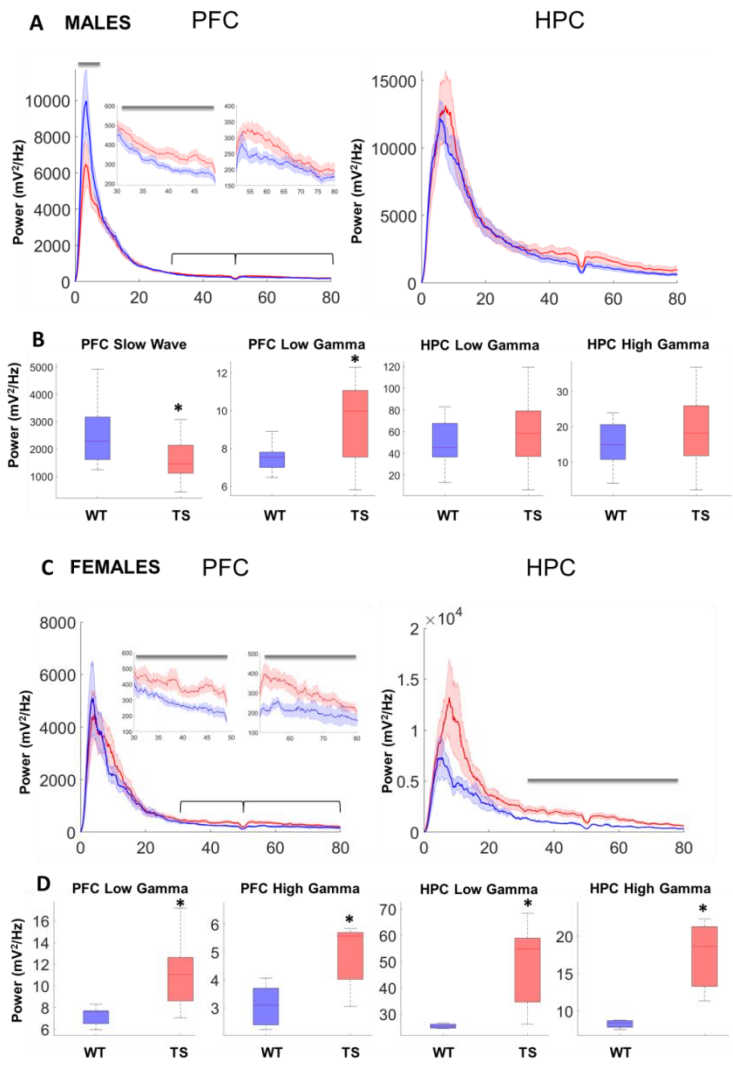

Figure 4.1.11: Oscillatory power in PFC and HPC of Ts65Dn and WT mice during NREM sleep - **(A**) Power spectra of neural signals in PFC and HPC of WT (blue) and TS (red) male mice; grey bars depict significant differences between genotypes. **(B)** Power quantification of selective bands in PFC and HPC of WT and TS male mice. **(C**) Power spectra of neural signals in PFC and HPC of WT and TS female mice. **(D)** Power quantification of gamma bands in PFC and HPC of WT and TS female mice.

However, ripple entropy was similar to WT animals (Fig. 4.1.12B). TS female ripples had also a tendency to occur at lower frequencies (P = 0.16) and higher amplitudes (P = 0.002), and had lower entropy (P = 0.05) (Fig. 4.1.12C). This indicates that ripples in TS animals are slower, with larger power and more organized than ripples in WT animals.

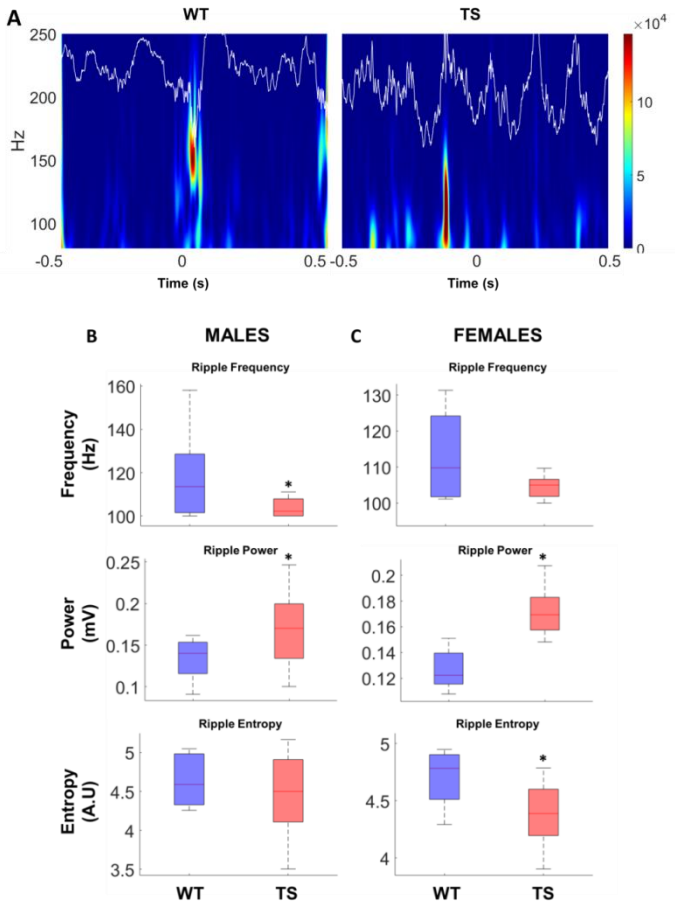

Figure 4.1.12: Hippocampal ripples in WT and Ts65Dn mice during NREM sleep -(A) Examples of sharp-wave ripples recorded in representative WT (blue) and TS (red) mice during NREM sleep. **(B**) Ripple frequency (top), power (middle) and entropy (low) of WT and TS male and **(C**) female mice.

Furthermore, PFC-HPC theta phase synchronization during NREM sleep was exaggerated in TS male mice as in quiet wakefulness (P = 0.04) (Fig. 4.1.13A,C) while in TS female mice PFC-HPC low gamma synchronization was remarkably higher than in WT mice (P = 0.00002) (Fig. 4.1.13B,D).

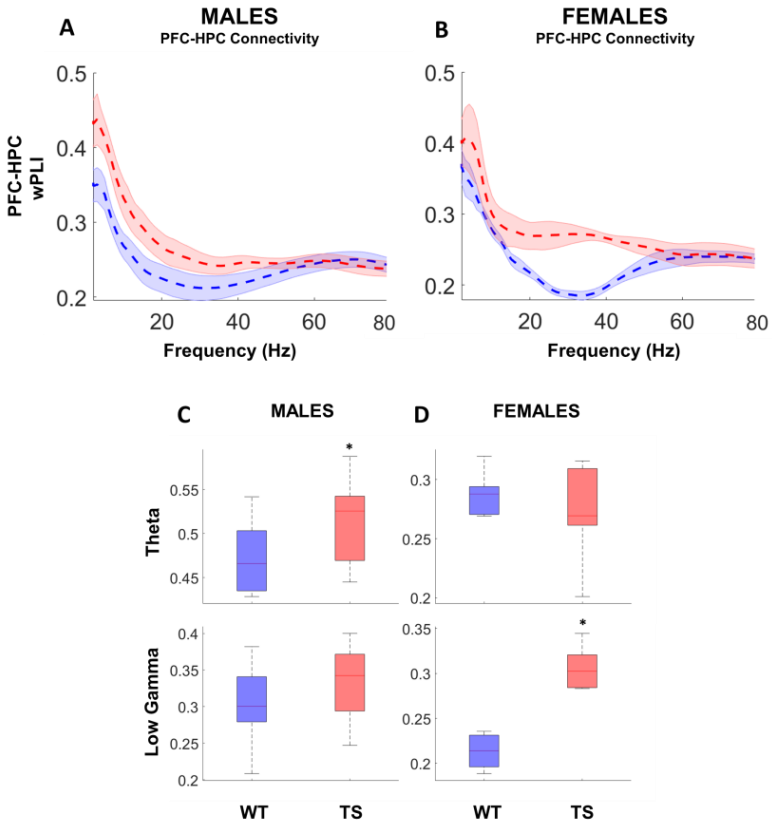

Figure 4.1.13: Phase synchronization of prefronto-hippocampal circuits in Ts65Dn and WT mice during NREM sleep - (A) Mean weighted Phase Lag Index (wPLI) between the PFC and the HPC in WT and TS male and **(B)** female mice. **(C)** PFC-HPC wPLI at theta and low gamma frequencies in WT and TS male and **(D)** female mice.

4.1.2.2. REM sleep

Memory processing during sleep can occur also during rapid eye movement (REM) episodes, a faster brain state characterized by prominent theta oscillations in the HPC along with cortical gamma oscillations. REM-associated HPC theta oscillations appear to support the consolidation of certain types of memories (Boyce et al., 2016). During REM episodes, PFC theta and beta oscillations were increased in TS males (WT n = 8, TS n = 11 mice; P = 0.001; P = 0.02) (Fig. 4.1.14A,B). In addition, TS females also showed excessive PFC theta oscillations and increased PFC and HPC low gamma activity in REM sleep (WT n = 5, TS n = 7 mice; P = 0.06 ; P = 0.05; P = 0.02, respectively) (Fig. 4.1.14C,D).

HPC phase-amplitude theta-gamma coupling is not only prevailing during alertness but also during REM sleep. Both TS male and female mice showed a tendency to display an increased theta-to-HFO modulation in HPC compared to WT mice (independent T test, P = 0.1 for both) (Fig. 4.1.15). Again, these results unravel an aberrant local hypersynchronisation in the HPC of TS mice.

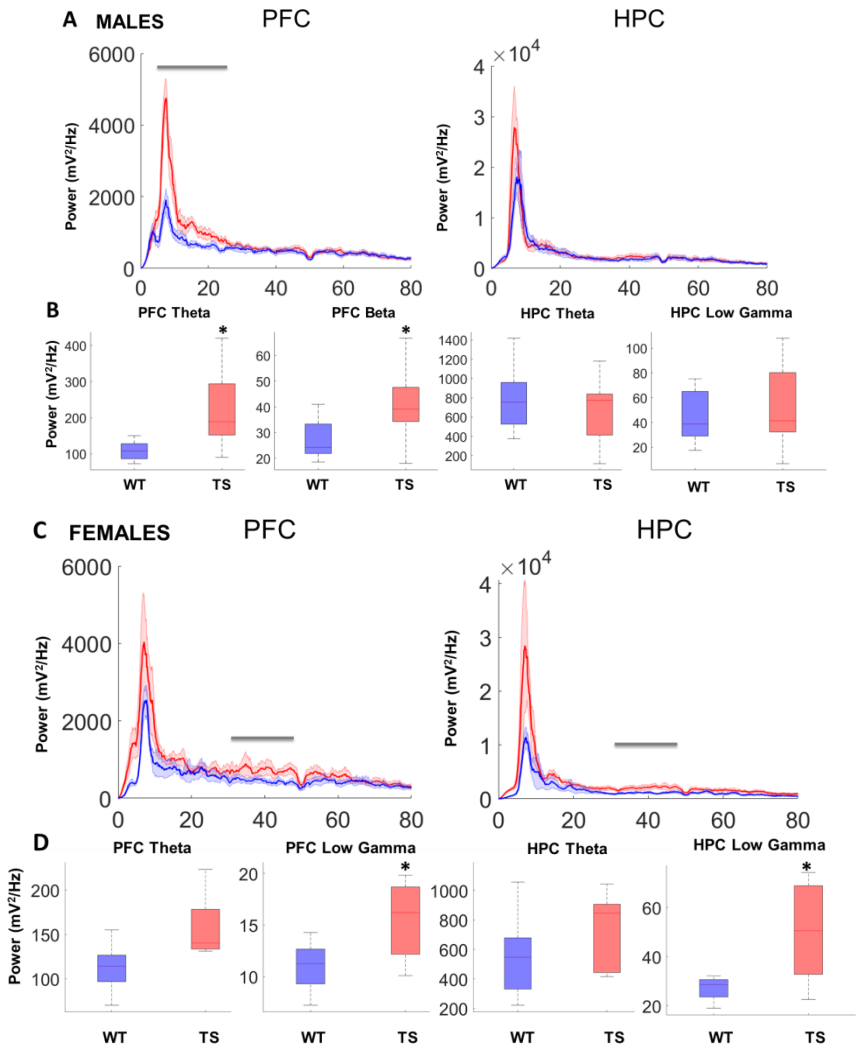

Figure 4.1.14: Oscillatory power in PFC and HPC of Ts65Dn and WT mice during REM sleep - (A) Power spectra of neural signals in PFC and HPC of WT and TS male mice; grey bars depict significant differences between genotypes. **(B)** Power quantification of selective bands in PFC and HPC of WT and TS male mice. **(C**) Power spectra of neural signals in PFC and HPC of WT and TS female mice **(D)** Power quantification of selective bands in PFC and HPC of WT and TS female mice.

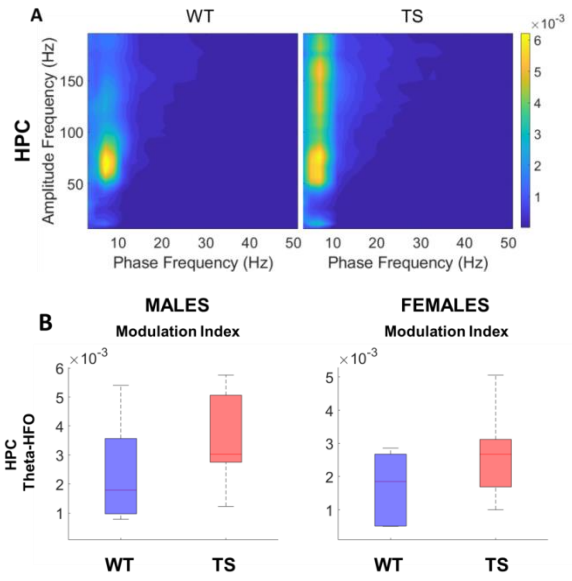

Figure 4.1.15: Prefrontal and hippocampal phase-amplitude comodulograms in WT and Ts65Dn mice during REM sleep - (A) Mean phase-amplitude comodulogram map of WT and TS male mice for HPC LFPs. **(B)** HPC theta-HFO MI in WT and TS males and females.

Regarding functional connectivity during REM sleep, PFC-HPC synchronization was also stronger at low gamma ranges (independent T test; P = 0.002) in TS male mice compared to WT animals (Fig. 4.1.16A).

Collectively, our results show that during sleep TS mice show PFC-HPC hyperactivity at theta and gamma frequencies and slower and more powerful ripples during NREM sleep.

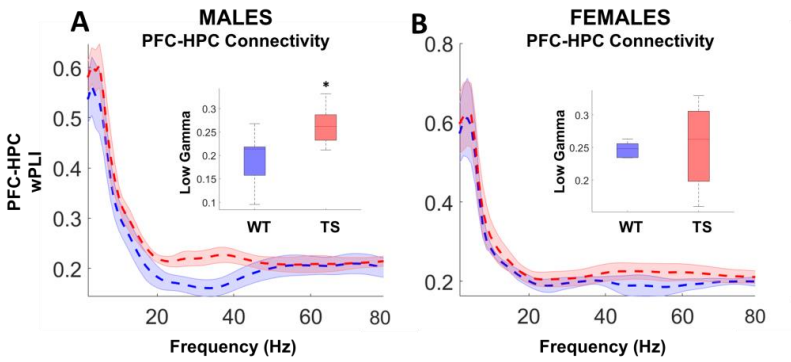

Figure 4.1.16: Phase synchronization of prefronto-hippocampal circuits in WT and Ts65Dn mice during REM sleep - (A) Mean weighted Phase Lag Index (wPLI) between the PFC and the HPC in WT and TS male and **(B)** female mice. Insets show PFC-HPC wPLI at low gamma frequencies in WT and TS mice.

4.2. Prefronto-hippocampal circuit alterations during memory acquisition and retrieval in Ts65Dn mice

We next assessed memory abilities with the novel object recognition task (NOR). We used this task because it is well-validated in mice, it is non-operant and therefore does not require any training, and it depends on the PFC and HPC (Warburton and Brown, 2015). More importantly, the performance on this task is profoundly impaired in Ts65Dn mice (Fernandez et al., 2007; Fernandez and Garner, 2008; Braudeau et al., 2011a; Faizi et al., 2011; de la Torre et al., 2016). Recognition memory refers to the ability to determine if an item is novel or has been experienced before, and it is necessary to store experiences into memory. The NOR task leverages on mice innate motivation to explore novel items in the environment. The task consists in 3 phases of 10 minutes each: habituation to the maze without objects,

familiarization of two identical objects placed at the end of the two lateral arms, and memory test 24 hours after familiarization when one of the familiar objects has been replaced with a novel one (Fig. 4.2.1). We designed and built a custom T-maze adapted for electrophysiological recordings (wider and higher arms than the standard mazes, shielded and grounded; see Methods).

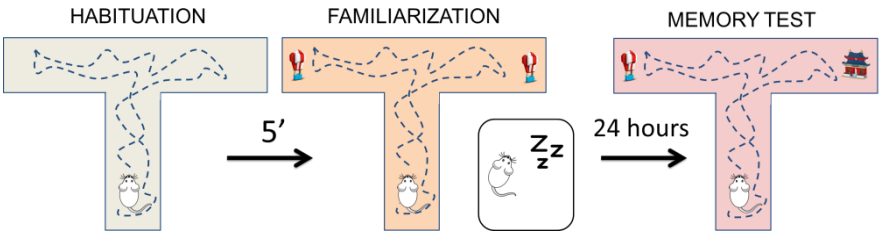

Figure 4.2.1: Different phases of the novel object recognition test.

Animals' interactions with objects were aligned online to the electrophysiological system by pressing a right or left button on a custom-designed joystick for the duration of object explorations (see Methods) (Fig. 4.2.2). We used this online system to automatize the analyses of several behavioural measures during the performance of the task and to analyse the neural mechanisms underlying these behaviours.

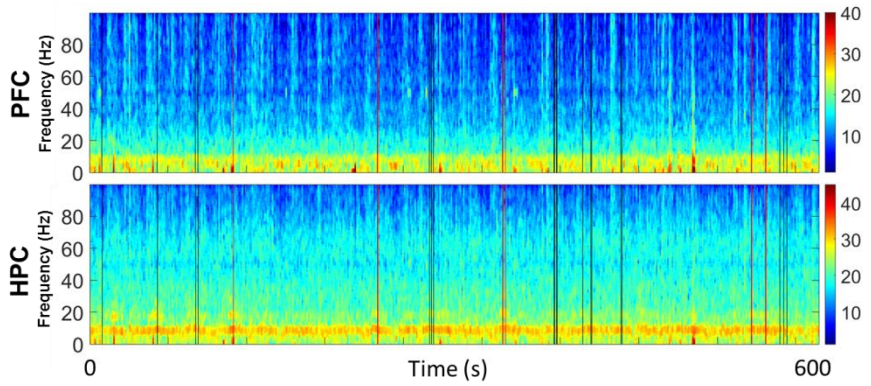

Figure 4.2.2: PFC and HPC activity recorded during the novel object recognition test in a WT mouse - Example spectrograms in PFC and HPC of a 24-hour memory test session. Black and red lines indicate the onset of individual interactions with novel and familiar objects, respectively, aligned to the electrophysiological system via button presses on a joystick.

4.2.1. Recognition memory impairment in Ts65Dn mice

Consistent with the literature (Fernandez and Garner, 2008; Dierssen, 2012; Navarro-Romero et al., 2019), WT mice explored novel objects more than familiar objects in the 24-hour memory test. By contrast, TS mice explored novel and familiar objects equally, an indication of poor long-term recognition memory. This was reflected by smaller familiar vs. novel discrimination indices (DIs) with respect to WTs (males, WT n = 10 vs. TS n = 11 mice; independent T test; $P < 0.00005$; females, WT n = 6 vs. TS n = 7 mice; $P < 0.00005$) (Fig. 4.2.3).

The smaller DIs were not due to differences in the total time of explorations or in the total number of explorations but in their individual duration (males, P = 0.00005; females, P = 0.00001) (Fig. 4.2.3). More specifically, WT mice explored novel objects longer than familiar objects (paired T test; male, P = 0.04; female, P = 0.0001) whereas TS mice explored them equally and for shorter periods of time (males, P = 0.6; females, P = 0.3) (Fig. 4.2.4), perhaps indicating poor attention (Driscoll et al., 2004). A repeated measures ANOVA with duration of novel and familiar explorations as within factor and genotype as between factor showed a significant novelty x genotype interaction (males, $F_{1,18}$ = 5,38; P = 0.032; females, $F_{1,10}$ = 25,04; P = 0.001), indicating that familiar and novel interactions were not equal across genotypes. WT mice also showed prolonged exploration times when interacting with novel versus familiar objects (males, P = 0.007; $F_{1,19}$ = 11,922; P = 0.003; females, P = 0.002; $F_{1,10}$ = 22,68; P = 0.001) whereas TS mice explored both objects during the same time (Fig. 4.2.4).

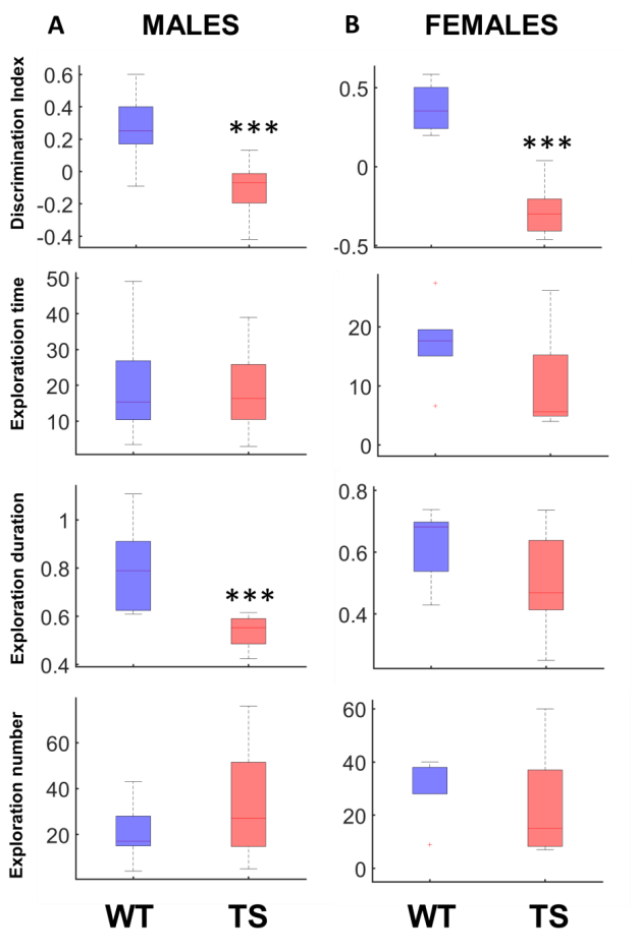

Figure 4.2.3: Behavioural readouts of the NOR task in WT and Ts65Dn mice - **(A)** Discrimination indices (DI), total exploration time, total duration of individual explorations and total number of explorations in WT and TS male and **(B)** female mice during the NOR test.

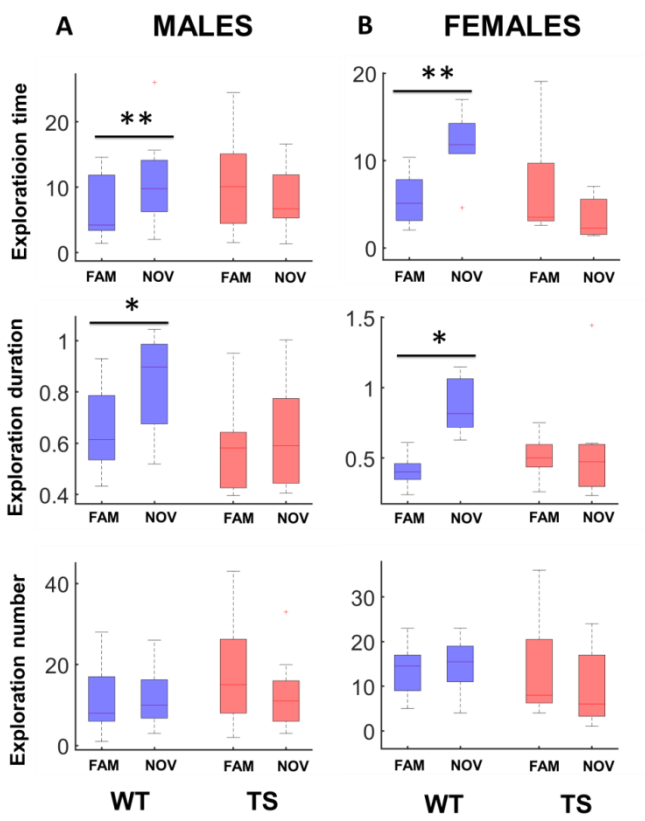

Figure 4.2.4: Behavioural readouts of novel and familiar explorations in WT and Ts65Dn mice - (A) Exploration time, duration of individual explorations and number of explorations of familiar and novel objects in WT and TS male and **(B)** female mice during the NOR task.

4.2.2. Neural substrates of memory acquisition and retrieval in healthy mice

We first aimed to understand the neural mechanisms underlying memory acquisition and retrieval in WT mice. We investigated memory acquisition during the familiarization phase when mice were presented with two identical objects that were stored in

memory. We investigated memory retrieval during the 24-hour memory test when mice were tested for recognition memory of the familiar object.

4.2.2.1 Memory acquisition

To investigate neural mechanisms of memory acquisition, we measured changes in neural activity during the familiarization phase by comparing the first 5 (early) vs. the last 5 (late) explorations of the object irrespective of location (i.e., any of the two lateral arms of the maze) (Fig. 4.2.5). Individual explorations were analysed in 1 second non-overlapping windows starting from the button presses (see Methods). We first found a selective decrease of theta power in HPC during memory acquisition (WT males, n = 10 mice; early vs. late HPC theta, paired T test; P = 0.01; WT females, n = 6 mice; early vs. late HPC theta; P = 0.005) (Fig. 4.2.6). In addition, we detected that PFC-HPC phase synchronization (wPLI) was selectively enhanced at low gamma during late explorations (male, P = 0.003; female, P = 0.09) (Fig. 4.2.6). We also investigated the directionality of information flow between the PFC and the HPC with the Phase Slope Index (PSI, see also Methods), that quantifies the consistency of phase differences between two signals. Interestingly, these analyses pointed to a shift of directionality from hippocampal-to-prefrontal (HPC-to-PFC) theta connectivity during early explo-rations to prefrontal-to-hippocampal (PFC-to-HPC) theta connec-tivity during late explorations (male, early vs. late PFC-to-HPC theta PSI, paired T test; P = 0.002) (Fig. 4.2.6A).

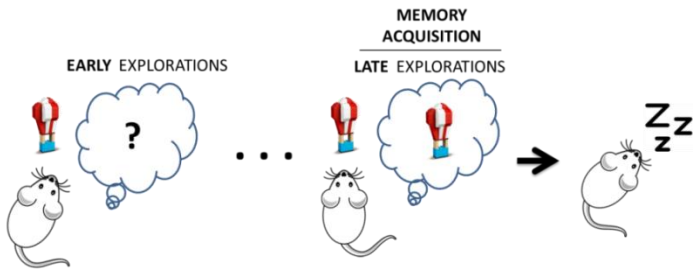

Figure 4.2.5: Schematic representation of memory acquisition in the familiarization phase of the NOR task.

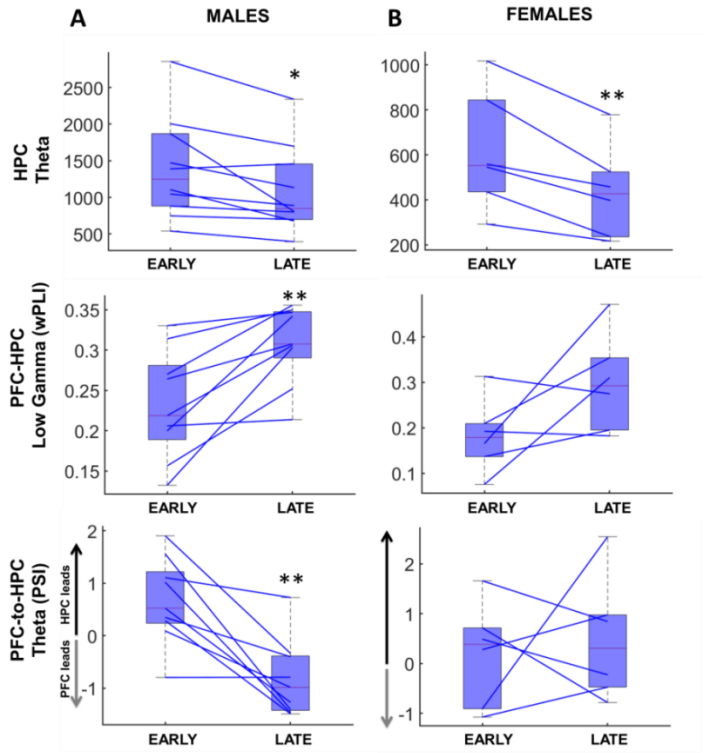

Figure 4.2.6: PFC-HPC network activity during memory acquisition in WT mice - (A) HPC theta power, PFC-HPC low gamma connectivity (wPLI) and PFC-to-HPC theta directionality (PSI) for early and late explorations in WT male and **(B)** female mice during the NOR familiarization phase.

4.2.2.2 Memory retrieval

To investigate neural mechanisms of memory retrieval, we quantified differences in neural activity during the 24-hour memory test by comparing all explorations of the familiar versus the novel objects (Fig. 4.2.7). Like in previous analyses, individual explorations were dissected in 1 second non-overlapping windows starting from the button presses.

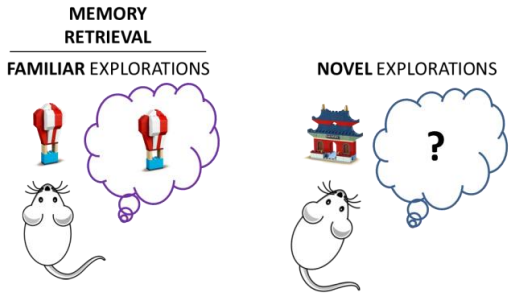

Figure 4.2.7: Schematic representation of memory retrieval in the 24-hour memory test of the NOR task.

The strongest and most consistent effects during memory retrieval were observed at gamma ranges in both genders. First, we found a selective decrease of low gamma power in HPC and PFC-HPC high gamma phase synchronization (wPLI) during familiar explorations relative to novel explorations (WT males, n = 10 mice; familiar vs. novel, paired T test; P = 0.009 and P = 0.006, respectively; WT females, n = 6 mice; P = 0.05 and P = 0.004, respectively) (Fig. 4.2.8). We also investigated the directionality of information (PSI) between the PFC and the HPC and identified a selective HPC-to-PFC flow of information at low gamma during memory retrieval (paired T test; males, P = 0.002; females, P = 0.04) (Fig. 4.2.8).

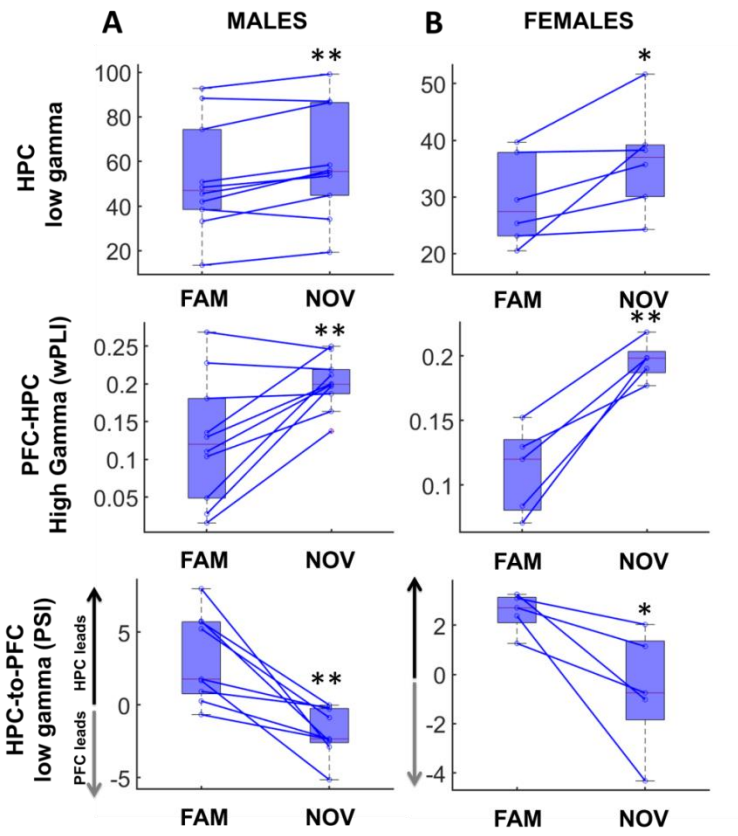

Figure 4.2.8: PFC-HPC network activity during memory retrieval in WT mice - (A) HPC low gamma power, PFC-HPC high gamma connectivity (wPLI) and HPC-to-PFC low gamma PSI for familiar and novel explorations in WT male and **(B)** female mice in the NOR task.

Taken together, if we consider only neural activity that emerges during late explorations in the familiarization phase, a selective PFC-to-HPC theta connectivity is required for memory acquisition. On the other hand, if we consider only neural activity that emerges during familiar object explorations in the 24-hour memory test, a

selective HPC-to-PFC low gamma connectivity may be necessary for memory retrieval (Fig. 4.2.9)

Figure 4.2.9: PFC-HPC theta and gamma connectivity during memory acquisition (familiarization phase) and retrieval (24-hour memory test) in the NOR task.

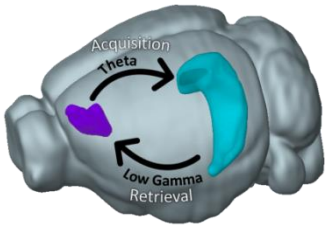

4.2.3 Neural substrates of memory acquisition and retrieval impairments in Ts65Dn mice

We next examined the PFC-HPC circuit during the NOR task in TS mice. Interestingly, most neurophysiological biomarkers of memory acquisition identified in WT mice were not present in TS mice. A repeated measures ANOVA with time (early or late explorations) as within factor and genotype as between factor showed a significant time x genotype interaction for PFC-to-HPC theta PSI and PFC-HPC low gamma wPLI (males, n = 19; $F_{1,15} = 5.11$; P = 0.039; $F_{1,14} = 6.08$; P = 0.027, respectively) (Fig. 4.2.10A), indicating that early-to-late transitions were not equal across genotypes during the familiarization phase. However, HPC theta power did decrease during late explorations as in WT males ($F_{1,16} = 0.4$; P = 0.53 for interaction; $F_{1,16} = 9.45$; P = 0.007 for time) (Fig. 4.2.10A). WT female mice did not show proper memory acquisition biomarkers probably due to the reduced sample size but TS females showed abnormal PFC-HPC wPLI and PFC-to-HPC theta PSI similar to those observed in TS males (Fig. 4.2.10B).

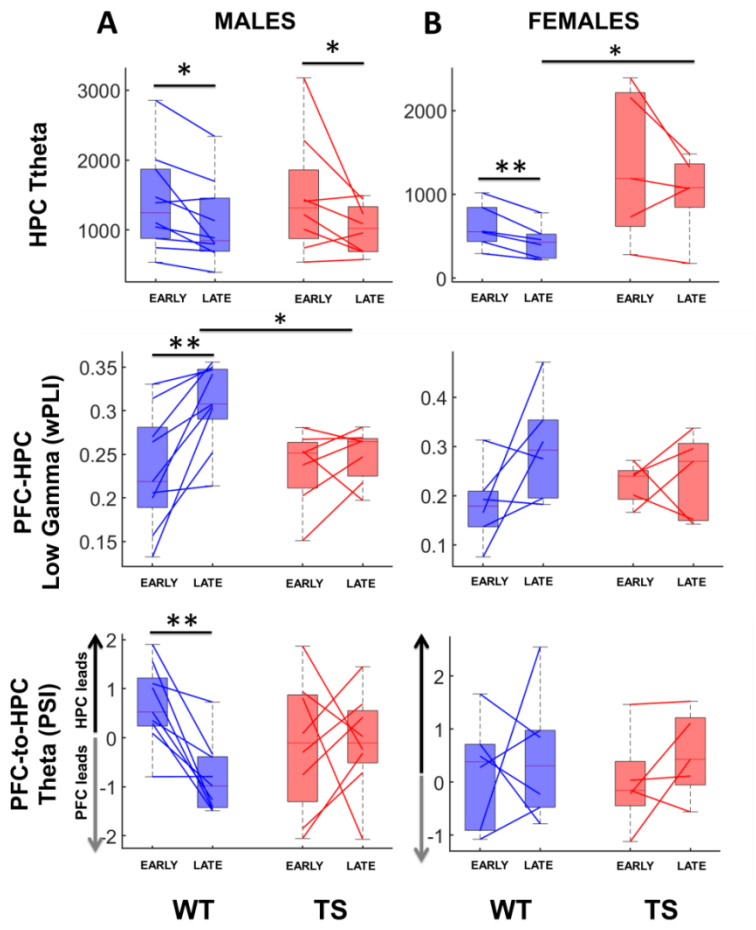

Figure 4.2.10: Network activity in the PFC-HPC circuit during object familiarization in WT and Ts65Dn mice - (A) HPC theta power, PFC-HPC low gamma connectivity (wPLI) and PFC-to-HPC theta connectivity (PSI) for early and late explorations in WT and TS male and **(B)** female mice.

Furthermore, the three neurophysiological biomarkers associated with memory retrieval in WT mice were not present in TS mice. First, HPC low gamma power was not different when exploring familiar vs. novel objects (TS males, n = 9 mice; paired T test, P = 0.34; TS females, n = 7 mice, P = 0.66) (Fig. 4.2.11A,B). Moreover,

although familiar vs. novel PFC-HPC high gamma synchronization was not different in TS males, it changed in TS females but in the opposite direction than in WT females (P = 0.47 and 0.04 for TS males and females, respectively) (Fig. 4.2.11A,B). Accordingly, repeated measures ANOVA showed a significant novelty x genotype interaction for both parameters (males, $F_{1,16}$ = 5.11; P = 0.04; $F_{1,17}$ = 5.23; P = 0.012, respectively; females, $F_{1,11}$ = 2.28; P = 0.15; $F_{1,11}$ = 13.022; P = 0.004, respectively), indicating that familiar vs. novel interactions were not equal across genotypes.

The absence of familiar vs. novel differences emerged because power and PFC-HPC wPLI at gamma were exaggerated during familiar explorations in TS mice (familiar explorations in WTs vs. familiar explorations in TS mice; males, n = 10 WT vs. n = 9 TS; independent T test; P = 0.04, 0.05, respectively; females, n = 6 WT vs. n = 7 TS; P = 0.003, 0.04, respectively) (Fig. 4.2.11A,B), in accord with a hypersynchronisation of PFC-HPC networks. In fact, both measures during retrieval in TS male mice were not different from those when WT mice explored novel objects (independent T test, P = 0.1 and P = 0.73, respectively), as if trisomic mice were considering familiar objects as new. Interestingly, HPC-to-PFC low gamma directionality (PSI) did not differ either during exploration of novel and familiar objects in TS mice (paired T test; males, P = 0.67; females, P = 0.64) because it was decreased during familiar explorations (male, P = 0.01; female, P = 0.0001) (Fig. 4.2.11A,B).

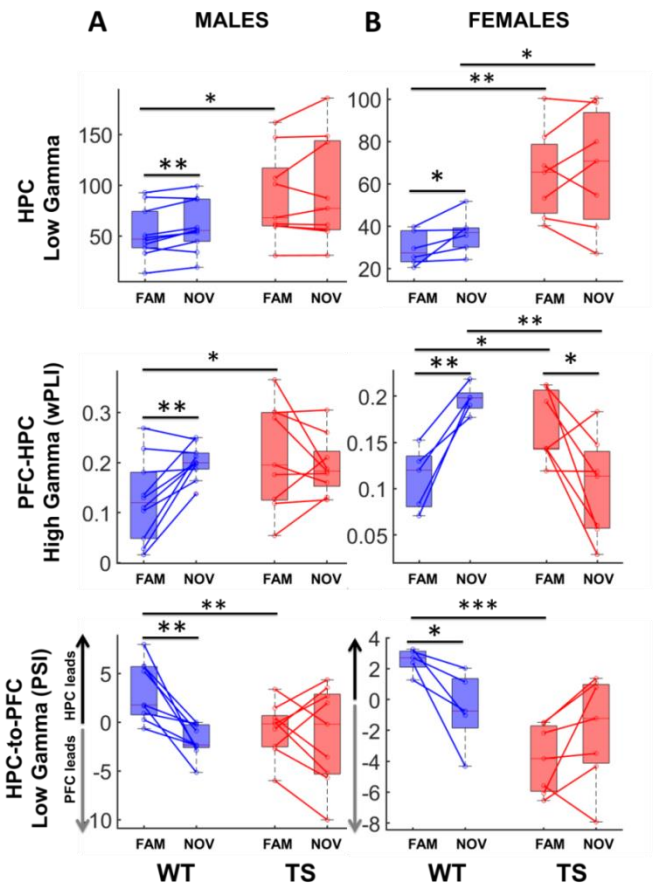

Figure 4.2.11: Network activity in the PFC-HPC circuit during the 24-hour memory test in WT and Ts65Dn mice. (A) HPC low gamma power, PFC-HPC high gamma connectivity (wPLI) and HPC-to-PFC low gamma connectivity (PSI) during familiar and novel object explorations in WT and TS male and **(B)** female mice.

Again, repeated measures ANOVA showed a significant novelty x genotype interaction for HPC-to-PFC low gamma PSI (males, $F_{1,16}$ = 6.34; P = 0.023; females, $F_{1,10}$ = 10.69; P = 0.008), indicating that PSI during familiar and novel interactions were not equal across genotypes.

Moreover, we detected two additional neural activity alterations in TS females during the 24-hour memory test. They showed increased PFC low gamma and HPC high gamma activity during familiar explorations compared to WT females (independent T test, P = 0.007 and P = 0.03, respectively) (Fig. 4.2.12A,B).

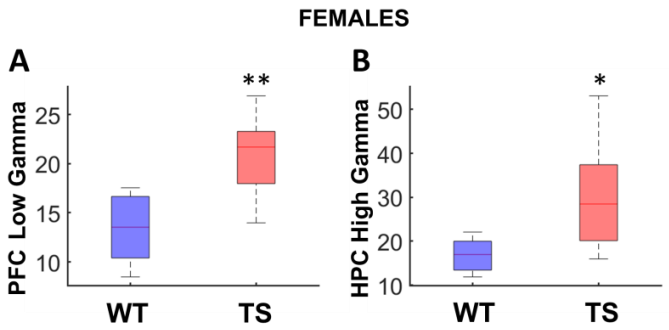

Figure 4.2.12: Network activity in the PFC-HPC circuit during the 24-hour memory test in WT and Ts65Dn specific to female mice. (A) PFC low gamma and **(B)** HPC high gamma power during exploration of familiar objects in WT and TS mice.

Altogether, TS mice showed abnormal neural activity during memory acquisition and retrieval that could underlie their recognition memory deficits in the NOR task.

		QUIET		NREM		REM	
MEASURE	BANDS	M	F	M	F	M	F
PFC Power	δ						
	θ						
	β						
	lγ						
	hγ						
PFC MI	δ-hγ						
HPC Power	δ						
	θ						
	β						
	lγ						
	hγ						
HPC MI	θ-hγ						
	θ-HFO						
HPC Ripples	*Freq.*						
	Power						
	Entropy						
PFC-HPC wPLI	δ						
	θ						
	β						
	lγ						
	hγ						

MEMORY		M	F
Acquisition	PFC-to-HPC Theta (PSI)	✕	✕
Retrieval	HPC low gamma		
	PFC-HPC High Gamma (wPLI)		
	HPC-to-PFC Low Gamma (PSI)	✕	✕

Table 3 – PFC-HPC network alterations in Ts65Dn mice compared to WT mice. Red indicates increase, blue decrease of activity and black cross depicts disruption.

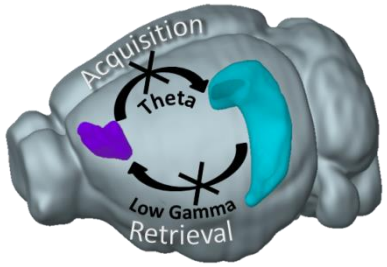

Figure 4.2.13 - Putative alterations of the PFC-HPC circuit during memory acquisition and retrieval in Ts65Dn mice.

4.3. Prefronto-hippocampal neurophysiological biomarkers predict memory performance

The results presented above raised the possibility of a causal link between PFC-HPC network alterations and deficient memory in TS mice. Such causal link is supported by significant correlations between several neural activity biomarkers and cognitive performance (discrimination index - DI) in the 24-hour memory test

in male mice. We note that several of these pairs of biomarkers were collected in separate sessions and brain states. First, the power of PFC theta oscillations recorded during quiet wake correlated negatively with memory performances when including both genotypes (correlation; n = 20 males, 10 WT and 10 TS; R = -0.61; P = 0.004) (Fig. 4.3.1A). Overall, a high PFC theta amplitude predicted poor memory performance. In fact, discrimination indices showed a strong dependence on PFC theta power in TS mice but not in WT mice (WT: R = -0.28, P = 0.43; TS: R = -0.69, P = 0.025), suggesting that pathological theta rhythms may occur in the PFC of TS animals. Other abnormal measures identified during quiet wakefulness (HPC theta power, theta-gamma modulation index, PFC-HPC wPLI at theta and beta) and REM sleep (PFC theta and beta power, PFC-HPC wPLI at low gamma) did not correlate with memory performance. During NREM sleep, however, we observed strong correlations between ripple frequency and DIs when combining both genotypes (R = 0.66; P = 0.002). In this case, higher ripple frequency predicted better memory performance in WT mice (R = 0.61; P = 0.06), but not in TS mice (R = 0.4; P = 0.28) (Fig. 4.3.1B). Conversely, ripple power, that was increased in TS mice, correlated positively in TS mice (R = 0.63; P = 0.04) but not in WT mice (R = -0.11; P = 0.54) (Fig. 4.3.1C), implying that pathological rhythms also emerge during sleep.

Next, we investigated whether neurophysiological biomarkers associated with memory acquisition and retrieval correlated with animals' memory performance. In WT mice, PFC-to-HPC theta

connectivity during memory acquisition correlated negatively with DIs (R = -0.78; P = 0.013; note that this directionality is represented by negative PSI values), underscoring that a flow of information from the PFC to the HPC at theta frequencies is important for proper memory acquisition (Fig. 4.3.1D). Furthermore, PFC-HPC high gamma phase synchronization during memory retrieval correlated negatively with DIs (both genotypes, R = -0.51; P = 0.027), but more in TS mice (R = -0.61; P = 0.08) than in WT mice (R = 0.06; P = 0.98) (Fig. 4.3.1E). This suggests that elevated PFC-HPC high gamma connectivity in TS mice results in worse memory recognition highlighting yet again that a pathological PFC-HPC gamma synchronization in TS mice may interfere with normal memory processing during retrieval. Conversely, HPC-to-PFC low gamma connectivity during memory retrieval positively correlated with memory performance (correlation; R = 0.62; P = 0.006), being those animals with higher HPC low gamma input to the PFC the best performers. In agreement, WT animals showed strong correlations between HPC-to-PFC low gamma connectivity and DIs (R = 0.7, P = 0.036) while TS mice did not (R = -0.11, P = 0.12) (Fig. 4.3.1F).

The fact that PFC-to-HPC theta connectivity during memory acquisition and HPC-to-PFC low gamma connectivity during memory retrieval correlated with memory performance in WT mice provide further support to a selective flow of information between the two areas during distinct stages of memory processing (Fig. 4.2.9).

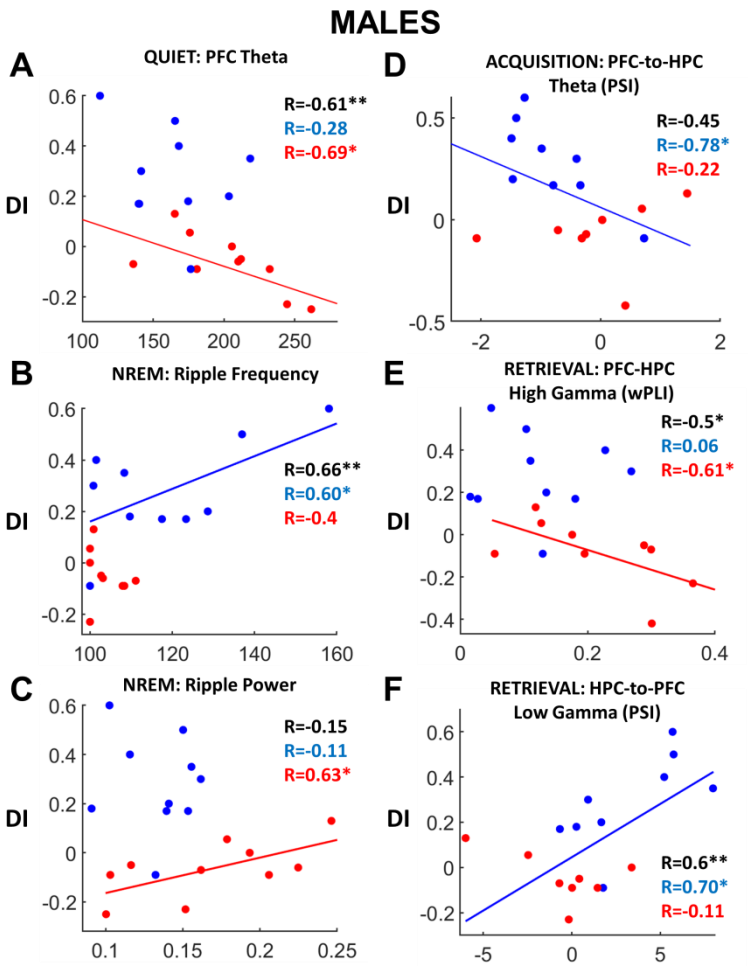

Figure 4.3.1: Correlations between PFC-HPC neurophysiological biomarkers and memory performance in WT and Ts65Dn male mice - (A) Correlations between DIs and PFC theta power recorded during quiet wakefulness, **(B)** NREM ripple frequency and **(C)** ripple power in WT and TS mice. **(D)** Correlations between DIs and PFC-to-HPC theta directionality (PSI) during memory acquisition. **(E)** Correlations between DIs and PFC-HPC high gamma connectivity (wPLI) and **(F)** PFC-to-HPC low gamma connectivity (PSI) during memory retrieval.

In female mice we also found some correlations between neurophysiological biomarkers and DIs, even though the sample size was smaller. First, PFC theta power during quiet wake predicted poor memory performances (R = -0.7 P = 0.002), as reported in males. Again, DIs showed a strong dependence on PFC theta power in TS females (R = -0.9, P = 0.01) but not in WT females (R = 0.14, P = 0.97) (Fig. 4.3.2A), pointing to pathological theta rhythms in the PFC of TS females as well. During NREM sleep we observed negative correlations between ripple power and DIs when combining both genotypes (R = -0.79; P = 0.002), and this was more pronounced for TS mice (R = -0.51; P = 0.29) (Fig. 4.3.2B). In this case, larger ripple power predicted poorer memory performance. Unique to female mice, we observed positive correlations between ripple entropy and DIs when combining both genotypes (R = 0.60; P = 0.03), and this was more pronounced for TS mice (R = 0.72; P = 0.06), suggesting that higher ripple entropy predicted better memory performance (Fig. 4.3.2C). Also unique to females, PFC high gamma power during NREM sleep correlated negatively with DIs in TS (R = -0.78; P = 0.03) but not in WT females (R = 0.26; P = 0.61) (Fig. 4.3.2D). Finally, as in males, we detected a positive correlation when combining both genotypes between HPC-to-PFC low gamma connectivity during memory retrieval and DIs (R = 0.71, P = 0.009) (Fig. 4.3.2E).

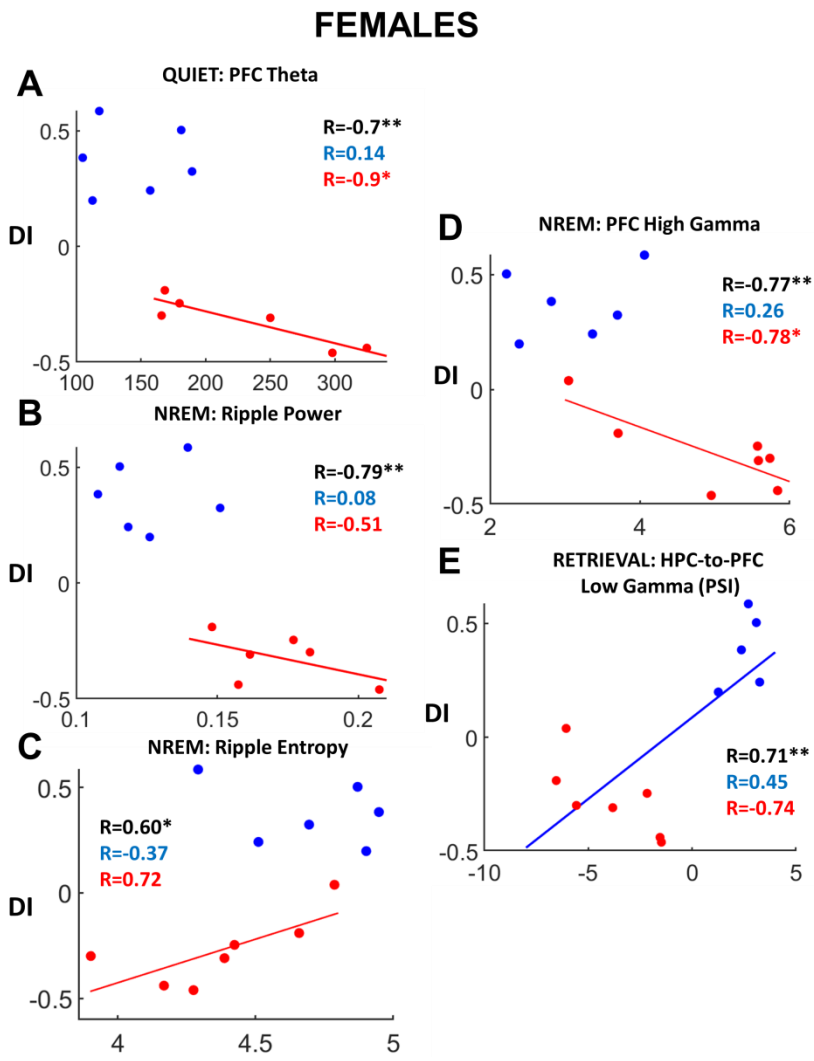

Figure 4.3.2: Correlations between PFC-HPC neurophysiological biomarkers and memory performance in TS and WT female mice - (A) Correlation between DIs and PFC theta power during quiet wakefulness, **(B)** NREM ripple power, **(C)** NREM ripple entropy, **(D)** NREM PFC high gamma power in TS and WT mice, and **(E)** HPC-to-PFC low gamma connectivity (PSI) during memory retrieval.

5. CHAPTER II. NEURAL CORRELATES OF COGNITIVE AMELIORATION IN Ts65Dn MICE

5. CHAPTER II. NEURAL CORRELATES OF COGNITIVE AMELIORATION IN Ts65Dn MICE

In this chapter we explored the neural substrates of cognitive amelioration in TS mice. We used three pro-cognitive strategies able to rescue memory deficits in both DS human subjects and TS mice. First, we studied the pro-cognitive effects of a chronic treatment with the natural compound epigallocatechin-3-gallate (EGCG) in young adult TS male mice. Second, we assessed the effects of an acute treatment with the selective $GABA_A$ α5IA in the same male mice at the age of 5-6 months. Third, we assessed the effects of post-weaning enriched environment (EE) in young adult WT and TS female mice.

5.1. Chronic oral treatment with epigallocatechin-3-gallate in young adult Ts65Dn male mice

Here we aimed to unravel the neural substrates of the pro-cognitive compound EGCG, a flavonoid found in green tea leaves that ameliorates executive function in individuals with DS and rescues cognitive deficits TS mice (De La Torre et al., 2013; de la Torre et al., 2016). TS and WT mice were administered EGCG in the drinking water for one month following procedures reported previously (De La Torre et al., 2013), and neural activity was then recorded as in pre-EGCG epochs (Fig. 5.1.1). Some animals that only received water were used as controls.

Figure 5.1.1: Protocol for the behavioural and neurophysiological assessment of chronic oral EGCG treatment of as a memory enhancer.

EGCG rescued memory deficits in 6 of 8 TS male mice (DI pre vs. post EGCG, paired T test; TS n = 8 mice; P = 0.02) (Fig. 5.1.2A). After treatment, the mean duration of individual explorations increased and now explorations of novel objects were longer than explorations of familiar objects in the 6 EGCG-responding mice (pre-EGCG vs. post-EGCG; paired T test, P = 0.005 and P = 0.024, respectively) (Fig. 5.1.2B,C). A repeated measures ANOVA with duration of novel and familiar explorations as within factor and genotype (WT pre-EGCG and TS post-EGCG) as between factor did not show a significant novelty x genotype interaction ($F_{1,12}$ = 1.31; P = 0.27) but a significant effect of duration ($F_{1,12}$ = 8.89; P = 0.01). In addition, EGCG increased significantly the total exploration time in TS mice (paired T test, P = 0.001) (Fig. 5.1.2D). None of these measures were rescued in TS control mice that received water or the two mice that did not respond behaviourally to EGCG, with the exception of total exploration time that was increased in one EGCG-nonresponding mice (see individual black dots for control mice and red dots for EGCG non-responding mice in Fig. 5.1.2D).

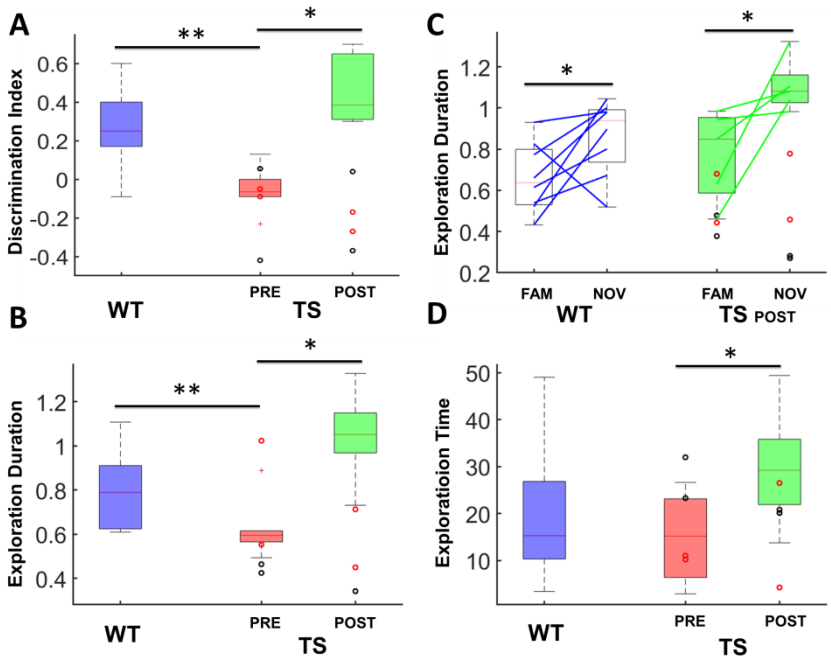

Figure 5.1.2: Behavioural effects of chronic oral treatment with EGCG in male mice - (A) Discrimination indices (DI), **(B)** mean duration of individual explorations, **(C)** mean duration of familiar and novel explorations and **(D)** total exploration time in WT (blue), TS pre-EGCG (red) and TS post-EGCG (green) mice in the NOR task.

We next investigated the neural substrates of EGCG´s pro-cognitive effects in TS mice. EGCG normalized excessive power of PFC theta oscillations in TS male mice to WT levels during quiet wakefulness (paired T test; TS n = 6 mice; P = 0.02), while in TS control animals and EGCG-nonresponders it remained elevated (Fig. 5.1.3A). Accordingly, dependence of DIs on PFC theta subsided with EGCG in the six responders (pre-EGCG: R = -0.69, P = 0.02; post-EGCG: R = 0.25; P = 0.62) (Fig. 5.1.3A). Moreover, EGCG partly corrected low ripple frequency (P = 0.18) (Fig.

5.1.3B) and fully rescued increased ripple power during NREM sleep (P = 0.04) (Fig. 5.1.3C). Again, aberrant correlation between DIs and ripple power was normalized by EGCG in the 6 responders (R = -0.25; P = 0.68) (Fig. 5.1.3C).

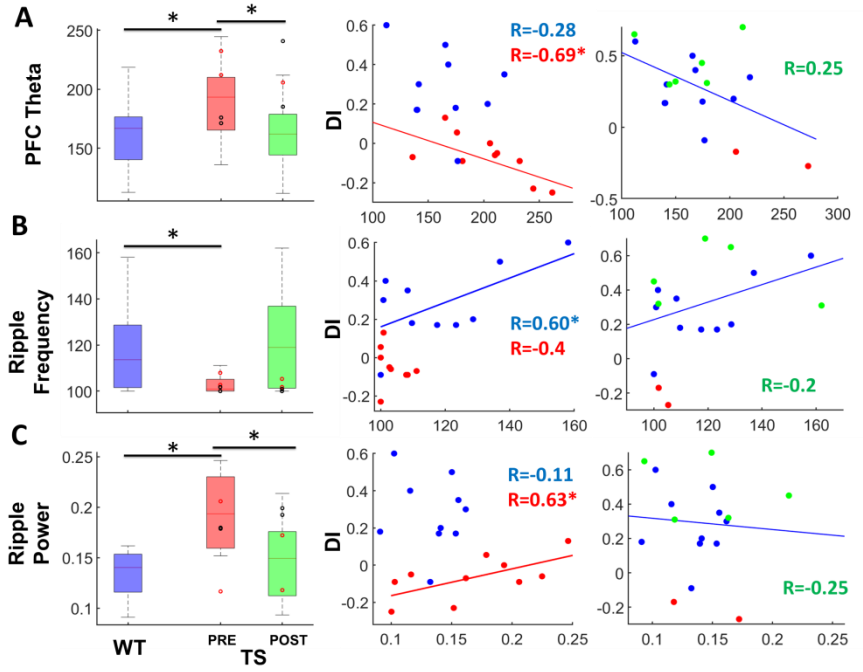

Figure 5.1.3: Effects of chronic EGCG on neural activity of the PFC-HPC circuit during quiet wakefulness and sleep - (A) PFC theta power during quiet wakefulness, **(B)** NREM ripple frequency and **(C)** NREM ripple power in WT (blue), TS pre-EGCG (red) and TS post-EGCG (green) mice. Corresponding correlations with DIs in pre- and post-EGCG conditions are shown on the right panels.

We also assessed EGCG´s effects on the neural signatures of memory acquisition and retrieval in the NOR task. Noteworthy, selective neurophysiological biomarkers were corrected in five

EGCG-responders (in one animal the quality of neural recordings deteriorated over time and became insufficient for proper signal analysis). More specifically, PFC-to-HPC theta PSI was now different between early and late explorations during memory acquisition (paired T test; TS n = 5 mice, P = 0.01) (Fig. 5.1.4A), whereas in control TS animals and EGCG-nonresponders it remained equal. In agreement, correlation between DIs and PFC-to-HPC theta PSI was normalized by EGCG in the 5 responders (R = -0.76; P = 0.13) (Fig. 5.1.4A). During memory retrieval, excessive HPC low gamma power in TS mice decreased to WT levels (pre- vs. post-EGCG; paired T test, P = 0.01), however the familiar vs. novel differences remained as in pre-EGCG conditions (familiar vs. novel explorations; P = 0.14; data not shown). More robust effects were observed in PFC-HPC high gamma phase synchronization (wPLI) and HPC-to-PFC low gamma connectivity (PSI), that were fully rescued by EGCG in the 5 responders (P = 0.01 and 0.03 for familiar vs. novel, respectively) (Fig. 5.1.4B,C).

Collectively, EGCG normalized PFC-HPC theta and gamma connectivity during memory acquisition and retrieval in TS mice, pointing to precise cellular mechanisms underlying its pro-cognitive actions.

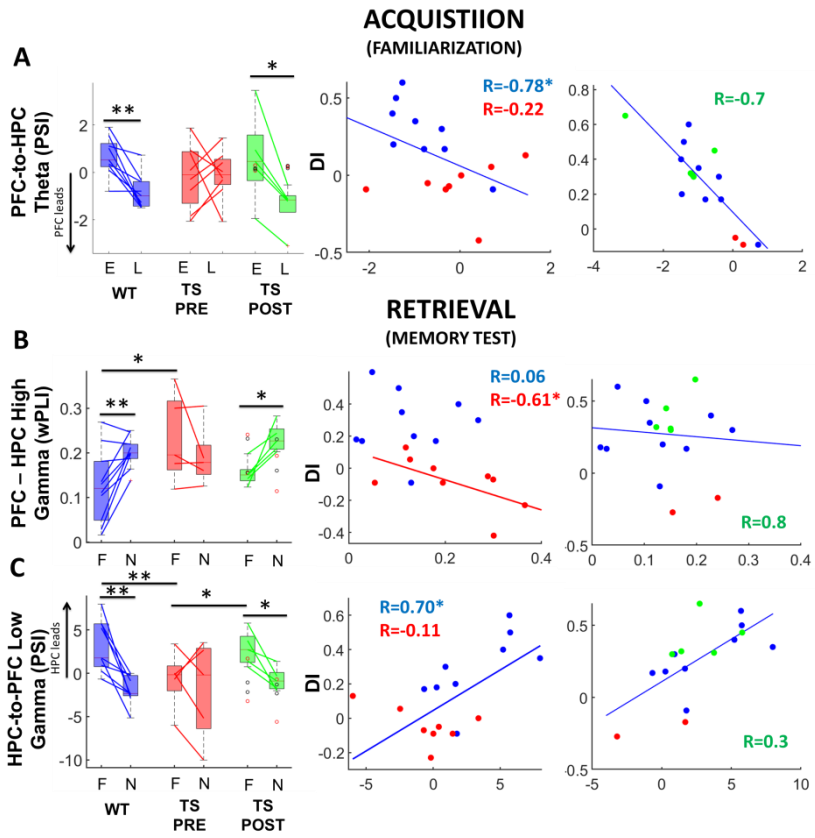

Figure 5.1.4: Effects of chronic EGCG on neural activity of the PFC-HPC circuit during memory acquisition and retrieval (A) - PFC-to-HPC theta connectivity (PSI) during early and late explorations in the familiarization phase, **(B)** PFC-HPC high gamma connectivity (wPLI) and **(C)** HPC-to-PFC low gamma directionality (PSI) for familiar and novel object explorations in WT (blue), TS pre-EGCG (red) and TS post-EGCG (green) mice. Corresponding correlations with DIs in pre- and post-EGCG conditions are shown on the right panels.

5.2. Acute IP treatment with α5IA in old adult Ts65Dn male mice

We next assessed the effects of a $GABA_A$ receptor inverse agonist selective for the α5 subunits (α5IA). This compound was first described as a pro-cognitive agent by (Sternfeld et al., 2004) and later (Braudeau et al., 2011a) demonstrated its memory enhancing abilities in TS mice. More specifically, acute α5IA improved learning and memory in TS mice when tested in the Morris water maze and NOR task. In addition, α5IA boosts learning-evoked immediate early gene products in both CA1 and perirhinal cortices, two brain areas tightly involved in recognition memory (Braudeau et al., 2011a). Here we investigated the effects of acute α5IA on the PFC-HPC circuit in 7 WT and 8 TS male adult mice (5-6 months old). These mice were previously used for EGCG chronic treatment and were washed out for a month (Fig. 5.2.1). Mice were first habituated to the maze for 10 min and later placed in an open arena where they were injected with either vehicle or α5IA 5 mg/kg intraperitoneally. Thirty minutes after injections, mice were placed back in the maze containing two identical objects (familiarization) for 10 min. As before, we assessed long-term memory after a 24-hour retention interval. Mice received vehicle and α5IA treatments in two consecutive weeks and were tested with different pairs of objects (Fig. 5.2.1).

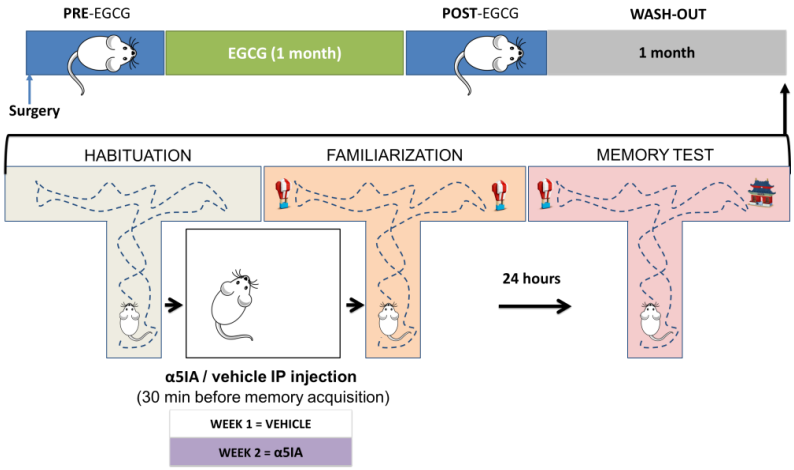

Figure 5.2.1: Protocol for the behavioural and neurophysiological assessment of an acute injection of α5IA as a memory enhancer.

First, we found that α5IA had pro-cognitive effects in long-term recognition memory (24-hour test) in our TS mice, in line with the short-term recognition memory (10 min) amelioration reported by (Braudeau et al., 2011b). Specifically, α5IA improved DIs in TS mice (DIs after vehicle vs. α5IA; paired T test; TS n = 7 mice; P = 0.002) (Fig. 5.2.2A). Interestingly, α5IA did not improve memory in WT mice. A repeated measures ANOVA with treatment (vehicle or α5IA) as within factor and genotype as between factor showed a significant drug x genotype interaction ($F_{1,12}$ = 13.16; P = 0.003), indicating that the treatments exerted distinct effects across genotypes. Following α5IA injections, but not vehicle, TS mice explored novel objects more than familiar objects because individual explorations were longer (α5IA: P = 0.00008, 0.005, respectively; treatment x novelty interaction: $F_{1,12}$ = 12.81; P = 0.004; vehicle: P = 0.4, 0.63, respectively; $F_{1,12}$ = 4.31; P = 0.06).

Again, these changes were not observed in WT mice, the behavioural parameters associated with better memory were not potentiated after α5IA compared to vehicle (treatment x novelty interaction; exploration time: $F_{1,12}$ = 0.19, P = 0.67; duration of individual explorations: $F_{1,11}$ = 0.39, P = 0.54) (Fig. 5.2.2B,C).

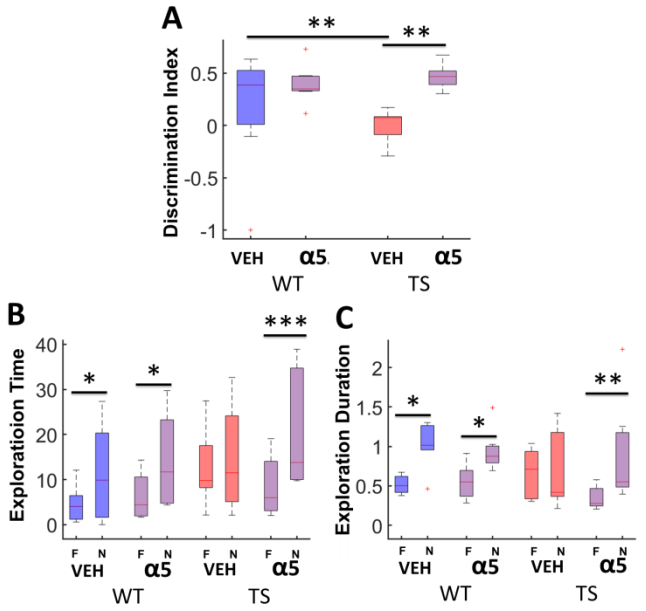

Figure 5.2.2: Behavioural effects of acute α5IA in Ts65Dn mice - (A) Discrimination indices (DI), **(B)** total exploration time and **(C)** mean duration of individual explorations of familiar (F) and novel (N) objects in WT and TS male mice injected with vehicle and α5IA thirty minutes before the familiarization phase of the NOR task.

We next evaluated the neural substrates of the pro-cognitive actions of α5IA on the PFC-HPC circuit in an open field. With age (2-3 months older), TS mice also showed alterations of PFC-HPC neural activity. We note that recordings were carried out in an open field and not in a box as when they were young adults. At this age, PFC

theta power was still exaggerated compared to their WT littermates (independent T test; WT n = 5 mice, TS n = 5, P = 0.002), together with increases of HPC theta, beta, low gamma and high gamma power (P = 0.02, 0.004, 0.005, 0.027, respectively). In addition, PFC-HPC phase synchronization at theta was still exacerbated (P = 0.01) (Fig. 5.2.3).

We compared the acute effects of α5IA with those of vehicle 25 min after the injections, for a period of five minutes (25-30 min after the injections). First, α5IA normalized excessive power of PFC theta oscillations in TS mice (paired T test, P = 0.004) and tended to reduce PFC theta in WT mice (WT n = 7 mice; P = 0.12) (Fig. 5.2.3A). A repeated measures ANOVA with drug (vehicle or α5IA) as within factor and genotype as between factor showed significance for drug with no interaction ($F_{1,12}$ = 13.16; P = 0.003). Moreover, α5IA decreased PFC low gamma activity in TS mice (P = 0.005) but not in WT mice (P = 0.8) (Fig. 6.3A). In accord, a repeated measures ANOVA showed a significant drug x genotype interaction for PFC low gamma ($F_{1,10}$ = 4.64; P = 0.05). Interestingly, α5IA effects were broader and stronger in the HPC than in the PFC. α5IA alleviated excessive HPC theta, beta, low and high gamma activity in TS mice (P = 0.007, 0.01, 0.007 and 0.02, respectively) (Fig. 5.2.3B). A repeated measures ANOVA showed a significant drug x genotype interaction for HPC theta ($F_{1,10}$ = 4.69; P = 0.05) and significant drug factor for HPC beta, low and high gamma ($F_{1,12}$ = 4.86, P = 0.04; $F_{1,12}$ = 7.01, P = 0.02; $F_{1,12}$ = 5.76, P = 0.03, respectively). Moreover, excessive PFC-HPC phase

synchronization at theta frequency was also reduced by α5IA in TS mice (paired T test, P = 0.04) (Fig. 5.2.3C). We note that despite locomotion rates were higher in TS mice compared to WT mice (WT n = 7, TS n = 8; independent T test, P = 0.005), α5IA had no effect on TS mice locomotion (α5IA vs. vehicle; TS n = 8 mice; paired T test, P = 0.6). We finally investigated the effects of α5IA on the neural signatures of memory acquisition and retrieval in the NOR task. As reported in chapter I, PFC-to-HPC theta connectivity built up during memory acquisition (late explorations during the familiarization phase) in WT young mice (Fig. 4.2.6). A PFC-to-HPC connectivity was also present in aged WT mice during memory acquisition but at a lower frequency, at delta. We speculate that this occurred because aged brain circuits generate slower rhythms. The injection of α5IA however disrupted this connectivity in WT mice as PSI became closer to zero (vehicle vs. α5IA delta PSI; paired T test; n = 5, P = 0.26). Interestingly, TS mice presented abnormal PFC-to-HPC delta connectivity that was corrected by α5IA (TS n = 5 mice, paired T test, P = 0.002) (Fig. 5.2.4A). A repeated measures ANOVA showed a significant treatment x genotype interaction for PFC-to-HPC delta PSI ($F_{1,8}$ = 17.26 P = 0.003). Moreover, α5IA nearly normalized increased PFC-HPC low gamma phase synchronization (wPLI) during memory acquisition in TS mice (P = 0.08) (Fig. 5.2.4B). Intriguingly, α5IA did not change the measures that correlated with memory retrieval in WT young adults (i.e., HPC low gamma power, PFC-HPC high gamma wPLI and HPC-to-PFC PSI at low gamma).

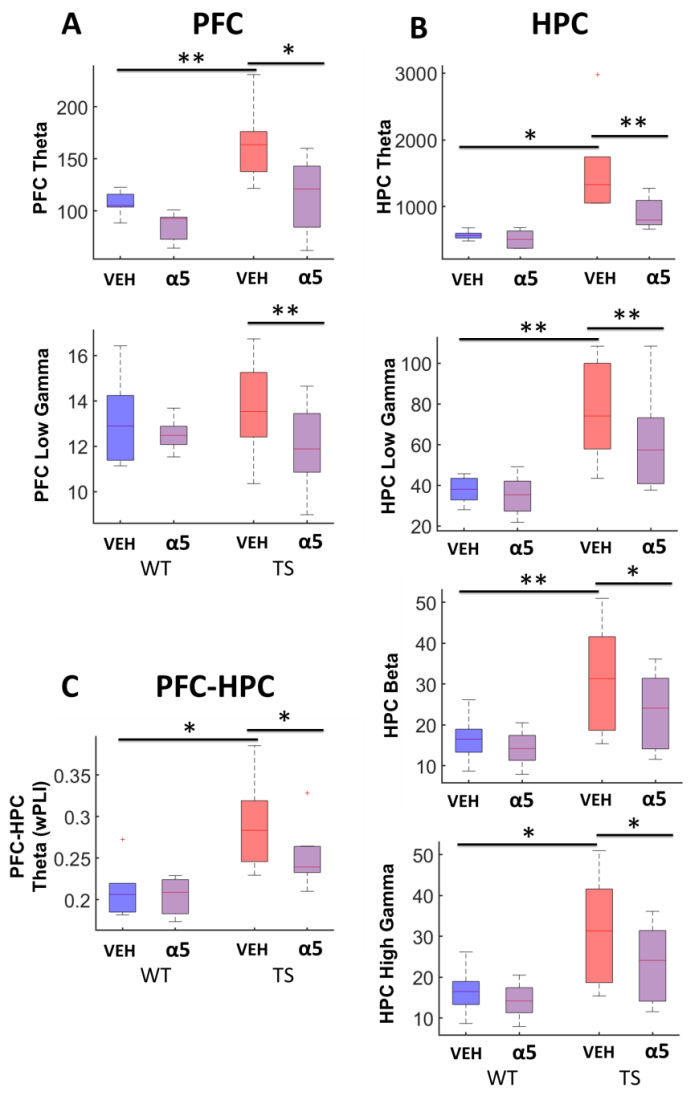

Figure 5.2.3: Acute α5IA effects on neural activity of the PFC-HPC network in Ts65Dn mice - (A) PFC theta and low gamma power, **(B)** HPC theta, beta, low and high gamma power and **(C)** PFC-HPC theta phase synchronization (wPLI) in WT and TS mice after injection with vehicle and α5IA.

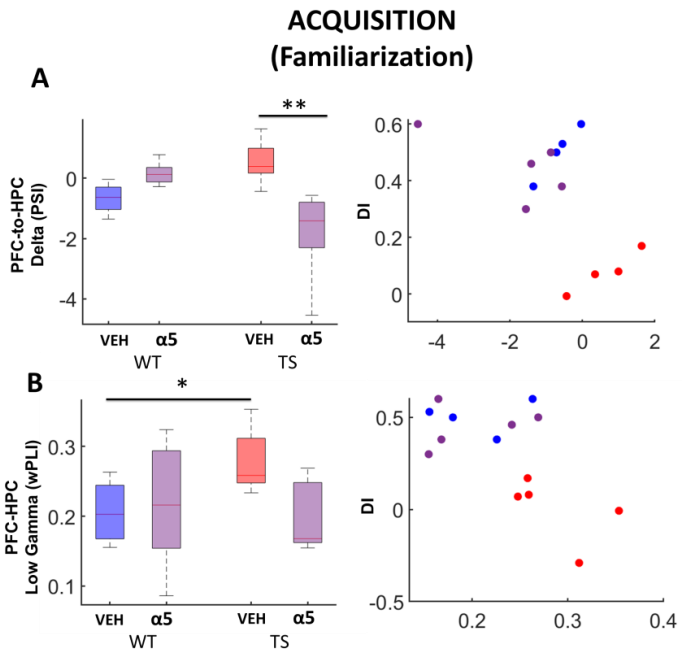

Figure 5.2.4: Acute α5IA effects on the neural activity of PFC-HPC network in Ts65Dn mice during memory acquisition in the NOR task - (A) HPC-to-PFC delta connectivity (PSI) and **(B)** PFC-HPC low gamma connectivity (wPLI) during memory acquisition in WT and TS mice after injection of vehicle (VEH) and α5IA (α5). Corresponding correlations with DIs in WT-veh (blue), TS-veh (red) and TS-α5IA (purple) are shown on the right panels.

More thorough analyses of the data will be necessary to understand the neural substrates of memory retrieval in aged mice and their susceptibility to α5IA.

Collectively, these findings suggest that α5IA might ameliorate recognition memory in TS mice by alleviating PFC-HPC increased local oscillatory activity and synchrony and, particularly, by targeting PFC-HPC communication during memory acquisition.

5.3. Environmental enrichment in Ts65Dn female mice

We finally examined the effects of an exposure to enriched environments (EE) for 7 weeks after weaning on recognition memory and the PFC-HPC circuit in TS female mice. EE ameliorates spatial memory in TS female mice, but not in TS males (Martínez-Cué et al., 2002), and improves short-term recognition memory when combined with EGCG in TS females (Catuara-Solarz et al., 2016). At a cellular level, EE increases cortical thickness, boosts the number of synapses and spines per neuron, augments dendritic branching and stimulates neurogenesis in some brain areas (Kempermann et al., n.d.; Jones and Greenough, 1996; Nilsson et al., 1999). EE also promotes HPC long-term synaptic potentiation in rats *in vitro* (Cortese et al., 2018). However, little is known about the *in vivo* effects of EE on the PFC-HPC functional circuit and the neural basis of its pro-cognitive actions remain elusive.

After weaning, natural litters composed of 2-6 TS and WT female mice were randomly exposed to either a standard non-enriched environment or an enriched environment (EE) for 7 weeks. The non-enriched environment consisted in standard Plexiglas cages (20x12x12cm) where mice were housed in groups of 2 or 3. Mice in EE conditions were housed in groups of 4-6 in cages with two levels (55x80x50 cm) with various plastic toys that were replaced every 3 days to maintain novelty. Mice were implanted during the first week after completing the 7-week rearing in both conditions and were recorded after the one-week post-surgical recovery period (Fig. 5.3.1).

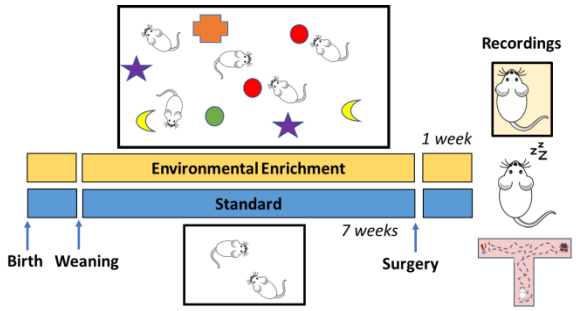

Figure 5.3.1: Protocol for the behavioural and neurophysiological assessment of post-weaning environmental enrichment.

We recorded neural activity simultaneously in the PFC and HPC of WT and TS female mice during quiet wakefulness, natural sleep and memory acquisition and retrieval via the NOR task. Overall, EE exerted strong behavioural and neurophysiological effects on TS mice. First, TS mice reared in standard conditions showed recognition memory deficits in the 24-hour memory test that were not present in 6 of 7 TS mice reared in EE conditions (DIs of standard vs. EE; independent T test; TS control, n = 7 mice, TS EE, n = 6 mice; P = 0.000005) (Fig. 5.3.2A). In WT mice, EE favoured only small improvements of memory performance, perhaps because of a ceiling effect. A two-way ANOVA with rearing condition (standard or EE) as within factor and genotype as between factor showed significance for rearing condition x genotype interaction ($F_{1,20}$ = 13.17; P = 0.002), indicating that the influence of EE on memory performance was unequal across genotypes. Discrimination indices were corrected in EE TS mice because the total exploration time and the mean duration of individual explorations were increased with respect to controls (standard vs EE; independent T

test; P = 0.013, P = 0.002, respectively), particularly explorations of novel objects (P = 0.001; P = 0.0002) (Fig. 5.3.2B,C). A repeated measures ANOVA with novel and familiar explorations (novelty) as within factor and rearing condition as between factor showed a significant novelty x rearing condition interaction for both total time and mean duration of explorations in TS mice ($F_{1,10}$ = 5,07; P = 0.048; $F_{1,10}$ = 53,57; P = 0.00002, respectively).

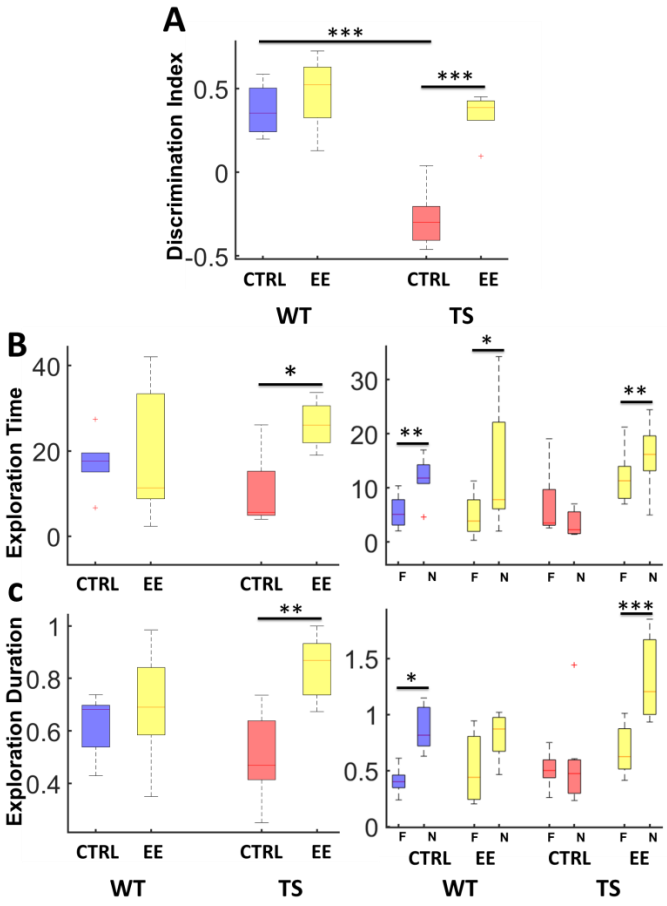

Figure 5.3.2: Behavioural effects of environmental enrichment during post-weaning periods in WT and Ts65Dn female mice - (A) Discrimination indices (DI), **(B)** total exploration time and **(C)** mean duration of individual explorations in the NOR task in WT and TS mice reared in standard and EE conditions.

Exposing post-weaning WT and TS mice to an enriched environment had profound effects on the PFC-HPC circuit during quiet wakefulness (i.e., recordings carried out in a small box where mice could move but not walk). First, EE tend to reduce TS hyperactivity (standard vs. EE accelerometer rates; independent T test; TS standard, n = 7 mice, TS EE, n = 6; P = 0.11) while slightly increasing activity in WT mice (Fig. 5.3.3A). A two-way ANOVA showed a nearly significant rearing condition x genotype interaction ($F_{1,20}$ = 3.72; P = 0.06). Interestingly, EE increased PFC and HPC single unit firing rate only in WT mice (WT standard, n = 6 mice, WT EE, n = 6 mice; P = 0.003 and 0.002, respectively), so a two-way ANOVA showed a significant rearing condition x genotype interaction (PFC FR: $F_{1,19}$ = 9.96, P = 0.005; HPC FR: $F_{1,19}$ = 6.06; P = 0.024) (Fig. 5.3.3B). In addition, EE enhanced delta oscillations in PFC and HPC and most robustly in TS mice (TS PFC delta: P = 0.007; TS HPC delta: 0.003). Moreover, EE decreased excessive PFC theta in TS mice (P = 0.06) with no effect in WT mice (Fig. 5.3.3C). Interestingly, greater EE effects were found at gamma frequencies, in line with a study by (Shinohara et al., 2013) that reported that environmental experience enhanced gamma oscillations in the HPC of Long-Evans rats. In accord, EE tended to increase low gamma power in the HPC of WT mice (P = 0.08, rearing condition x genotype interaction: $F_{1,20}$ = 9.22; P = 0.007). In TS mice it exerted the opposite by decreasing exaggerated PFC and HPC low gamma activity (P = 0.07; P = 0.02, respectively). These effects were more dramatic at high gamma frequencies. EE normalized excessive PFC and HPC high gamma activity to WT

levels in TS mice (P = 0.04; P = 0.007, respectively) while had an inverse effect in the HPC of WT mice (P = 0.02) (Fig. 5.3.3C). In agreement, a two-way ANOVA showed a significant rearing condition x genotype interaction for HPC high gamma ($F_{1,19}$ = 15.42, P = 0.001). Remarkably, EE increased specifically HPC theta-high gamma coupling in WT mice (P = 0.01; rearing condition x genotype interaction: $F_{1,21}$ = 5.28; P = 0.032) (Fig. 5.3.3D).

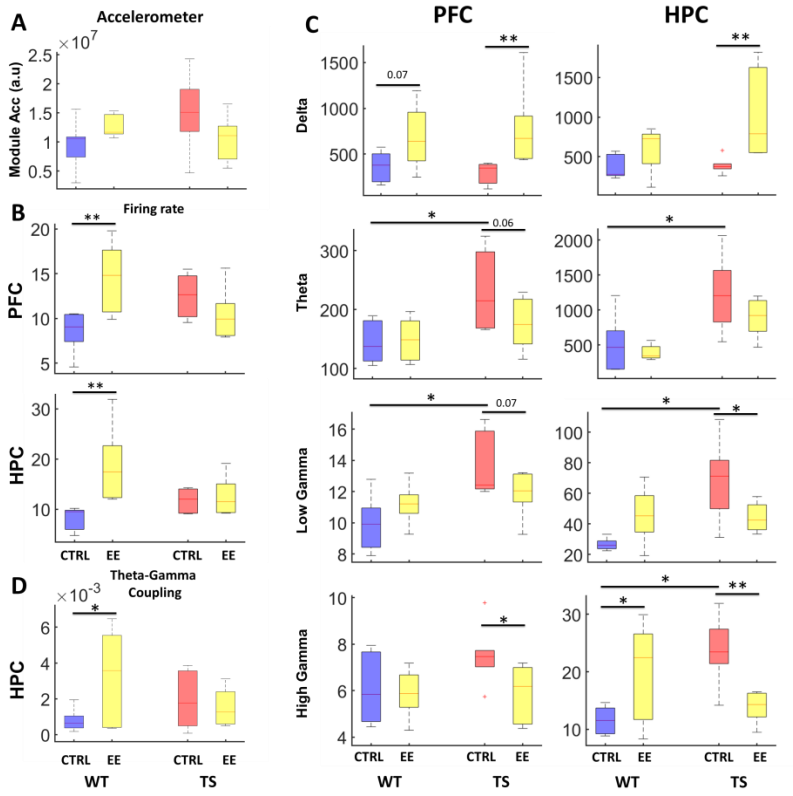

Figure 5.3.3: Effects of EE on neural activity of the PFC-HPC circuit in WT and Ts65Dn female mice during quiet wakefulness - (A) Mean locomotion (variance of the acceleration module), **(B)** mean firing rate of single neurons in PFC and HPC, **(C)** PFC and HPC power at delta, theta, low gamma and high

gamma frequencies and **(D)** HPC theta-high gamma coupling in WT and TS mice reared in standard and EE conditions.

Furthermore, exposing post-weaning WT and TS female mice to an enriched environment dramatically influenced neural activity of the HPC during NREM and REM sleep. EE fully normalized excessive HPC low and high gamma power to WT levels in TS mice ($P = 0.02$; $P = 0.0004$, respectively; rearing condition x genotype interaction: $F_{1,16} = 8.07$; $P = 0.01$; $F_{1,17} = 17.54$; $P = 0.001$, respectively) (Fig. 5.3.4A). In addition, EE normalized excessive ripple power and reduced ripple entropy in TS mice ($P = 0.007$; $P = 0.012$, respectively; rearing condition x genotype interaction: $F_{1,20} = 8.28$; $P = 0.009$; $F_{1,21} = 8.56$; $P = 0.008$, respectively), while not affecting ripple frequency (Fig. 5.3.4B). More interestingly, EE specifically decreased the excessive PFC-HPC phase synchronization (wPLI) at low gamma in TS mice ($P = 0.005$; rearing condition x genotype interaction: $F_{1,20} = 10.1$; $P = 0.005$) (Fig. 5.3.4C).

During REM sleep, EE normalized excessive HPC high gamma activity in TS mice while increasing it in WT mice (TS: $P = 0.008$; WT: $P = 0.02$; rearing condition x genotype interaction: $F_{1,16} = 14.67$; $P = 0.001$), as during NREM sleep episodes (Fig. 5.3.5A). And again, EE selectively increased HPC theta-high gamma coupling only in WT mice ($P = 0.01$) as reported in quiet wakefulness (Fig. 5.3.5B).

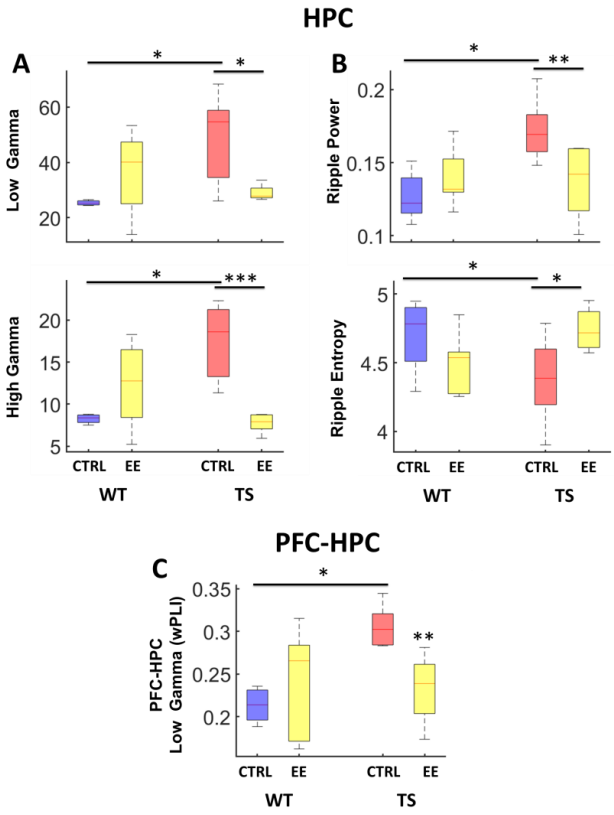

Figure 5.3.4: Effects of EE on neural activity of the PFC-HPC circuit in WT and Ts65Dn female mice during NREM sleep. (A) HPC low and high gamma power, **(B)** NREM ripple power and entropy and **(G)** PFC-HPC low gamma phase synchronization (wPLI) in WT and TS mice reared in standard and EE conditions.

Remarkably, this REM-associated HPC theta-high gamma coupling in WT mice, control and enriched combined, positively correlated with DIs (WT n = 9 mice, R = 0.66; P = 0.05), suggesting that stronger HPC theta-high gamma coupling predicts better memory performance in WT female mice (data not shown).

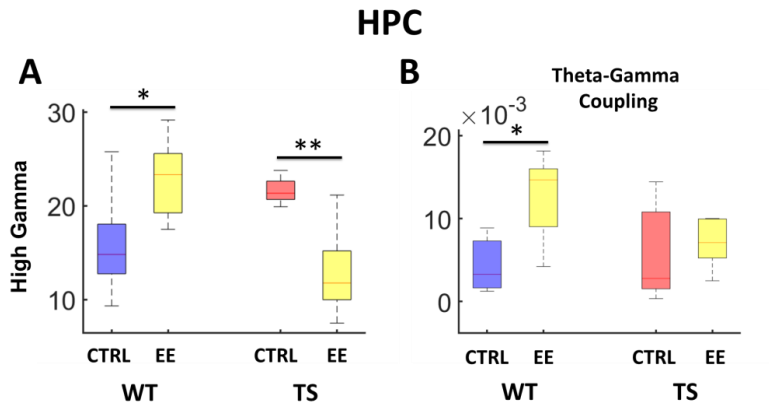

Figure 5.3.5: Effects of EE on neural activity of the PFC-HPC circuit in WT and Ts65Dn female mice during REM sleep. (A) HPC high gamma power and **(B)** HPC theta-high gamma coupling in WT and TS mice reared in standard and EE conditions. unpaired T test when comparing genotypes and posthoc differences identified by multiple comparisons in the ANOVAs with Bonferroni correction.

Noteworthy, EE selectively corrected key neurophysiological biomarkers of memory acquisition and retrieval TS mice. During memory acquisition TS females exhibited aberrant PFC-to-HPC theta PSI (Fig. 4.2.1). In addition, during memory retrieval TS females showed exaggerated HPC low and high gamma activity and altered HPC-to-PFC low gamma PSI (Fig. 4.2.11). We found that EE shifted the flow of information from PFC to HPC at theta frequencies (PSI) during events associated with memory acquisition (late explorations during the familiarization phase) in TS mice (independent T test; P = 0.06) (Fig. 5.3.6A). Unfortunately, the WT control group exhibited abnormal theta PSI during memory acquisition, advising for further replication of the experiments. However, EE also tended to shift PFC-to-HPC PSI theta in WT

mice (independent T test; P = 0.1) and a two-way ANOVA showed significance for rearing condition ($F_{1,17}$ = 6.592, P = 0.02) and not for rearing condition x genotype interaction ($F_{1,17}$ = 0.102, P = 0.7), suggesting that EE had effect in PSI theta in both genotypes. Nevertheless, EE normalized excessive HPC low and high gamma power when TS mice explored familiar objects in the 24-hour memory test (P = 0.004; P = 0.01, respectively; rearing condition x genotype interaction: $F_{1,19}$ = 13.41, P = 0.002; $F_{1,19}$ = 16.1, P = 0.001) (Fig. 5.3.6B,C). Moreover, as in quiet wakefulness and REM sleep, EE also increased HPC high gamma power in WT mice (P = 0.006) (Fig. 5.3.6C). More importantly, EE rescued the HPC-to-PFC functional connectivity at low gamma required for a proper memory retrieval (P = 0.002; rearing condition x genotype interaction: $F_{1,19}$ = 5.37, P = 0.03) (Fig. 5.3.6D).

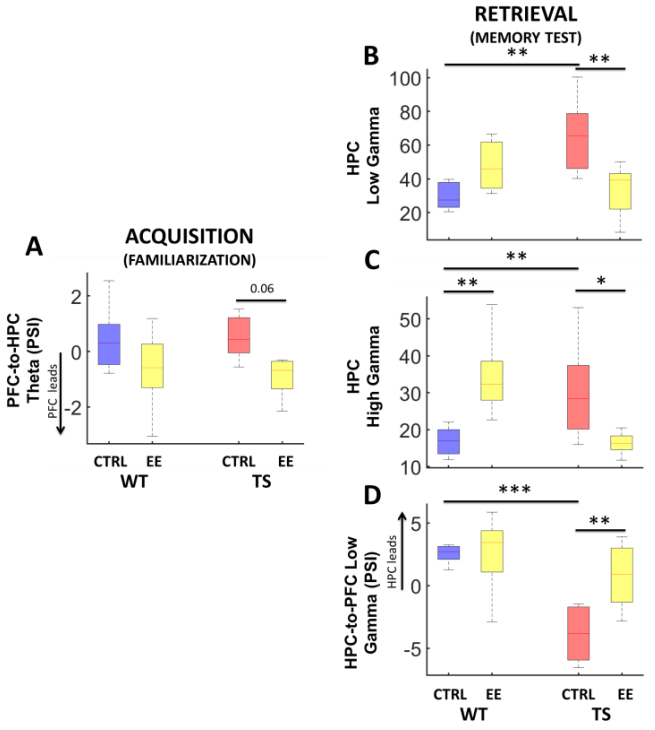

Figure 5.3.6: Effects of EE on neural activity of PFC-HPC network in WT and Ts65Dn mice during memory acquisition and retrieval in the NOR task. **(A)** PFC-to-HPC theta directionality (PSI) during memory acquisition in the NOR task. **(B)** HPC low and **(C)** high gamma power and **(D)** HPC-to-PFC low gamma directionality (PSI) during memory retrieval in the 24-hour memory test in the NOR task.

Interestingly, EE normalized pathological correlations present in control TS mice between DIs and PFC theta (Fig. 5.3.7A), ripple power (Fig. 5.3.7B) and ripple entropy (Fig. 5.3.7CIn addition, enriched TS mice showed better recognition memory accompanied by a normalization of the HPC-to-PFC low gamma PSI during memory retrieval.

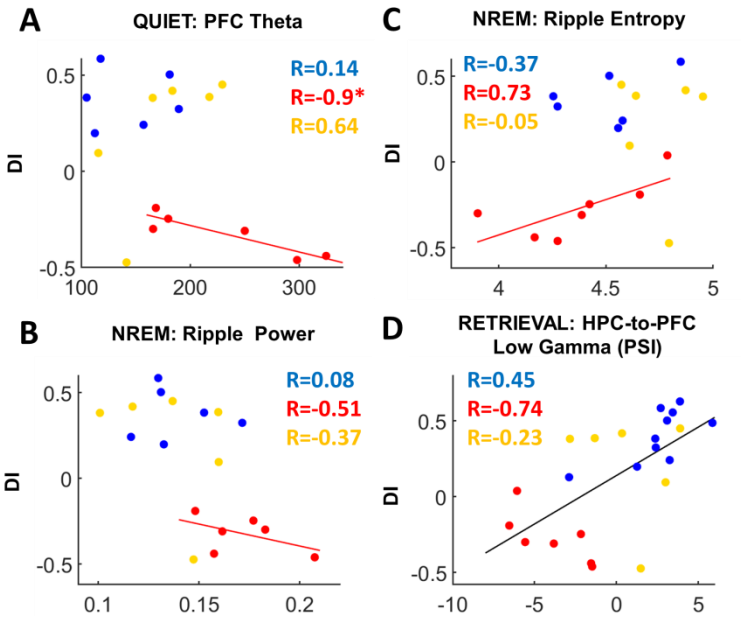

Figure 5.3.7: Effects of EE on correlations between PFC-HPC neurophysiological biomarkers and memory performance in WT and Ts65Dn mice - (A) Correlations between DIs and PFC theta power recorded during quiet wakefulness, **(B)** NREM ripple power and **(C)** ripple entropy in control WT (blue), control TS (red) and TS reared in EE conditions (yellow). **(D)** Correlations between DIs and HPC-to-PFC low gamma directionality (PSI) during memory retrieval in control WT, control TS and TS reared in EE conditions.

All three groups together showed a positive correlation between DIs and HPC-to-PFC low gamma (PSI) (n = 18; R = 0.527, P = 0.02) (Fig. 5.3.7D), supporting further the hypothesis that stronger low gamma connectivity favours better memory retrieval.

In this second chapter we have evaluated the neural substrates of three different pro-cognitive treatments in TS mice that were able to correct their memory deficits in the NOR task. EGCG, α5IA and EE normalized excessive PFC theta activity in TS mice. EGCG and EE also normalized exaggerated ripple's power in TS mice even though we could not assess α5IA effects on it. Moreover, α5IA and EE normalized increased low and high gamma activity in the HPC while α5IA also normalized theta and beta activity in the HPC. Regarding PFC-HPC communication, only α5IA could rescue exacerbated PFC-HPC theta connectivity in TS mice. However, EE normalized PFC-HPC low gamma connectivity in TS female mice.

While exploring the pro-cognitive effects underlying memory acquisition and retrieval we found that both EGCG and α5IA corrected the PFC-to-HPC theta connectivity (PSI) during memory acquisition while EGCG and EE normalized PFC-HPC gamma biomarkers during memory retrieval (see Table 4). Interestingly, EE showed a clear enhancer effect in high gamma activity in WT mice specifically in the HPC.

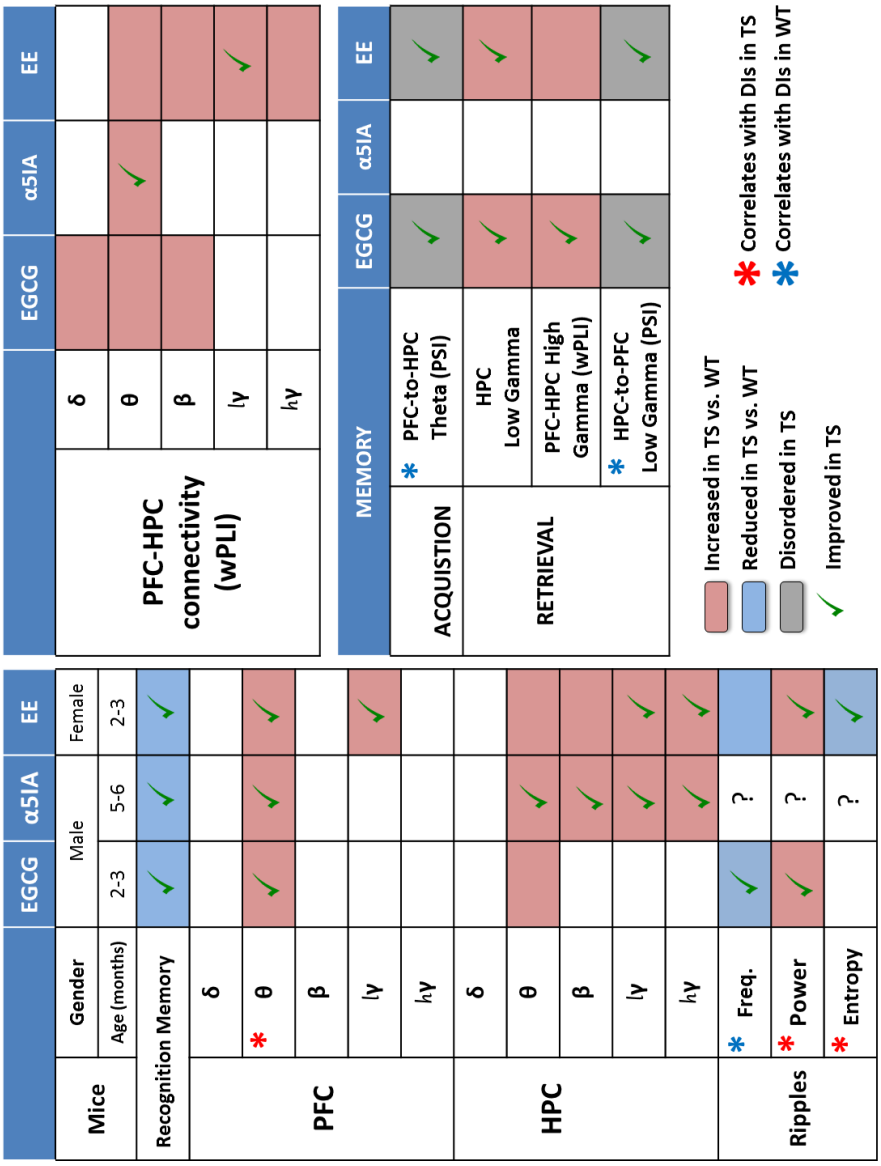

Table 4 – Summary of the pro-cognitive and neural activity effects of the three treatments on the PFC-HPC circuit in TS mice: comparison between EGCG, α5IA and EE.

6. DISCUSSION

6. DISCUSSION

In this thesis we show that Ts65Dn mice, a well-established model of DS, exhibit hypersynchronised neural activity in the PFC-HPC circuit during distinct brain states, including quiet wakefulness, natural sleep and memory performance. TS mice also showed disordered PFC-HPC communication during memory acquisition and retrieval. We postulate that this abnormal network activity could underlie cognitive deficits in DS since several of these measures correlated strongly with memory performance. The fact that three different pro-cognitive strategies rescued memory impairment and normalised some of these biomarkers in TS mice provide further support for this hypothesis.

Neurophysiological characterization of the PFC-HPC circuit was performed in male and female mice, where exaggerated oscillations and connectivity in PFC-HPC circuits were noticeable. Although cognitive measures and many PFC-HPC neurophysiological alterations were comparable across genders, in general, TS females showed broader hypersynchronisation than TS males, particularly at gamma ranges and in the HPC (Table 3). We consider that these results add scientific and social value to this work as female presence in animal models for research is under-represented. In fact, little is known about gender differences in the neuropathology of DS as most of the studies have been carried out in males. However, significant gender differences exist in patterns of gene expression (Yang et al., 2006) and in protein levels across the brain (Block et

al., 2015). Further studies are therefore necessary to determine how gender influences neuropathology in DS.

During wakefulness, TS mice of both genders displayed exaggerated theta power in the PFC and HPC. Excessive prefrontal theta oscillations correlated strongly with poor memory performance only in TS mice and were corrected by the three pro-cognitive interventions. Remarkably, PFC theta was the most consistent biomarker normalized by EGCG, α5IA and EE, so it may be a key neuropathological hallmark in trisomy 21 that contribute to cognitive impairment. Cortical theta oscillations emerge during working memory and cognitive flexibility (Lee et al., 2005; Benchenane et al., 2010; O'Neill et al., 2013) but their role during quiet wakefulness is unresolved. A DI-cortical theta correlation was not observed in WT mice, so we conclude that this amplified cortical theta in TS mice is pathological and reflects cortical hypersynchronisation of neural networks in resting states. Interestingly, previous studies have suggested that LFPs primarily reflect inhibitory neuron activity (Teleńczuk et al., 2017) and that theta oscillations in the mPFC might arise through local activity of specific subtypes of interneurons (Beierlein et al., 2000; Blatow et al., 2003). Therefore, dysregulated GABAergic neurotransmission could cause excessive theta rhythms in DS (Kleschevnikov et al., 2004). More specifically, excessive PFC theta oscillations in TS mice might originate from overinhibition produced by augmented spiking activity of local interneurons. In agreement, individual neurons in the PFC exhibited augmented firing rates in TS mice.

However, more detailed analyses of the data presented here will be necessary to determine whether increased spiking of pyramidal and/or inhibitory neurons exist in the PFC of TS mice. Additionally, TS mice overexpress G-protein coupled inward-rectifying potassium channels (GIRK2) (Best et al., 2012) that regulate frontal theta oscillations (Hesselbrock, 2012). So, excessive interneuron synchronization and GIRK2 overexpression in TS mice could result in the pathological cortical theta reported here.

Hippocampal theta oscillations were also increased in TS mice. HPC theta rhythms are involved in several cognitive processes such as spatial, time and memory processing (Korotkova et al., 2018). In agreement, Ts65Dn mice are impaired in the Morris water maze that requires proper spatial memory (Demas et al., 1998) and in the HPC-dependent spatial radial arm maze (Hyde et al., 2001). Enlarged HPC theta oscillations in our TS mice did not correlate with memory performance and were only normalized by acute α5IA. Thus, reducing overinhibition with a blocker of $GABA_A$ receptors normalises increased theta oscillations in the PFC and HPC of TS mice. These findings however disagree with those from (Hajós et al., 2004) that showed that the $GABA_A$ inverse agonist FG-7142 enhances theta oscillations in the HPC. Nevertheless, these results highlight the importance of GABAergic receptors in regulating network oscillations probably via inhibitory interneurons that generate theta oscillations (Buzsáki et al., 1983).

Cross-frequency coupling was stronger in TS male and female mice both in PFC and HPC, another sign of increased local neural synchronization. Lower-to-faster phase-amplitude modulation has been proposed to play a relevant role in information processing. In HPC, theta-gamma coupling has been linked to associative memory (Tort et al., 2009) and is enhanced in a mouse model of epilepsy that concurs with memory impairment (Maheshwari et al., 2017). The aberrant phase-amplitude coupling in TS mice may reflect a pathological state in which neural network activity is highly restricted, rendering it less able to respond dynamically to other neural signals. However, excessive cross-frequency coupling in TS mice did not correlate with DIs and was not normalized by any pro-cognitive treatment. Interestingly, EE promoted HPC theta-high gamma coupling both during quiet wakefulness and REM sleep but only in WT mice. HPC theta-gamma coupling in REM sleep has been recently suggested to underlie offline mnemonic processing (Bandarabadi et al., 2017). In fact, stronger HPC theta-gamma coupling during REM sleep predicted better memory performance in WT mice, suggesting that EE might boost cognition in healthy conditions via cross-frequency modulation.

We also investigated functional connectivity between the PFC and the HPC in TS mice. TS male mice exhibited increased PFC-HPC phase synchronization at lower frequencies, including theta ranges. TS female mice exhibited increased PFC-HPC phase synchronization at higher frequencies, including theta and gamma ranges. Further work will need to elucidate the behavioural

consequences of these gender differences in synchrony. Nevertheless, it seems as if **the PFC-HPC circuit was locked to theta oscillatory regimes in both genders**, with increased local theta power in PFC and HPC and cross-regional theta synchronization. Proper PFC-HPC synchrony is key for diverse behavioural and cognitive functions such as memory encoding, retrieval and consolidation (Preston and Eichenbaum, 2013) and PFC-HPC synchrony at theta is involved in learning processes (Benchenane et al., 2010; Sigurdsson et al., 2010; Backus et al., 2016). PFC-HPC disruption contributes to psychiatric and neurological disorders such as schizophrenia, where reduced PFC-HPC functional connectivity correlates with poor cognitive performance both in human subjects and animal models (Henseler et al., 2010; Sigurdsson et al., 2010). However, our results are consistent with the increased functional connectivity detected in the frontal cortices and temporal lobes of individuals with Down syndrome (Anderson et al., 2013; Pujol et al., 2015). Remarkably, as with PFC and HPC excessive theta, PFC-HPC theta hypersynchronisation was only rescued by the $GABA_A$ α5IA in TS mice. This strongly suggests that **augmented theta in PFC-HPC circuits may result from increased inhibitory transmission**. In TS females, EE corrected PFC-HPC theta hyperactivity in the PFC, whereas it fully rescued gamma hyperactivity (gamma power in PFC and HPC and phase synchronisation.

We also examined the PFC-HPC circuit in TS mice during natural sleep as DS subjects suffer from sleep abnormalities including

prolonged sleep latency, sustained light sleep and sleep fragmentation (Nisbet et al., 2015). TS mice experience similar symptoms that are accompanied by increased cortical theta power in the EEG during NREM and REM sleep (Colas et al., 2008). We extend these observations by reporting that TS mice exhibit smaller slow waves and amplified low gamma oscillations in the PFC during NREM sleep, likely reflecting superficial sleep states. And again, PFC-HPC theta and gamma phase synchronization was augmented compared to WT controls. During REM sleep, the "wake-like" sleep, PFC theta oscillations were larger as in quiet alertness. Our observations of increased cortical activity and cross-regional synchronization during sleep in Ts65Dn mice may explain insomnia in DS, as recently suggested by studies conducted in human subjects (Leerssen et al., 2018). In addition, we recorded HPC sharp-wave ripples during NREM sleep after the familiarization phase of the NOR task as they promote synaptic plasticity necessary for memory consolidation (Buzsáki, 1986; Wilson and McNaughton, 1994). We hypothesized that abnormal ripples could contribute to memory impairment in TS mice. In WT mice ripple frequency, but not power, correlated positively with memory performances, suggesting that animals with faster ripples consolidated memories more robustly. Conversely, ripples were remarkably slow and of larger amplitude in TS mice, as previously reported in a mouse model of Alzheimer disease (Cayzac et al., 2015), and this ripple amplification correlated negatively with memory performance. Moreover, TS females also showed more organized ripples (less entropy) than their WT peers and correlated

positively with memory performance only in TS mice. EGCG corrected ripple power in TS males whereas EE corrected both ripple power and entropy in TS females. Correlation of ripple features with memory performances and their normalisation by the pro-cognitive treatments provide strong evidence that **ripple alterations may have contributed to poor memory performance in TS mice by preventing appropriate consolidation of memories about familiar objects**.

Deficits in declarative memory in DS, including recognition memory, could arise from deficient memory consolidation, but also from poor memory acquisition, retrieval or faulty learning strategies (Vicari et al., 2000). TS mice exhibit deficient declarative memory, as revealed by abnormal spatial navigation in the Morris water maze (Reeves et al., 1995) and poor recognition of novel versus familiar objects in the NOR task (Fernandez et al., 2007; Fernandez and Garner, 2008; Dierssen, 2012; Navarro-Romero et al., 2019). In this study we further demonstrate that TS mice show smaller DIs than WT mice because the mean duration of individual explorations is shorter, particularly when interacting with novel objects. We hypothesize that this behaviour may reflect impaired attention (Alkam et al., 2011; Heller et al., 2014). In fact, EGCG, α5IA and EE normalized DIs by prolonging the duration of novel object explorations in TS mice, suggesting an amelioration of memory processing but not excluding a beneficial action on attention.

One key challenge of this thesis was to explore neural activities of the PFC-HPC circuit as candidate cellular mechanisms for memory acquisition and retrieval in the NOR task. A robust consensus exists about the key role of the HPC in recognition memory based on previous damage and lesion studies in humans and monkeys (Squire et al., 2007), while a contribution of the PFC is also acknowledged (Lepage et al., 2003). Trimper (Trimper et al., 2014) and Zheng (Zheng et al., 2016) reported that prominent gamma power arises in the HPC of rats during novel object explorations in an object-location task likely underlying memory encoding. We replicate these findings in mice by showing that HPC low gamma power increases when mice explore novel objects in the 24-hour memory test. However, in rodents, there are discrepancies about the roles played by the PFC and HPC in recognition memory beyond the agreed critical involvement of the perirhinal cortex (Brown and Aggleton, 2001; Brown and Banks, 2015). Our study strongly suggests the participation of both structures in memory acquisition and retrieval and highlights that a correct cross-regional communication is crucial. More specifically, we propose two main complementary neural mechanisms that could underlie memory acquisition and retrieval in the NOR task. Following multiple explorations of an object during the familiarization phase mice strengthened the communication between the PFC to the HPC at theta frequencies while this communication shifted directions at low gamma frequencies when they explored familiar objects in the 24-hour memory test. Crucially, greater PFC-to-HPC theta connectivity during memory acquisition and greater HPC-to-PFC gamma

connectivity during memory retrieval strongly predicted good recognition memory in WT mice. So, we conclude that **memory acquisition depends on PFC-to-HPC theta connectivity whereas memory retrieval depends on HPC-to-PFC low gamma connectivity**. Our observations agree with a previous study reporting a PFC-to-HPC theta connectivity during object sampling in a context-guided object-reward association task (Place et al., 2016). The abovementioned hypothesis is further supported by the fact that acquisition and retrieval biomarkers in WT mice were abnormal in TS mice and were consistently rescued by EGGG and EE in TS males and females, respectively.

We note that this thesis presents several limitations that should be taken into account when interpreting the results. First, treatments were not age or gender matched. Specifically, EGCG and α5IA were used in young-adult and old-adult male mice, respectively, while EE was investigated in young-adult female mice. Therefore, treatment effects on the PFC-HPC network cannot be fully compared between groups. In fact, we identified gener-specific differences in non-treated TS mice that need further investigation. More importantly, more detailed longitudinal analyses are necessary to understand the PFC-HPC circuit in aged TS mice. This is particularly relevant as TS mice show early-onset Alzheimer's disease with progressive memory loss (Granholm et al., 2000). Moreover, time and protocols where also different among the experiments examining the three therapeutic approaches. EE and EGCG were chronically administered, while α5IA was injected

acutely. Thus, further studies will be needed to comprehend α5IA chronic effects in cognition and the PFC-HPC network. In addition, it would be of high interest to combine α5IA with EGCG in a chronic protocol to assess the complementary effects of targeting both GABAergic signalling and Dyrk1A kinase over-activity in DS.

Collectively, we identified unique neurophysiological biomarkers in the PFC-HPC circuit of TS mice during distinct brain states that are candidate cellular mechanisms underlying deficient memory acquisition, memory retrieval and sleep disturbances in DS. This thesis also highlights potential neural substrates of memory rescue taking advantage of three promising therapeutic strategies in DS, EGCG, α5IA and EE.

7. CONCLUSIONS

7. CONCLUSIONS

1/ TS male and female mice show hypersynchronised neural activity in the PFC and HPC and excessive PFC-HPC connectivity during distinct brain states, particularly at theta ranges.

2/ Ripple alterations during NREM sleep may contribute to poor memory performance in TS mice.

3/ In WT mice memory acquisition is encoded by PFC-to-HPC theta connectivity whereas memory retrieval is encoded by HPC-to-PFC low gamma connectivity.

4/ In young TS mice PFC-HPC connectivity during memory acquisition and retrieval is disrupted and is corrected by chronic treatment with EGCG and EE.

5/ EGCG and cognitive stimulation may correct memory impairment in TS mice via the normalisation of HPC ripples and PFC theta hyperactivity. Cognitive stimulation has broader effects on the PFC-HPC circuit than EGCG, particularly in the HPC.

6/ Acute α5IA normalises PFC-HPC theta hypersynchronisation preferentially in the HPC. Therefore, a pathological theta in DS may results from increased GABAergic signalling.

8. BIBLIOGRAPHY

8. BIBLIOGRAPHY

Abbeduto L, Warren SF, Conners FA (2007) Language development in Down syndrome: From the prelinguistic period to the acquisition of literacy. Ment Retard Dev Disabil Res Rev 13:247–261

Adhikari A, Topiwala MA, Gordon JA (2010) Synchronized activity between the ventral hippocampus and the medial prefrontal cortex during anxiety. Neuron 65:257–269

Alkam T, Hiramatsu M, Mamiya T, Aoyama Y, Nitta A, Yamada K, Kim H-C, Nabeshima T (2011) Evaluation of object-based attention in mice. Behav Brain Res 220:185–193

Altafaj X, Dierssen M, Baamonde C, Martí E, Visa J, Guimerà J, Oset M, González JR, Flórez J, Fillat C, Estivill X (2001) Neurodevelopmental delay, motor abnormalities and cognitive deficits in transgenic mice overexpressing Dyrk1A (minibrain), a murine model of Down's syndrome. Hum Mol Genet 10:1915–1923

Alvarez P, Squire LR (1994) Memory consolidation and the medial temporal lobe: a simple network model. Proc Natl Acad Sci U S A 91:7041–7045

Anderson JS, Nielsen JA, Ferguson MA, Burback MC, Cox ET, Dai L, Gerig G, Edgin JO, Korenberg JR (2013) NeuroImage : Clinical Abnormal brain synchrony in Down Syndrome. YNICL 2:703–715

Aru J, Aru J, Priesemann V, Wibral M, Lana L, Pipa G, Singer W, Vicente R (2015) Untangling cross-frequency coupling in neuroscience. Curr Opin Neurobiol 31:51–61

Ayberk Kurt M, Ilker Kafa M, Dierssen M, Ceri Davies D (2004) Deficits of neuronal density in CA1 and synaptic density in the dentate gyrus, CA3 and CA1, in a mouse model of Down syndrome. Brain Res 1022:101–109

Backus AR, Schoffelen J-M, Szebényi S, Hanslmayr S, Doeller CF

(2016) Hippocampal-Prefrontal Theta Oscillations Support Memory Integration. Curr Biol 26:450–457

Bähner F, Demanuele C, Schweiger J, Gerchen MF, Zamoscik V, Ueltzhöffer K, Hahn T, Meyer P, Flor H, Durstewitz D, Tost H, Kirsch P, Plichta MM, Meyer-Lindenberg A (2015) Hippocampal-dorsolateral prefrontal coupling as a species-conserved cognitive mechanism: a human translational imaging study. Neuropsychopharmacology 40:1674–1681

Bandarabadi M, Boyce R, Herrera CG, Bassetti C, Williams S, Schindler K, Adamantidis A (2017) Dynamical modulation of theta-gamma coupling during REM sleep. bioRxiv:169656

Baroncelli L, Braschi C, Spolidoro M, Begenisic T, Sale A, Maffei L (2009) Nurturing brain plasticity : impact of environmental enrichment. Cell Death Differ 17:1092–1103

Baroncelli L, Braschi C, Spolidoro M, Begenisic T, Sale A, Maffei L (2010) Nurturing brain plasticity: impact of environmental enrichment. Cell Death Differ 17:1092–1103

Bastos AM, Schoffelen J-M (2016) A Tutorial Review of Functional Connectivity Analysis Methods and Their Interpretational Pitfalls. Front Syst Neurosci 9:175

Becker LE, Armstrong DL, Chan F (1986) Dendritic atrophy in children with Down's syndrome. Ann Neurol 20:520–526

Begenisic T, Spolidoro M, Braschi C, Baroncelli L, Milanese M, Pietra G, Fabbri ME, Bonanno G, Cioni G, Maffei L, Sale A (2011) Environmental enrichment decreases GABAergic inhibition and improves cognitive abilities, synaptic plasticity, and visual functions in a mouse model of Down syndrome. Front Cell Neurosci 5:29

Beierlein M, Gibson JR, Connors BW (2000) A network of electrically coupled interneurons drives synchronized inhibition in neocortex. Nat Neurosci 3:904–910

Belichenko P V., Kleschevnikov AM, Salehi A, Epstein CJ, Mobley WC (2007) Synaptic and cognitive abnormalities in mouse models of down syndrome: Exploring genotype-phenotype

relationships. J Comp Neurol 504:329–345

Benchenane K, Peyrache A, Khamassi M, Tierney PL, Gioanni Y, Battaglia FP, Wiener SI (2010) Coherent theta oscillations and reorganization of spike timing in the hippocampal- prefrontal network upon learning. Neuron 66:921–936

Best TK, Cramer NP, Chakrabarti L, Haydar TF, Galdzicki Z (2012) Dysfunctional hippocampal inhibition in the Ts65Dn mouse model of Down syndrome. Exp Neurol 233:749–757

Blatow M, Rozov A, Katona I, Hormuzdi SG, Meyer AH, Whittington MA, Caputi A, Monyer H (2003) A novel network of multipolar bursting interneurons generates theta frequency oscillations in neocortex. Neuron 38:805–817

Block A, Ahmed MM, Dhanasekaran AR, Tong S, Gardiner KJ (2015) Sex differences in protein expression in the mouse brain and their perturbations in a model of Down syndrome. Biol Sex Differ 6:24

Bokil H, Andrews P, Kulkarni JE, Mehta S, Mitra PP (2010) Chronux: a platform for analyzing neural signals. J Neurosci Methods 192:146–151

Boyce R, Glasgow SD, Williams S, Adamantidis A (2016) Causal evidence for the role of REM sleep theta rhythm in contextual memory consolidation. Science (80-) 352:812–816

Bragin A, Jandó G, Nádasdy Z, Hetke J, Wise K, Buzsáki G (1995) Gamma (40-100 Hz) oscillation in the hippocampus of the behaving rat. J Neurosci 15:47–60

Braudeau J, Dauphinot L, Duchon A, Loistron A, Dodd RH (2011a) Chronic Treatment with a Promnesiant GABA-A α 5 - Selective Inverse Agonist Increases Immediate Early Genes Expression during Memory Processing in Mice and Rectifies Their Expression Levels in a Down Syndrome Mouse Model. 2011.

Braudeau J, Delatour B, Duchon A, Pereira PL, Dauphinot L, Chaumont F De, Dodd RH (2011b) Specific targeting of the GABA-A receptor a 5 subtype by a selective inverse agonist

restores cognitive deficits in Down syndrome mice.

Braudeau J, Delatour B, Duchon A, Pereira PL, Dauphinot L, de Chaumont F, Olivo-Marin J-C, Dodd R, Hérault Y, Potier M-C (2011c) Specific targeting of the GABA-A receptor α5 subtype by a selective inverse agonist restores cognitive deficits in Down syndrome mice. J Psychopharmacol 25:1030–1042

Brennan AR, Arnsten AFT (2008) Neuronal Mechanisms Underlying Attention Deficit Hyperactivity Disorder: The Influence of Arousal on Prefrontal Cortical Function. Ann N Y Acad Sci 1129:236

Brincat SL, Miller EK (2015) Frequency-specific hippocampal-prefrontal interactions during associative learning. Nat Neurosci 18:576–581

Brown MW, Aggleton JP (2001) Recognition memory: What are the roles of the perirhinal cortex and hippocampus? Nat Rev Neurosci 2:51–61

Brown MW, Banks PJ (2015) In search of a recognition memory engram. Neurosci Biobehav Rev 50:12–28 Available at: http://www.ncbi.nlm.nih.gov/pubmed/25280908

Buzsáki G (1986) Hippocampal sharp waves: their origin and significance. Brain Res 398:242–252

Buzsáki G (2015) Hippocampal sharp wave-ripple: A cognitive biomarker for episodic memory and planning. Hippocampus 25:1073–1188

Buzsaki G, Draguhn A (2004) Neuronal Oscillations in Cortical Networks. Science (80-) 304:1926–1929

Buzsáki G, Leung LW, Vanderwolf CH (1983) Cellular bases of hippocampal EEG in the behaving rat. Brain Res 287:139–171

Buzsáki G, Watson BO (2012) Brain rhythms and neural syntax: implications for efficient coding of cognitive content and neuropsychiatric disease. Dialogues Clin Neurosci 14:345–367

Carter CS, Perlstein W, Ganguli R, Brar J, Mintun M, Cohen JD (1998) Functional Hypofrontality and Working Memory

Dysfunction in Schizophrenia. Am J Psychiatry 155:1285–1287

Catuara-Solarz S, Espinosa-Carrasco J, Erb I, Langohr K, Gonzalez JR, Notredame C, Dierssen M (2016) Combined Treatment With Environmental Enrichment and (-)-Epigallocatechin-3-Gallate Ameliorates Learning Deficits and Hippocampal Alterations in a Mouse Model of Down Syndrome. eNeuro 3

Cayzac S, Mons N, Ginguay A, Allinquant B, Jeantet Y, Cho YH (2015) Altered hippocampal information coding and network synchrony in APP-PS1 mice. Neurobiol Aging 36:3200–3213

Chapman RS, Hesketh LJ (2000) Behavioral phenotype of individuals with Down syndrome. Ment Retard Dev Disabil Res Rev 6:84–95

Colas D, Valletta JS, Takimoto-Kimura R, Nishino S, Fujiki N, Mobley WC, Mignot E (2008) Sleep and EEG features in genetic models of Down syndrome. Neurobiol Dis 30:1–7

Condé F, Maire-Lepoivre E, Audinat E, Crépel F (1995) Afferent connections of the medial frontal cortex of the rat. II. Cortical and subcortical afferents. J Comp Neurol 352:567–593

Contestabile A, Magara S, Cancedda L (2017) The GABAergic Hypothesis for Cognitive Disabilities in Down Syndrome. Front Cell Neurosci 11:54

Corkin S, Amaral DG, González RG, Johnson KA, Hyman BT (1997) H. M.'s medial temporal lobe lesion: findings from magnetic resonance imaging. J Neurosci 17:3964–3979

Cortese GP, Olin A, O'Riordan K, Hullinger R, Burger C (2018) Environmental enrichment improves hippocampal function in aged rats by enhancing learning and memory, LTP, and mGluR5-Homer1c activity. Neurobiol Aging 63:1–11

Costa ACS, Grybko MJ (2005) Deficits in hippocampal CA1 LTP induced by TBS but not HFS in the Ts65Dn mouse: A model of Down syndrome. Neurosci Lett 382:317–322

Coussons-Read ME, Crnic LS (1996) Behavioral assessment of the

Ts65Dn mouse, a model for Down syndrome: altered behavior in the elevated plus maze and open field. Behav Genet 26:7–13

Crossley NA, Mechelli A, Fusar-Poli P, Broome MR, Matthiasson P, Johns LC, Bramon E, Valmaggia L, Williams SCR, McGuire PK (2009) Superior temporal lobe dysfunction and frontotemporal dysconnectivity in subjects at risk of psychosis and in first-episode psychosis. Hum Brain Mapp 30:4129–4137

Csicsvari J, O'Neill J, Allen K, Senior T (2007) Place-selective firing contributes to the reverse-order reactivation of CA1 pyramidal cells during sharp waves in open-field exploration. Eur J Neurosci 26:704–716

Dawson GR, Maubach KA, Collinson N, Cobain M, Everitt BJ, MacLeod AM, Choudhury HI, McDonald LM, Pillai G, Rycroft W, Smith AJ, Sternfeld F, Tattersall FD, Wafford KA, Reynolds DS, Seabrook GR, Atack JR (2005) An Inverse Agonist Selective for 5 Subunit-Containing GABAA Receptors Enhances Cognition. J Pharmacol Exp Ther 316:1335–1345

de la Torre R et al. (2016) Safety and efficacy of cognitive training plus epigallocatechin-3-gallate in young adults with Down's syndrome (TESDAD): a double-blind, randomised, placebo-controlled, phase 2 trial. Lancet Neurol 15:801–810.

de la Torre R et al. (2019) A phase 1, randomized double-blind, placebo controlled trial to evaluate safety and efficacy of epigallocatechin-3-gallate and cognitive training in adults with Fragile X syndrome. Clin Nutr

De la Torre R et al. (2014) Epigallocatechin-3-gallate, a DYRK1A inhibitor, rescues cognitive deficits in Down syndrome mouse models and in humans. Mol Nutr Food Res.

De La Torre R et al. (2013) Epigallocatechin-3-gallate, a DYRK1A inhibitor, rescues cognitive deficits in Down syndrome mouse models and in humans. Mol Nutr Food Res Mol Nutr Food Res 0:1–11.

del Pino I, García-Frigola C, Dehorter N, Brotons-Mas JR, Alvarez-

Salvado E, Martínez de Lagrán M, Ciceri G, Gabaldón MV, Moratal D, Dierssen M, Canals S, Marín O, Rico B (2013) Erbb4 Deletion from Fast-Spiking Interneurons Causes Schizophrenia-like Phenotypes. Neuron 79:1152–1168

Demas GE, Nelson RJ, Krueger BK, Yarowsky PJ (1998) Impaired spatial working and reference memory in segmental trisomy (Ts65Dn) mice. Behav Brain Res 90:199–201

Dierssen M (2003) Alterations of Neocortical Pyramidal Cell Phenotype in the Ts65Dn Mouse Model of Down Syndrome : Effects of Environmental Enrichment. :758–764.

Dierssen M (2012) Down syndrome: the brain in trisomic mode. Nat Rev Neurosci 13:844–858

Driscoll LL, Carroll JC, Moon J, Crnic LS, Levitsky DA, Strupp BJ (2004) Impaired Sustained Attention and Error-Induced Stereotypy in the Aged Ts65Dn Mouse: A Mouse Model of Down Syndrome and Alzheimer's Disease. Behav Neurosci 118:1196–1205

Duchon A, Raveau M, Chevalier C, Nalesso V, Sharp AJ, Herault Y (2011) Identification of the translocation breakpoints in the Ts65Dn and Ts1Cje mouse lines: relevance for modeling Down syndrome. Mamm Genome 22:674–684

Ego-Stengel V, Wilson MA (2009) Disruption of ripple-associated hippocampal activity during rest impairs spatial learning in the rat. Hippocampus 20:NA-NA

Eichenbaum H (2004) Review Hippocampus: Cognitive Processes and Neural Representations that Underlie Declarative Memory A Simple Model of Hippocampal Information Processing There are many diverse views about the underlying mechanisms by which hippocampus supports declara-tive memory. Differing perspectives emphasize the pro.

Ellingson RJ, Peters JF (1980) Development of EEG and daytime sleep patterns in Trisomy-21 infants during the first year of life: longitudinal observations. Electroencephalogr Clin Neurophysiol 50:457–466 Available at: http://www.ncbi.nlm.nih.gov/pubmed/6160988

Engevik LI, Næss K-AB, Hagtvet BE (2016) Cognitive stimulation of pupils with Down syndrome: A study of inferential talk during book-sharing. Res Dev Disabil 55:287–300

Escorihuela RM, Vallina IF, Martínez-Cué C, Baamonde C, Dierssen M, Tobeña A, Flórez J, Fernández-Teruel A (1998) Impaired short- and long-term memory in Ts65Dn mice, a model for Down syndrome. Neurosci Lett 247:171–174

Faizi M, Bader PL, Tun C, Encarnacion A, Kleschevnikov A, Belichenko P, Saw N, Priestley M, Tsien RW, Mobley WC, Shamloo M (2011) Comprehensive behavioral phenotyping of Ts65Dn mouse model of Down Syndrome: Activation of β1-adrenergic receptor by xamoterol as a potential cognitive enhancer. Neurobiol Dis 43:397–413

Fernandez F, Edgin JO (2013) Poor Sleep as a Precursor to Cognitive Decline in Down Syndrome : A Hypothesis. J Alzheimer's Dis Park 3:124

Fernandez F, Garner CC (2008) Episodic-like memory in Ts65Dn, a mouse model of Down syndrome. Behav Brain Res 188:233–237

Fernandez F, Morishita W, Zuniga E, Nguyen J, Blank M, Malenka RC, Garner CC (2007) Pharmacotherapy for cognitive impairment in a mouse model of Down syndrome. Nat Neurosci 10:411–413

Friese U, Köster M, Hassler U, Martens U, Trujillo-Barreto N, Gruber T (2013) Successful memory encoding is associated with increased cross-frequency coupling between frontal theta and posterior gamma oscillations in human scalp-recorded EEG. Neuroimage 66:642–647

Godfrey M, Lee NR (2018) Memory profiles in Down syndrome across development: a review of memory abilities through the lifespan. J Neurodev Disord 10:5

Grady CL, McIntosh AR, Beig S, Keightley ML, Burian H, Black SE (2003) Evidence from functional neuroimaging of a compensatory prefrontal network in Alzheimer's disease. J Neurosci 23:986–993

Granholm A-CE, Sanders LA, Crnic LS (2000) Loss of Cholinergic Phenotype in Basal Forebrain Coincides with Cognitive Decline in a Mouse Model of Down's Syndrome. Exp Neurol 161:647–663

Guimera J, Casas C, Estivill X, Pritchard M (1999) HumanMinibrainHomologue (MNBH/DYRK1): Characterization, Alternative Splicing, Differential Tissue Expression, and Overexpression in Down Syndrome. Genomics 57:407–418

Gulinello M, Mitchell HA, Chang Q, Timothy O'brien W, Zhou Z, Abel T, Wang L, Corbin JG, Veeraragavan S, Samaco RC, Andrews NA, Fagiolini M, Cole TB, Burbacher TM, Crawley JN (2018) Rigor and reproducibility in rodent behavioral research.

Guralnick MJ (2016) Early Intervention for Children with Intellectual Disabilities:

Hajós M, Hoffmann WE, Orbán G, Kiss T, Érdi P (2004) Modulation of septo-hippocampal θ activity by GABAA receptors: an experimental and computational approach. Neuroscience 126:599–610

Hardmeier M, Hatz F, Bousleiman H, Schindler C, Stam CJ, Fuhr P (2014) Reproducibility of functional connectivity and graph measures based on the phase lag index (PLI) and weighted phase lag index (wPLI) derived from high resolution EEG. PLoS One 9:e108648

Headley DB, Paré D (2017) Common oscillatory mechanisms across multiple memory systems. npj Sci Learn 2:1

HEBB, DO (1947) The effects of early experience on problem-solving at maturity. Am Psychol 2:306–307

Helfrich RF, Knight RT (2016) Oscillatory Dynamics of Prefrontal Cognitive Control. Trends Cogn Sci 20:916–930

Heller HC, Salehi A, Chuluun B, Das D, Lin B, Moghadam S, Garner CC, Colas D (2014) Nest building is impaired in the Ts65Dn mouse model of Down syndrome and rescued by

blocking 5HT2a receptors. Neurobiol Learn Mem 116:162–171

Heller T, Hsieh K, Rimmer JH (2004) Attitudinal and Psychosocial Outcomes of a Fitness and Health Education Program on Adults With Down Syndrome. Am J Ment Retard 109:175

Henseler I, Falkai P, Gruber O (2010) Disturbed functional connectivity within brain networks subserving domain-specific subcomponents of working memory in schizophrenia: relation to performance and clinical symptoms. J Psychiatr Res 44:364–372

Hesselbrock VM (2012) Family-based Genome-wide Association Study of Frontal Theta Oscillations Identifies Potassium Channel Gene KCNJ6.

Hoffmire CA, Magyar CI, Connolly H V, Fernandez ID, van Wijngaarden E (2014) High prevalence of sleep disorders and associated comorbidities in a community sample of children with Down syndrome. J Clin Sleep Med 10:411–419

Horwitz B, McIntosh AR, Haxby J V, Furey M, Salerno JA, Schapiro MB, Rapoport SI, Grady CL (1995) Network analysis of PET-mapped visual pathways in Alzheimer type dementia. Neuroreport 6:2287–2292

Hunter CL, Bimonte HA, Granholm ACE (2003) Behavioral comparison of 4 and 6 month-old Ts65Dn mice: age-related impairments in working and reference memory. Behav Brain Res 138:121–131

Hyde LA, Frisone DF, Crnic LS (2001) Ts65Dn mice, a model for Down syndrome, have deficits in context discrimination learning suggesting impaired hippocampal function. Behav Brain Res 118:53–60

Jones MW, Wilson MA (2005) Theta rhythms coordinate hippocampal-prefrontal interactions in a spatial memory task. PLoS Biol 3:e402-

Jones TA, Greenough WT (1996) Ultrastructural Evidence for Increased Contact between Astrocytes and Synapses in Rats

Reared in a Complex Environment. Neurobiol Learn Mem 65:48–56

Kelley CM, Powers BE, Velazquez R, Ash JA, Ginsberg SD, Strupp BJ, Mufson EJ (2014) Sex Differences in the Cholinergic Basal Forebrain in the Ts65Dn Mouse Model of Down Syndrome and Alzheimer's Disease. Brain Pathol 24:33–44

Kempermann G, Brandon EP, Gage FH (n.d.) Environmental stimulation of 129/SvJ mice causes increased cell proliferation and neurogenesis in the adult dentate gyrus. Curr Biol 8:939–942

Kim JJ, Fanselow MS (1992) Modality-specific retrograde amnesia of fear. Science 256:675–677 Available at: http://www.ncbi.nlm.nih.gov/pubmed/1585183

Kleschevnikov AM, Belichenko P V, Villar AJ, Epstein CJ, Malenka RC, Mobley WC (2004) Hippocampal Long-Term Potentiation Suppressed by Increased Inhibition in the Ts65Dn Mouse, a Genetic Model of Down Syndrome. J Neurosci 24:8153–8160

Korotkova T, Ponomarenko A, Monaghan CK, Poulter SL, Cacucci F, Wills T, Hasselmo ME, Lever C (2018) Reconciling the different faces of hippocampal theta: The role of theta oscillations in cognitive, emotional and innate behaviors. Neurosci Biobehav Rev 85:65–80

Lee H, Simpson G V., Logothetis NK, Rainer G (2005) Phase Locking of Single Neuron Activity to Theta Oscillations during Working Memory in Monkey Extrastriate Visual Cortex. Neuron 45:147–156

Leerssen J, Wassing R, Ramautar JR, Stoffers D, Lakbila-Kamal O, Perrier J, Bruijel J, Foster-Dingley JC, Aghajani M, van Someren EJW (2018) Increased hippocampal-prefrontal functional connectivity in insomnia. Neurobiol Learn Mem

Leger M, Quiedeville A, Bouet V, Haelewyn B, Boulouard M, Schumann-Bard P, Freret T (2013) Object recognition test in mice. Nat Protoc 8:2531–2537

Lepage M, Brodeur M, Bourgouin P (2003) Prefrontal cortex contribution to associative recognition memory in humans: an event-related functional magnetic resonance imaging study. Neurosci Lett 346:73–76

Maheshwari A, Akbar A, Wang M, Marks RL, Yu K, Park S, Foster BL, Noebels JL (2017) Persistent aberrant cortical phase-amplitude coupling following seizure treatment in absence epilepsy models. J Physiol 595:7249–7260

Marin-Padilla M (1976) Pyramidal cell abnormalities in the motor cortex of a child with Down's syndrome. A Golgi study. J Comp Neurol 167:63–81 Available at: http://www.ncbi.nlm.nih.gov/pubmed/131810

Martínez-Cué C, Baamonde C, Lumbreras M, Paz J, Davisson MT, Schmidt C, Dierssen M, Flórez J (2002) Differential effects of environmental enrichment on behavior and learning of male and female Ts65Dn mice, a model for Down syndrome. Behav Brain Res 134:185–200

Martinez-Cue C, Rueda N, Garcia E, Florez J (2006) Anxiety and panic responses to a predator in male and female Ts65Dn mice, a model for Down syndrome. Genes, Brain Behav 5:413–422

Miller EK (2000) The prefontral cortex and cognitive control. Nat Rev Neurosci 1:59–65

Morgan M, Moni KB, Jobling A (2004) What's it all about? Investigating reading comprehension strategies in young adults with down syndrome. Down's Syndr Res Pract J Sarah Duffen Cent 9:37–44

Nadel L (2003) Down's syndrome: a genetic disorder in biobehavioral perspective. Genes, Brain Behav 2:156–166

Navarro-Romero A, Vázquez-Oliver A, Gomis-González M, Garzón-Montesinos C, Falcón-Moya R, Pastor A, Martín-García E, Pizarro N, Busquets-Garcia A, Revest J-M, Piazza P-V, Bosch F, Dierssen M, de la Torre R, Rodríguez-Moreno A, Maldonado R, Ozaita A (2019) Cannabinoid type-1 receptor blockade restores neurological phenotypes in two models for Down syndrome. Neurobiol Dis 125:92–106

Negrón-Oyarzo I, Espinosa N, Aguilar-Rivera M, Fuenzalida M, Aboitiz F, Fuentealba P (2018) Coordinated prefrontal–hippocampal activity and navigation strategy-related prefrontal firing during spatial memory formation. Proc Natl Acad Sci 115:7123–7128

Newpher TM, Ehlers MD (2009) Spine microdomains for postsynaptic signaling and plasticity. Trends Cell Biol 19:218–227

Nilsson M, Perfilieva E, Johansson U, Orwar O, Eriksson PS (1999) Enriched environment increases neurogenesis in the adult rat dentate gyrus and improves spatial memory. J Neurobiol 39:569–578

Nisbet LC, Phillips NN, Hoban TF, O'Brien LM (2015) Characterization of a sleep architectural phenotype in children with Down syndrome. Sleep Breath 19:1065–1071

Nolte G, Ziehe A, Nikulin V V, Schlögl A, Krämer N, Brismar T, Müller K-R (2007) Robustly Estimating the Flow Direction of Information in Complex Physical Systems.

Nyhus E, Curran T (2010) Functional role of gamma and theta oscillations in episodic memory. Neurosci Biobehav Rev 34:1023–1035

O'Neill P-K, Gordon JA, Sigurdsson T (2013) Theta Oscillations in the Medial Prefrontal Cortex Are Modulated by Spatial Working Memory and Synchronize with the Hippocampus through Its Ventral Subregion. J Neurosci 33:14211–14224

Paneri S, Gregoriou GG (2017) Top-Down Control of Visual Attention by the Prefrontal Cortex. Functional Specialization and Long-Range Interactions. Front Neurosci 11:545

Pennington BF, Moon J, Edgin J, Stedron J, Nadel L (n.d.) The neuropsychology of Down syndrome: evidence for hippocampal dysfunction. Child Dev 74:75–93

Place R, Farovik A, Brockmann M, Eichenbaum H (2016) Bidirectional prefrontal-hippocampal interactions support context-guided memory. Nat Neurosci.

Powers BE, Velazquez R, Kelley CM, Ash JA, Strawderman MS, Alldred MJ, Ginsberg SD, Mufson EJ, Strupp BJ (2016) Attentional function and basal forebrain cholinergic neuron morphology during aging in the Ts65Dn mouse model of Down syndrome. Brain Struct Funct.

Preston AR, Eichenbaum H (2013) Interplay of hippocampus and prefrontal cortex in memory. Curr Biol.

Pujol J, del Hoyo L, Blanco-Hinojo L, de Sola S, Macià D, Martínez-Vilavella G, Amor M, Deus J, Rodríguez J, Farré M, Dierssen M, de la Torre R (2015) Anomalous brain functional connectivity contributing to poor adaptive behavior in Down syndrome. Cortex.

Ramadan W, Eschenko O, Sara SJ (2009) Hippocampal Sharp Wave/Ripples during Sleep for Consolidation of Associative Memory Dickson CT, ed. PLoS One 4:e6697

Raveau M, Polygalov D, Boehringer R, Amano K, Yamakawa K, Mchugh TJ (2018) Alterations of in vivo CA1 network activity in Dp(16)1Yey Down syndrome model mice.

Reeves RH, Irving NG, Moran TH, Wohn A, Kitt C, Sisodia SS, Schmidt C, Bronson RT, Davisson MT (1995) A mouse model for Down syndrome exhibits learning and behaviour deficits. Nat Genet 11:177–184

Rosano C, Aizenstein HJ, Cochran JL, Saxton JA, De Kosky ST, Newman AB, Kuller LH, Lopez OL, Carter CS (2005) Event-related functional magnetic resonance imaging investigation of executive control in very old individuals with mild cognitive impairment. Biol Psychiatry 57:761–767

Rosen AM, Spellman T, Gordon JA (2015) Review Electrophysiological Endophenotypes in Rodent Models of Schizophrenia and Psychosis. Biol Psychiatry 77:1041–1049

Rueda N, Flórez J, Martínez-Cué C (2012) Mouse Models of Down Syndrome as a Tool to Unravel the Causes of Mental Disabilities. Neural Plast 2012:1–26

Ruiz-Mejias M, Martinez de Lagran M, Mattia M, Castano-Prat P,

Perez-Mendez L, Ciria-Suarez L, Gener T, Sancristobal B, García-Ojalvo J, Gruart A, Delgado-García JM, Sanchez-Vives M V., Dierssen M (2016) Overexpression of *Dyrk1A* , a Down Syndrome Candidate, Decreases Excitability and Impairs Gamma Oscillations in the Prefrontal Cortex. J Neurosci 36:3648–3659

Scoviille WB, Milner B (1957) LOSS OF RECENT MEMORY AFTER BILATERAL HIPPOCAMPAL LESIONS.

Shinohara Y, Hosoya A, Hirase H (2013) Experience enhances gamma oscillations and interhemispheric asymmetry in the hippocampus. Nat Commun 4:1652

Siapas AG, Lubenov E V, Wilson M a (2005) Prefrontal phase locking to hippocampal theta oscillations. Neuron 46:141–151

Siarey RJ, Carlson EJ, Epstein CJ, Balbo A, Rapoport SI, Galdzicki Z (1999) Increased synaptic depression in the Ts65Dn mouse, a model for mental retardation in Down syndrome. Neuropharmacology 38:1917–1920

Sigurdsson T, Duvarci S (2015) Hippocampal-Prefrontal Interactions in Cognition, Behavior and Psychiatric Disease. Front Syst Neurosci 9:190

Sigurdsson T, Stark KL, Karayiorgou M, Gogos JA, Gordon JA (2010) Impaired hippocampal-prefrontal synchrony in a genetic mouse model of schizophrenia. Nature 464:763–767

Smith C (2001) Sleep states and memory processes in humans: procedural versus declarative memory systems. Sleep Med Rev 5:491–506

Sorra KE, Harris KM (2000) Overview on the structure, composition, function, development, and plasticity of hippocampal dendritic spines. Hippocampus 10:501–511

Spellman T, Rigotti M, Ahmari SE, Fusi S, Gogos JA, Gordon JA (2015) Hippocampal-prefrontal input supports spatial encoding in working memory. Nature.

Squire LR, Wixted JT, Clark RE (2007) Recognition memory and

the medial temporal lobe: a new perspective. Nat Rev Neurosci 8:872–883

Sternfeld F, Carling RW, Jelley RA, Ladduwahetty T, Merchant KJ, Moore KW, Reeve AJ, Street LJ, O'Connor D, Sohal B, Atack JR, Cook S, Seabrook G, Wafford K, Tattersall FD, Collinson N, Dawson GR, Castro JL, MacLeod AM (2004) Selective, Orally Active γ-Aminobutyric Acid $_A$ α5 Receptor Inverse Agonists as Cognition Enhancers. J Med Chem 47:2176–2179

Suetsugu M, Mehraein P (1980) Spine distribution along the apical dendrites of the pyramidal neurons in Down's syndrome. A quantitative Golgi study. Acta Neuropathol 50:207–210

Teipel SJ, Schapiro MB, Alexander GE, Krasuski JS, Horwitz B, Hoehne C, Möller H-J, Rapoport SI, Hampel H (2003) Relation of Corpus Callosum and Hippocampal Size to Age in Nondemented Adults With Down's Syndrome. Am J Psychiatry 160:1870–1878

Tejedor FJ, Hämmerle B (2011) MNB/DYRK1A as a multiple regulator of neuronal development. FEBS J 278:223–235

Teleńczuk B, Dehghani N, Le Van Quyen M, Cash SS, Halgren E, Hatsopoulos NG, Destexhe A (2017) Local field potentials primarily reflect inhibitory neuron activity in human and monkey cortex. Sci Rep 7:40211

Tort ABL, Komorowski RW, Manns JR, Kopell NJ, Eichenbaum H (2009) Theta-gamma coupling increases during the learning of item-context associations. Proc Natl Acad Sci.

Trimper JB, Galloway CR, Jones AC, Mandi K, Manns JR (2017) Gamma Oscillations in Rat Hippocampal Subregions Dentate Gyrus, CA3, CA1, and Subiculum Underlie Associative Memory Encoding. Cell Rep.

Trimper JB, Stefanescu RA, Manns JR (2014) Recognition memory and theta-gamma interactions in the hippocampus. Hippocampus.

Uhlhaas P, Pipa G, Lima B, Melloni L, Neuenschwander S, Nikolić D, Singer W (2009) Neural synchrony in cortical networks:

history, concept and current status. Front Integr Neurosci 3:17

Valero M, Averkin RG, Fernandez-lamo I, Cid E, Tamas G, Valero M, Averkin RG, Fernandez-lamo I, Aguilar J, Lopez-pigozzi D, Brotons-mas JR, Cid E, Tamas G, Menendez L, Prida D (2017) Mechanisms for Selective Single-Cell Reactivation during Offline Sharp-Wave Ripples and Their Distortion by Fast Ripples Article Mechanisms for Selective Single-Cell Reactivation during Offline Sharp-Wave Ripples and Their Distortion by Fast Ripples. Neuron 94:1234–1247.e7

van Praag H, Kempermann G, Gage FH (2000) Neural consequences of enviromental enrichment. Nat Rev Neurosci 1:191–198

Verret L, Mann EO, Hang GB, Barth AMI, Cobos I, Ho K, Devidze N, Masliah E, Kreitzer AC, Mody I, Mucke L, Palop JJ (2012) Inhibitory interneuron deficit links altered network activity and cognitive dysfunction in Alzheimer model. Cell 149:708–721

Vertes RP (2006) Interactions among the medial prefrontal cortex, hippocampus and midline thalamus in emotional and cognitive processing in the rat. Neuroscience 142:1–20.

Vicari S, Bellucci S, Carlesimo GA (2000) Implicit and explicit memory: a functional dissociation in persons with Down syndrome. Neuropsychologia 38:240–251

Vinck M, Oostenveld R, Van Wingerden M, Battaglia F, Pennartz MA (2011) An improved index of phase-synchronization for electrophysiological data in the presence of volume-conduction, noise and sample-size bias.

Voss MW, Vivar C, Kramer AF, van Praag H (2013) Bridging animal and human models of exercise-induced brain plasticity. Trends Cogn Sci 17:525–544

Warburton EC, Brown MW (2015) Neural circuitry for rat recognition memory. Behav Brain Res 285:131–139

Ward LM (2003) Synchronous neural oscillations and cognitive processes. Trends Cogn Sci 7:553–559

Watson BO, Buzsáki G (2015) Sleep, Memory & Brain Rhythms. Daedalus 144:67–82

White NS, Alkire MT, Haier RJ (2003) A voxel-based morphometric study of nondemented adults with Down Syndrome. Neuroimage 20:393–403

Wilson MA, McNaughton BL (1994) Reactivation of hippocampal ensemble memories during sleep. Science 265:676–679

Xie W, Ramakrishna N, Wieraszko A, Hwang Y-W (2008) Promotion of Neuronal Plasticity by (−)-Epigallocatechin-3-Gallate. Neurochem Res 33:776–783

Yabut O, Domogauer J, D'Arcangelo G (2010) Dyrk1A overexpression inhibits proliferation and induces premature neuronal differentiation of neural progenitor cells. J Neurosci 30:4004–4014

Yang X, Schadt EE, Wang S, Wang H, Arnold AP, Ingram-Drake L, Drake TA, Lusis AJ (2006) Tissue-specific expression and regulation of sexually dimorphic genes in mice. Genome Res 16:995–1004

Zheng C, Bieri KW, Hwaun E, Colgin LL (2016) Fast Gamma Rhythms in the Hippocampus Promote Encoding of Novel Object – Place.